

**DESIGN AND SYNTHESIS OF CHROMONE DERIVATIVES AS
PLASMEPSIN II INHIBITORS**

PRADITH LERDSIRISUK

**A THESIS SUBMITTED IN PARTIAL FULFILLMENT
OF THE REQUIREMENTS FOR THE DEGREE OF
MASTER OF SCIENCE (PHARMACEUTICAL CHEMISTRY AND
PHYTOCHEMISTRY)
FACULTY OF GRADUATE STUDIES
MAHIDOL UNIVERSITY
2012**

COPYRIGHT OF MAHIDOL UNIVERSITY

Thesis
entitled
**DESIGN AND SYNTHESIS OF CHROMONE DERIVATIVES AS
PLASMEPSIN II INHIBITORS**

.....
Mr. Pradith Lerdsirisuk
Candidate

.....
Assoc. Prof. Jiraporn Ungwitayatorn,
Ph.D. (Medicinal Chemistry)
Major advisor

.....
Assoc. Prof. Chanpen Wiwat,
Ph.D. (Microbiology)
Co-advisor

.....
Prof. Banchong Mahaisavariya,
M.D., Dip Thai Board of Orthopedics
Dean
Faculty of Graduate Studies
Mahidol University

.....
Assoc. Prof. Weena Jiratchariyakul,
Dr.rer.nat (Pharmaceutical Chemistry)
Program Director
Master of Science Program in
Pharmaceutical Chemistry and
Phytochemistry
Faculty of Pharmacy, Mahidol University

Thesis
entitled
**DESIGN AND SYNTHESIS OF CHROMONE DERIVATIVES AS
PLASMEPSIN II INHIBITORS**

was submitted to the Faculty of Graduate Studies, Mahidol University
for the degree of Master of Science
(Pharmaceutical Chemistry and Phytochemistry)
on
November 29, 2012

.....
Mr. Pradith Lerdsirisuk
Candidate

.....
Assoc. Prof. Weerasak Samee,
Ph.D. (Pharmaceutical Chemistry and
Phytochemistry)
Chair

.....
Assoc. Prof. Jiraporn Ungwitayatorn,
Ph.D. (Medicinal Chemistry)
Member

.....
Assoc. Prof. Chanpen Wiwat,
Ph.D. (Microbiology)
Member

.....
Prof. Banchong Mahaisavariya,
M.D., Dip Thai Board of Orthopedics
Dean
Faculty of Graduate Studies
Mahidol University

.....
Assoc. Prof. Chuthamanee Suthisisang,
Ph.D. (Pharmacology)
Dean
Faculty of Pharmacy
Mahidol University

ACKNOWLEDGEMENTS

I am sincerely thankful to my thesis advisor, Associate Professor Dr. Jiraporn Ungwitayatorn, for her helpful suggestion of the problems, guidance, valuable advice, supervision and support throughout my entire study.

My sincere appreciation is also wish expressed to my thesis co-advisor, Associate Professor Dr. Chanpen Wiwat, for her valuable comments and suggestion in biological experimental section.

I would like to thank Associate Professor Dr. Weerasak Samee for being a committee in my thesis examination and giving valuable comments and suggestions.

I am sincerely grateful to Associate Professor Dr. Supanna Techasakul for her kindness to give me an opportunity to try some of organic reactions at Chulabhorn Research Institute (CRI) and also grateful to Dr. Nisachon Khunnawutmanotham and Mr. Nitirat Chimnoi, staff at CRI, for their suggestion in organic synthesis and mass spectrometry.

A special acknowledgement is extended to

- High Performance Computer Center (HPCC), National Electronic and Computer Technology Center (NECTEC) of Thailand for providing SYBYL version 8.0 facility.

- Bioassay laboratory of the National Center of Genetic Engineering and Biotechnology (BIOTEC) for testing the antimalarial activity.

I am also thankful to all graduate students and staffs at Mahidol University, for their helpful, friendship, kindness and encouragement.

Finally, I wish to express my sincere gratitude and especially thanks to my family for their concern and support me to gain invaluable experience throughout my life.

Pradith Lerdsirisuk

DESIGN AND SYNTHESIS OF CHROMONE DERIVATIVES AS PLASMEPSIN II INHIBITORS

PRADITH LERDSIRISUK 5237765 PYPP/M

M.Sc. (PHARMACEUTICAL CHEMISTRY AND PHYTOCHEMISTRY)

THESIS ADVISORY COMMITTEE: JIRAPORN UNGWITYATORN, Ph.D., CHANPEN WIWAT, Ph.D.

ABSTRACT

Plasmeprin II (Plm II) is an aspartic protease which is involved in the hemoglobin degradation inside the food vacuole during the erythrocytic phase of the malaria parasite's life cycle. This enzyme has received considerable attention as a promising target for antimalarial drug design. Since HIV-1 protease (HIV-1 PR) is also an aspartic protease, several HIV-1 PR inhibitors exhibit activity against Plm II and antimalarial activity against *P. falciparum*. These findings indicate that HIV-1 PR inhibitors may aid the removal of plasmodium parasites and be used as antimalarial drugs. The preliminary screening of Plm II inhibitory activity of the previous forty-six synthesized chromones with HIV-1 PR inhibitory activities was performed by docking study using AutoDock program. Chromone derivatives which showed good binding energy with Plm II and high HIV-1 PR inhibitory activity (more than 70 % inhibition) were selected to be evaluated for their antimalarial activity against *P. falciparum* (K1) by using the microculture radioisotope method. Chromone **35** was found to be the most active compound with IC_{50} value of $0.95 \mu M$ while primaquine and tafenoquine possessed $IC_{50} = 2.41 \pm 0.10$ and $1.95 \pm 0.06 \mu M$, respectively. Based on docking study of chromone structure, a series of newly designed chromones were synthesized as Plm II inhibitors. The synthetic route was mainly divided into two parts. Firstly, the chromone core structure was prepared by Baker-Venkataraman rearrangement and subsequent intramolecular cyclization with a catalytic amount of strong acid. This synthesis pathway was a practical and economical method for chromone structure preparation. Secondly, the esterification at positions 6 and 7 of the chromone structure was performed to provide the designed chromone derivatives. All of these new compounds were evaluated for their antimalarial activity. It was found that the new designed chromone was inactive against *P. falciparum*.

KEY WORDS: CHROMONE DERIVATIVES / PLASMEPSIN II INHIBITORS / ANTIMALARIAL AGENT / MOLECULAR DOCKING / SYNTHESIS

110 pages

การออกแบบและสังเคราะห์อนุพันธ์ของโครโมนเพื่อใช้เป็นสารยับยั้งเอนไซม์พลาสมิซิน II
DESIGN AND SYNTHESIS OF CHROMONE DERIVATIVES AS PLASMEPSIN II INHIBITORS

ประดิษฐ์ เลิศสิริสุข 5237765 PYPP/M

วท.ม. (เภสัชเคมีและพิษวิทยา)

คณะกรรมการที่ปรึกษาวิทยานิพนธ์: จิรกรณ์ อังวิทย์, Ph.D., จันทร์เพ็ญ วิวัฒน์, Ph.D.

บทคัดย่อ

พลาสมิซิน II เป็นเอนไซม์ในกลุ่มเอสพาดิกโปรตีเอส ที่เกี่ยวข้องกับกระบวนการย่อยสลายฮีโมโกลบินภายในถุงอาหารของเชื้อปรสิต ซึ่งเกิดขึ้นระหว่างช่วงวงจรชีวิตที่เชื้ออาศัยอยู่ในเม็ดเลือดแดง เอนไซม์ชนิดนี้ได้รับความสนใจในการเป็นเป้าหมายสำหรับการออกแบบยาที่คาดว่าจะยับยั้งการเจริญเติบโตของปรสิต เนื่องจากเอนไซม์-1 โปรตีเอส เป็นเอนไซม์ในกลุ่มของเอสพาดิกโปรตีเอสเช่นเดียวกับพลาสมิซิน สารซึ่งยับยั้งเอนไซม์-1 โปรตีเอสหลายชนิดสามารถออกฤทธิ์ยับยั้งพลาสมิซิน II และมีฤทธิ์ต้านมาลาเรียกับเชื้อพลาสมิเดียม ฟาลซิพารัมได้ จากการค้นพบเหล่านี้บ่งชี้ว่าสารยับยั้งเอนไซม์-1 โปรตีเอส อาจช่วยในการกำจัดเชื้อพลาสมิเดียมและใช้เป็นยาต้านมาลาเรียได้ การคัดกรองเบื้องต้นในการออกฤทธิ์ยับยั้งพลาสมิซิน II ของอนุพันธ์โครโมนจำนวน 46 อนุพันธ์ ซึ่งได้สังเคราะห์ในงานวิจัยก่อนหน้านี้และพบว่ามีฤทธิ์ยับยั้งเอนไซม์-1 โปรตีเอส ทำโดยวิธีคัดกรอง นำอนุพันธ์โครโมนที่แสดงค่าพลังงานการจับกับพลาสมิซิน II ได้ดีและมีฤทธิ์ในการยับยั้งเอนไซม์-1 โปรตีเอสที่ดี (ฤทธิ์ยับยั้งมากกว่า 70%) มาประเมินความสามารถในการออกฤทธิ์ต้านมาลาเรียกับเชื้อพลาสมิเดียม ฟาลซิพารัม (สายพันธุ์ K1) ด้วยวิธี microculture radioisotope พบว่าโครโมน 35 เป็นสารที่มีฤทธิ์ดีที่สุด โดยมีค่า IC_{50} เท่ากับ 0.95 ไมโครโมลาร์ ในขณะที่ primaquine และ tafenoquine มีค่า IC_{50} เท่ากับ 2.41 ± 0.10 และ 1.95 ± 0.06 ไมโครโมลาร์ ตามลำดับ ผลจากการศึกษาคัดกรองได้ทำการออกแบบและสังเคราะห์อนุพันธ์โครโมนกลุ่มใหม่เพื่อใช้เป็นสารยับยั้งพลาสมิซิน II วิธีการสังเคราะห์แบ่งออกเป็นสองส่วนหลัก ส่วนแรก คือ การสังเคราะห์โครงสร้างหลักของโครโมนเตรียมโดยปฏิกิริยา Baker-Venkataraman rearrangement และตามด้วยการปิดวงโดยมีกรดแก่เป็นตัวเร่งปฏิกิริยา วิธีการนี้เป็นวิธีที่เหมาะสมและประหยัดค่าใช้จ่ายในการสังเคราะห์โครงสร้างหลักของโครโมน ส่วนที่สอง คือ ทำการปฏิกิริยาเอสเทอร์ฟิเคชัน ที่ตำแหน่ง 6 และ 7 ของโครโมน เพื่อให้ได้อนุพันธ์โครโมนที่ได้ออกแบบไว้ สารประกอบที่สังเคราะห์ขึ้นใหม่นำไปประเมินทางชีวภาพสำหรับการออกฤทธิ์ต้านมาลาเรีย พบว่าสารที่ออกแบบขึ้นใหม่ไม่มีฤทธิ์ต้านเชื้อพลาสมิเดียม ฟาลซิพารัม

CONTENTS

	Page
ACKONWLAGEMENTS	iii
ABSTRACT (ENGLISH)	iv
ABSTRACT (THAI)	v
LIST OF TABLES	ix
LIST OF FIGURES	x
LIST OF SCHEMES	xii
LIST OF ABBREVIATIONS	xiii
CHAPTER I INTRODUCTION	1
CHAPTER II LITERATURE REVIEW	4
2.1 Malaria	4
1) Life cycle of malaria parasite	4
2) Current antimalarial drugs and drugs resistance	6
3) The approaches for antimalarial drugs development and the targets for antimalarial chemotherapy	9
4) Hemoglobin degradation	9
2.2 Plasmeprins	11
1) Crystal structure of Plm II	12
2) Aspartic protease inhibitors	15
3) Flavonoids as aspartic protease inhibitors and antimalarial agents	18
2.3 Antimalarial activity assay	22
CHAPTER III MOLECULAR MODELING EXPERIMENTAL	24
3.1 Materials	24
1) Computers	24
2) Softwares	24
3.2 Methods	24
1) Preparation and Validation of Plm II template	24

CONTENTS (cont.)

	Page
2) Ligand preparation	26
3) Docking studies of chromone derivatives with Plm II	26
4) Structural modification of chromone derivatives as Plm II inhibitors	27
CHAPTER IV CHEMICAL EXPERIMENTAL	28
4.1 Equipment and chemicals	28
1) Equipments	28
2) Chemicals	28
4.2 Methods	29
1) 2,4,5-Trihydroxyacetophenone	30
2) 4,5-Bisbenzyloxy-2-hydroxyacetophenone	31
3) 6,7-Dihydroxy-2-(3'-methoxyphenyl) chromone, 49 .	32
4) 6-(3''-Methoxybenzoate)-7-(3'''-methoxybenzoate)-2-(3'-methoxyphenyl) chromone, 49a .	33
5) 6-(4''-Methoxybenzoate)-7-(4'''-methoxybenzoate)-2-(3'-methoxyphenyl) chromone, 49b .	34
6) 6-(3'',4''-Dimethoxybenzoate)-7-(3''',4'''-dimethoxybenzoate)-2-(3'-methoxyphenyl) chromone, 49c .	35
7) 6-(3''-Chlorobenzoate)-7-(3'''-chlorobenzoate)-2-(3'-methoxyphenyl) chromone, 49d .	36
8) 6-(4''-Chlorobenzoate)-7-(4'''-chlorobenzoate)-2-(3'-methoxyphenyl) chromone, 49e .	37
9) 6-(3'',4''-Dichlorobenzoate)-7-(3''',4'''-dichlorobenzoate)-2-(3'-methoxyphenyl) chromone, 49f .	38
10) 6-(3''-Nitrobenzoate)-7-(3'''-nitrobenzoate)-2-(3'-methoxyphenyl) chromone, 49g .	39

CONTENTS (cont.)

	Page
12) 6-(3'',5''-Dinitrobenzoate)-7-(3''',5'''-dinitrobenzoate)-2-(3'-methoxy-phenyl) chromone, 49i .	41
CHAPTER V BIOLOGICAL EXPERIMENTAL	42
5.1 Equipment and chemicals	43
1) Equipments	43
2) Chemicals	43
5.2 Methods	43
CHAPTER VI RESULTS AND DISSUCSSION	44
6.1 Molecular modeling	46
1) Preparation and Validation of Plm II template	46
2) Docking studies of chromone derivatives with Plm II	47
3) Structural modification of chromone derivatives as Plm II inhibitors	50
6.2 Synthesis	56
1) Preparation of 6,7-dihydroxy-2-(3'-methoxyphenyl) chromone (49)	56
2) Synthesis of the modified chromone derivatives (49a-49i)	60
3) Structure elucidation	62
6.3 Antimalarial activity assay against <i>P. falciparum</i>	69
CHAPTER VII CONCLUSION	78
REFFERENCES	80
APPENDIX	85
BIOGRAPHY	110

LIST OF TABLES

Table	Page
2.1 The current important antimalarial drugs and their action as antimalarial agents.	7
2.2 The amino acid residues of each subsite of the active binding site of Plm II.	13
2.3 The commonly used <i>in vitro</i> antimalarial activity assay.	23
3.1 The structure of ligands complexed in the crystal structures of Plm II.	25
3.2 Grid parameters and docking parameters.	26
6.1 Validation results of Plm II template.	46
6.2 Structures and binding energy of chromone derivatives with Plm II (1SME).	48
6.3 Twenty chromone compounds which showed good binding energy and high inhibitory activity against HIV-1 PR (more than 70 % inhibition).	49
6.4 Structure of the chromone derivatives (47-52) and their binding energy.	50
6.5 Structure of the modified chromone derivatives and their binding energy.	51
6.6 The binding interactions of modified chromone derivatives (49a-49i) with Plm II.	54
6.7 Melting point (m.p.) and % yield of compound 49 and 49a-49i .	62
6.8 ¹ H-NMR data and ¹ H- ¹ H correlation of chromone 49c .	66
6.9 ¹ H-NMR data and ¹ H- ¹ H correlation of chromone 49d .	68
6.10 The high resolution mass spectrometry (ESI technique) of chromone 49 and chromones 49a-49h .	69
6.11 The antimalarial activity results of twenty selected chromone compounds and chromone 49 .	70
6.12 The results of antimalarial activity of chromones 49a-49h .	76

LIST OF FIGURES

Figure	Page
2.1 The life cycle of the malaria parasite in the human host and the mosquito vector. The trophozoite stage in the erythrocytic cycle is enlarged (3).	5
2.2 The 3D structure of oxyhemoglobin.	10
2.3 Degradation of hemoglobin by Plms and associated protease.	11
2.4 Ribbon structure of Plm II complex with EH58 ligand (PDB code 1LF3).	12
2.5 Catalytic mechanisms for Plm II-mediated hydrolysis of hemoglobin.	13
2.6 The active site of Plm II from S4 to S4' derived from substrate mimic (pepstatin A) (39).	14
2.7 Surface representations of a monomer of uncomplexed Plm II (a) and Plm II in complex with EH58 (b) and pepstatin A (c). The binding cavity of the complex with pepstatin A revealing a much tighter embrace of the inhibitor.	15
2.8 Transition-state analog units (TSA) in peptidomimetic inhibitors.	16
2.9 Peptidomimetic aspartic protease inhibitors, pepstatin A, lopinavir, saquinavir and ritonavir	17
2.10 General flavonoid structure.	17
2.11 Structure of flavonoid compounds with antimalarial activity (10).	19
2.12 The effect of luteolin of the intraerythrocytic growth of <i>P. falciparum</i> (10).	19
2.13 Some naturally flavonoids which exhibited antimalarial activity.	20
2.14 Structure of flavonoid derivatives containing a piperaziny chain (13).	21
2.15 The three most active HIV-1 PR inhibitors in chromone series.	21
6.1 The summary diagram of screening process.	45
6.2 The binding mode of nine modified chromone derivatives (49a-49i) comparing with the pepstatin A (navy blue color).	53
6.3 Schematic picture of binding interactions between modified chromones (49a-49i) and Plm II.	53

LIST OF FIGURES (cont.)

Figure	Page
6.4 IR spectrum of chromone 49 .	62
6.5 ¹ H-NMR spectra (300 MHz, DMSO-d ₆) of chromone 49 .	63
6.6 IR spectrum of chromone 49c .	64
6.7 ¹ H-NMR spectra (300 MHz, CDCl ₃) of chromone 49c .	65
6.8 ¹ H- ¹ H COSY spectra (300 MHz, CDCl ₃) of chromone 49c .	66
6.9 ¹ H-NMR spectra (300 MHz, CDCl ₃) of chromone 49d .	67
6.10 ¹ H- ¹ H COSY spectra (300 MHz, CDCl ₃) of chromone 49d .	68
6.11 Structure of HIV-1 PR enzyme.	73
6.12 Hydrophobic interaction of chromone 31 in the active site of HIV-1PR (a) and schematic view of the protease active site pockets binding with chromone 31 (b) (9).	74
6.13 The binding interaction of chromone 35 with Plm II from AutoDock 4.0 program (a) and schematic picture showing the interactions between binding pocket of Plm II and chromone 35 (b).	75

LIST OF SCHEMES

Scheme	Page
6.1 Synthesis route of 6,7-dihydroxy-2-(3'-methoxyphenyl) chromone (49) preparation (a) AlCl ₃ , PhCl, reflux, 12 hours (49, 50); (b) BnBr, K ₂ CO ₃ , acetone, reflux, 5 hours (51); (c) 3-methoxybenzoyl chloride, K ₂ CO ₃ , acetone, reflux, 24 hours (17); (d) conc. H ₂ SO ₄ , glacial acetic acid, 120 °C, 3 hours (18).	56
6.2 The demethylation reaction of 2,4,5-trimethoxyacetophenone	57
6.3 The selective protection of 2,4,5-trihydroxyacetophenone.	57
6.4 Baker-Venkataraman rearrangement, intramolecular cyclization and debenzylation reactions.	58
6.5 The proposed mechanism of Baker-Venkataraman rearrangement.	58
6.6 The proposed mechanism of intramolecular cyclization and debenylation of chromone 49 .	59
6.7 The esterification of chromone 49a , 49b and 49d-49i .	60
6.8 The esterification of chromone 49c (53).	60
6.9 The proposed mechanism of esterification of chromone 49c .	61

LIST OF ABBREVIATIONS

α	alpha
α -C	alpha carbon
Å	angstrom
AcOH	acetic acid
AIDS	acquired immunodeficiency syndrome
Ala	alanine
AR	analytical reagent
Arg	arginine
Asn	asparagine
Asp	aspartic acid
β	beta
BnBr	benzyl bromide
Cpd	compound
CPM	count per minute
cm ⁻¹	per centimeter
cont.	continued
°C	degree Celsius
calcd	calculated
Conc.	concentration
d	doublet
δ	chemical shift
DBU	1,8-diazabicyclo [5,4,0] undec-7-ene
dd	doublet of doublet
ddd	doublet of doublet of doublet
DHA	dihydrosrtemisinine
DHFR	dihydrofolate reductase
DHPS	dihydrofolate synthase

LIST OF ABBREVIATIONS (cont.)

DMF	dimethylformamide
DMSO	dimethyl sulfoxide
DMSO-d ₆	deuterated dimethylsulfoxide
DOXP	1-deoxy-D-xylose-5-phosphate
dt	doublet of triplet
EDAC.HCl	1-ethyl-3-(3'-dimethylaminopropyl)carbodiimide.HCl
ESI	electro spray ionization
FAS	fatty-acid synthase
FTIR	Fourier transforms infrared spectroscopy
g	gram
GA	genetic algorithm
Gly	glycine
³ H	tritium
HAP	histo-aspartic protease
HCl	hydrochloric acid
HEPES	N-2-hydroethylpiperazine-N'-2-ethanesulfonic acid
HGPR	hypoxanthine-guanine phosphoribosyl
HIV-1 PR	human immunodeficiency virus-1 protease
HOBt	hydroxylbenzotriazole
HPLC	high performance liquid chromatography
HRMS	high resolution mass spectrometer
HRP2	histidine-rich protein II
IC ₅₀	half maximal inhibitory concentration
Ile	isoleucine
IR	infrared
Iva	isovaleryl
<i>J</i>	coupling constant
KBr	potassium bromide

LIST OF ABBREVIATIONS (cont.)

K_2CO_3	potassium carbonate
kcal/mole	kilo calorie per mole
kDa	kilo Dalton
K_i	inhibition constant
Leu	leucine
LRMS	low resolution mass spectrometer
M	molar
m	multiplet
μCi	microcurie
MEF	mefloquine
Met	methionine
mg	milligram
μg	microgram
MHz	mega hertz
min.	minute
mL	milliliter
μM	micromolar
mmol	millimole
m.p.	melting point
MS	mass spectrometer
m/z	mass to charge ratio
nM	nanomolar
NMR	Nuclear Magnetic Resonance spectroscopy
PCR	polymerase chain reaction
PDB	protein data bank
PhCl	chlorobenzene
Phe	phenylalanine
pLDH	parasite lactate dehydrogenase

LIST OF ABBREVIATIONS (cont.)

Plms	plasmepsins
ppm	parts per million
Pro	proline
R _f	retention factor
RMSD	root mean square deviation
RPMI-1640	Roswell Park Memorial Institute-1640
s	singlet
SAR	structure-activity relationship
Ser	serine
st.	stretching
Sta	statine
TEA	triethylamine
TLC	thin layer chromatography
Thr	threonine
TSA	transition-state analog
Tyr	tyrosine
Val	valine

CHAPTER I

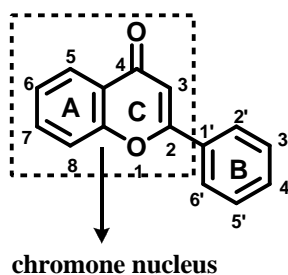
INTRODUCTION

Nowadays, malaria is still one of the major causes of ailment and mortality in the world (1-2). The causative agents of malaria are four different species of Plasmodium, but almost all deaths are due to infection by *P. falciparum* (3-4). Malaria has become more difficult to treat because of an increase in multi-drug resistant strains (5). This increasing drug resistance leads to the importance of identifying new antimalarial agents with novel mechanisms of action. One of the crucial drug targets in malaria are plasmepsins.

Plasmepsins (Plms) are groups of aspartic protease enzymes inside the digestive food vacuole of parasite. Four aspartic proteases, i.e., Plm I, II, IV and histidine aspartic protease (HAP) are involved in the initial step of human hemoglobin degradation process that digests the human hemoglobin as a source of amino acids for growth and maturation during the erythrocytic phase of its life cycle (2). These enzymes efficiently degrade 75% of host hemoglobin. Plm I and II make the first strategic cleavage of hemoglobin at α -chain between Phe33 and Leu34 in the hinge region, which is highly conserved and responsible for the stability of hemoglobin tetramer, resulting in protein unfolding (5). Plms have been given considerable attention as the promising targets for designing novel antimalarial agents because the inhibition of Plms results in the starvation of the malaria parasite. Among these enzymes, Plm II is the most thoroughly studied enzyme to discover novel antimalarial agents, most likely because it is the easiest one to crystallize (4).

The effective aspartic protease inhibitor is peptidomimetic aspartic protease inhibitors. A key structural feature in these inhibitors is the presence of hydroxyl or hydroxyl-like moiety that mimics the transition state of amide hydrolysis. Since HIV-1 protease (HIV-1 PR) is also an aspartic protease enzyme, several HIV-1 PR inhibitors exhibit activity against Plm II, e.g., pepstatin A, the known potent peptidomimetic aspartic protease inhibitor, can inhibit HIV-1 PR, several types of

Plms and cultured malaria parasites (6). HIV-1 PR inhibitors currently used in AIDS patients such as saquinavir, ritonavir and lopinavir can directly inhibit Plm II and the *in vitro* growth of both drug-sensitive and drug-resistant *P. falciparum* strains. These findings indicate that HIV-1 PR inhibitors may aid in the removal of Plasmodium parasite and used as antimalarial drugs (7-8). However, peptidomimetic inhibitors normally exhibit low bioavailability due to their high molecular weight, poor solubility and synthesis difficulties. Therefore, the non-peptidomimetic inhibitors are more interesting for developing the new aspartic protease inhibitors. In our search for new potent aspartic protease inhibitors, we concentrate on flavonoids or chromone compounds.



Flavonoids have been reported that they can exhibit the antimalarial activity against *P. falciparum* (10). Luteolin and some of naturally flavonoids have been reported that they can exhibit the antimalarial activity against *P. falciparum* (10-12). Moreover, a series of flavonoid derivatives, which had a 2,3,4-trimethoxybenzyl-piperazinyl chain attached to the flavone at the 7-phenol group, showed the IC_{50} values in micromolar to submicromolar range against *P. falciparum* (13).

The previous study of chromone derivatives as HIV-1 PR inhibitors, forty-six chromone derivatives have been previously synthesized and evaluated the *in vitro* inhibitory activity against HIV-1 PR (9). The three most potent inhibitors showed $IC_{50} = 0.34, 0.65$ and $2.53 \mu M$, respectively, while amprenavir exhibited $IC_{50} = 0.084 \mu M$ (14). Therefore, these chromone derivatives were selected to investigate their inhibitory activity against Plm II.

In this study the chromone derivatives were designed and synthesized as non-peptidomimetic Plm II inhibitors. The preliminary screening of the Plm II inhibitory activity of forty-six chromone derivatives that have been previously

synthesized and evaluated as HIV-1 PR inhibitors was performed by using docking simulation technique with AutoDock program (15). Chromone compounds which showed good binding energy with Plm II from docking study and high HIV-1 PR inhibitory activity (more than 70 % inhibition) were selected to evaluate for their antimalarial activity against *P. falciparum* using the microculture radioisotope method (16). Moreover, a new series of chromone derivatives were designed based on docking simulation results. The designed chromone derivatives were synthesized using the commercially available 2,4,5-trimethoxyacetophenone as starting material. The synthesis route of chromone derivatives was divided into two major parts. Firstly, the chromone core structure was prepared by Baker-Venkataraman rearrangement and subsequent intramolecular cyclization with strong acid as catalyst (17-18). Then esterification at positions 6 and 7 of the chromone structure was performed to obtain the designed chromone derivatives. These compounds were also tested for their antimalarial activity against *P. falciparum*.

CHAPTER II

LITERATURE REVIEW

2.1 Malaria

Malaria is one of the world's most common disease and still one of the major causes of ailment and mortality in the world. It is estimated that 300-500 million people become ailment and up to 2.7 million of them die, particularly among young children and pregnant women (19). Almost half of the world's population lives in malaria endemic areas that are centered in tropical and subtropical regions. The distribution of the disease is dependent on present of the parasite mosquito vector. Malaria is transmitted into human by the bite of inflect female *Anopheles* mosquitoes. The causative agents of malaria that responsible in human are four different species of Plasmodium, namely, *P. falciparum*, *P. vivax*, *P. malariae* and *P. ovale* (2). The inflections of *P. falciparum* are the most serious and commonly lethal. *P. vivax* inflection is less dangerous but more widespread, and the other two species are found much less frequently (20).

1) Life cycle of malaria parasite

The malaria parasites have a complicated life cycle that requires a human host for the asexual cycle and a female *Anopheles* mosquito for completion of the sexual cycle (21). In the human host, the asexual cycle can be further divided into a liver stage or a preerythrocytic stage and an erythrocytic stage (Figure 2.1). During the bite of inflected mosquito, the sporozoites in the mosquito's saliva are injected into the human host and migrate through the host bloodstream to the liver, where they invade the hepatocytes. Inside the hepatocyte, the sporozoite is changed into a trophozoite. Then a trophozoite divides into schizonts and each of schizont develops into the mature merozoite. After the development, the merozoites burst the hepatocyte and are released into the host bloodstream. This development and multiplication of the parasite in the hepatocytes constitutes the preerythrocytic stage. The subsequent erythrocytic

stage begins with the merozoite invades a host red blood cell (erythrocyte) and transforms into the ring stages, which grows and matures into a trophozoite. The mature trophozoite divides into schizonts, which each of them contains many daughter merozoites. Then the merozoites rupture the host cell and invade the new erythrocyte to continue asexual erythrocytic cycle. Some of merozoites develop into the sexual stages gametocytes and when the human host is bitten by the *Anopheles* mosquito, the gametocytes are taken up into the mosquito vector and finish the sexual stage (22).

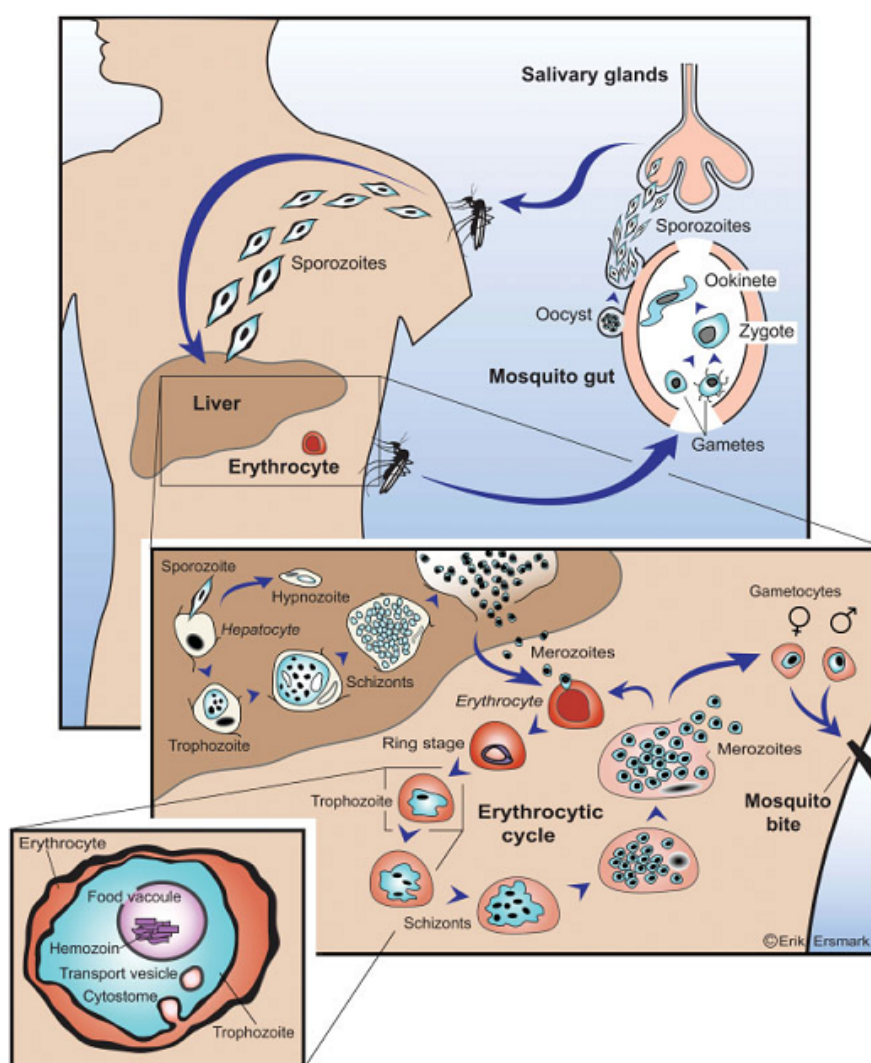


Figure 2.1 The life cycle of the malaria parasite in the human host and the mosquito vector. The trophozoite stage in the erythrocytic cycle is enlarged (3).

2) Current antimalarial drugs and drugs resistance

The most well known effective antimalarial agent in the Western world for hundreds of years was quinine, an alkaloid isolate of the bark of the cinchona tree (*Cinchona officinalis* L) (23). Until World War I and II, quinine was not used due to the drastically diminished supplies that caused attention to be turned to developing synthetic antimalarial agents. Nowadays several synthetic antimalarial drugs have been developed to act at the different stages of the parasite life cycle. Current important antimalarial drugs and their mechanism of action as antimalarial agents are shown in Table 2.1. The activities of current antimalarial drugs range from very specific stage, broader activities that interfere with several stages and against all stages of parasite in man. The majority of the current antimalarial drugs act on the blood stage parasites (erythrocytic stage), which are responsible for nearly all malaria symptoms. Despite the antimalarial agents have been developed and provided many available antimalarial agents against *P. falciparum* for treatment the malaria patient, malaria has become more difficult to treat due to an increase in multi-drug resistant strains (5). In 1910, the first parasite resistance to be reported was against quinine in Brazil (24). Since then, the number of reports of antimalarial resistance has been constantly increasing throughout the world (25). Regarding the parasite species infecting humans, resistance has primarily been documented for *P. falciparum* and *P. vivax*, the two species accounting for more than 95% of all cases (25). Additionally, multi-drug resistant strains of *P. falciparum* are emerging in several parts of the world (4). The molecular mechanisms behind resistance vary and depend on the chemical class of the antimalarial and its mechanism of action. Generally, resistance arises from mutations in genes encoding either the parasite drug targets or influx/efflux pumps that affect the concentration of the drug at the target (26). This increasing resistance to available drugs leads to the importance of identifying the new antimalarial drugs.

Table 2.1 The current important antimalarial drugs and their action as antimalarial agents.

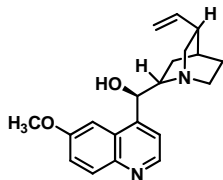

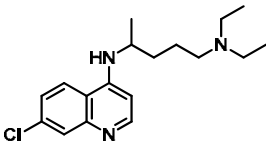
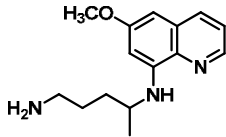
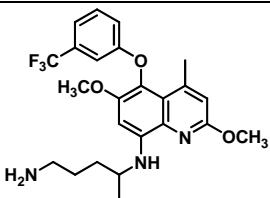
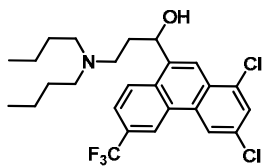
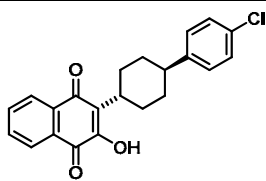
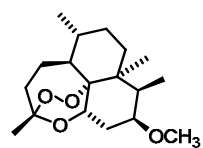
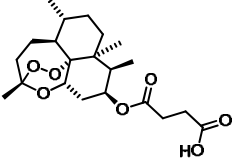
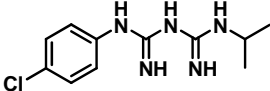
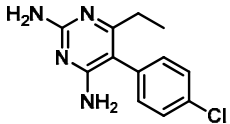
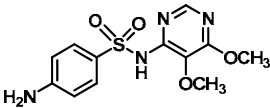
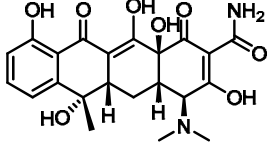
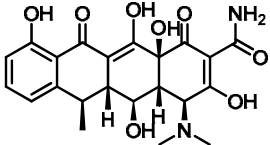
Drugs	Structure	Mechanism of action	References
Quinine		Interfering the heme detoxification process (Anti-hemozoin formation)	(24), (27)
Mefloquine		Interfering the heme detoxification process (Anti-hemozoin formation)	(24), (27)
Chloroquine		Interfering the heme detoxification process (Anti-hemozoin formation)	(24), (27)
Primaquine		Interfering the cellular respiration of the parasite by generating oxygen free radicals and deregulating the electron transport	(24), (28)
Tafenoquine		Interfering the cellular respiration of the parasite by generating oxygen free radicals and deregulating the electron transport	(28)
Halofantrine		Unknown mechanism of action	(29)
Atovaquone		Blocking the mitochondrial electron transport and collapse the mitochondrial membrane	(24)
Artemether		Probably generating the reactive oxygen intermediate (ROI) which is toxic to the malaria parasites	(24), (30)

Table 2.1 The current important antimalarial drugs and their action as antimalarial agents (cont.).

Drugs	Structure	Mechanism of action	References
Artesunate		Probably generating the reactive oxygen intermediate (ROI) which is toxic to the malaria parasites	(24), (30)
Proguanil		Antifolates (dihydrofolate reductase [DHFR] inhibitor)	(24), (31)
Pyrimethamine		Antifolates (dihydrofolate reductase [DHFR] inhibitor)	(24), (31)
Sulfadoxine		Antifolates (dihydrofolate synthase [DHPS] inhibitor)	(24), (31)
Tetracycline		Impairing the progeny of the apicoplast genes	(24), (29)
Doxycycline		Impairing the progeny of the apicoplast genes	(24), (29)

3) The approaches for antimalarial drugs development and the targets for antimalarial chemotherapy

Two major approaches have been employed in the search for new antimalarial drugs. The first method is the development of chemically related analogs to existing antimalarial drugs and the other method is the identification of novel drug targets and the design of chemical entities acting on these targets (32). The targets for antimalarial chemotherapy have been broadly classified into three categories. The first is targets involved in the hemoglobin metabolism and heme detoxification, e.g., protease enzyme such as plasmepsins and falcipains. The second is targets responsible for macromolecular and metabolite synthesis, e.g., 1-deoxy-D-xylose-5-phosphate (DOXP) reductoisomerase, farnesyl transferase, fatty-acid synthase (FAS) enzymes, parasite hypoxanthine-guanine phosphoribosyl (HGPR) transferase and lactate dehydrogenase. The third is targets engaged in membrane transport and signaling, e.g., the choline transporter and protein kinase (33). Among of these targets, the targets that involve in hemoglobin degradation are the crucial drug targets to search the new drugs for antimalarial chemotherapy (21).

4) Hemoglobin degradation

Hemoglobin is the iron-containing oxygen-transport protein in the red blood cell of human. Hemoglobin carries oxygen from the lung to the tissues where it releases the oxygen to burn nutrients and then provides energy to power the functions of the organism. Hemoglobin also collects the resultant carbon dioxide and brings it back to the lung to be dispensed from the organism. The structure of hemoglobin molecule is a tetramer that contains two α -chains (α -globins) and two β -chains (β -globins). The numbers of amino acid residues for α -chain and β -chain are 141 and 146 amino acids respectively. Most of the amino acids in hemoglobin form α -helixes (8 α -helixes), connected by short non-helical segments. Hydrogen bonds stabilize the helical sections inside this protein, causing attractions within the molecule, folding each polypeptide chain into a specific shape (34). Hemoglobin's quaternary structure comes from its four subunits in roughly a tetrahedral arrangement as shown in Figure 2.2.

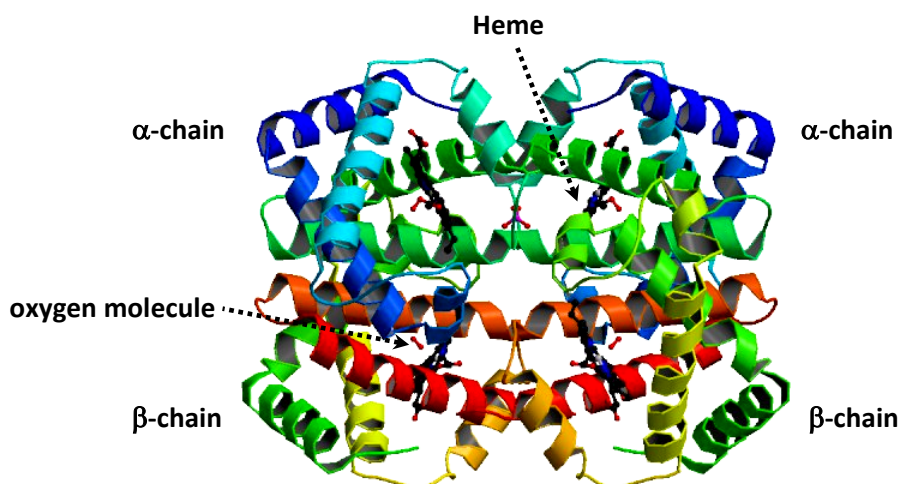


Figure 2.2 The 3D structure of oxyhemoglobin.

During the erythrocytic stage of malaria parasite life cycle, the parasite degrades most of the host hemoglobin as a source of amino acids for growth and maturation. The metabolic activity varies between the different phases. Some hemoglobin degradation is seen during the ring and early schizont stages of development, but it is most pronounced during the trophozoite stage (35). The enzymes that involved in this process are aspartic proteases (plasmepsins), cysteine proteases (falcipains), a metalloprotease (falcilysin) and cytoplasmic aminopeptidase. The human hemoglobin degradation is initiated by four aspartic proteases, i.e., plasmepsin (Plm) I, II, IV and histo-aspartic protease (HAP) inside the digestive food vacuole. These enzymes efficiently degrade 75% of host hemoglobin (5). Plm I and II make the first strategic cleavage of hemoglobin at α -chain between Phe33 and Leu34 in the hinge region, which is highly conserve and responsible for the stability of hemoglobin tetramer (21). It results in the protein unfolding and release of the heme moiety. Subsequent degradation steps are catalyzed by falcipains, falcilysin and cytoplasmic amino-peptidase (Figure 2.3) (5). All of those enzymes, Plms have been had considerable attention as the promising targets for design the novel antimalarial agents as the inhibition of Plms lead the starvation of the malaria parasite (4).

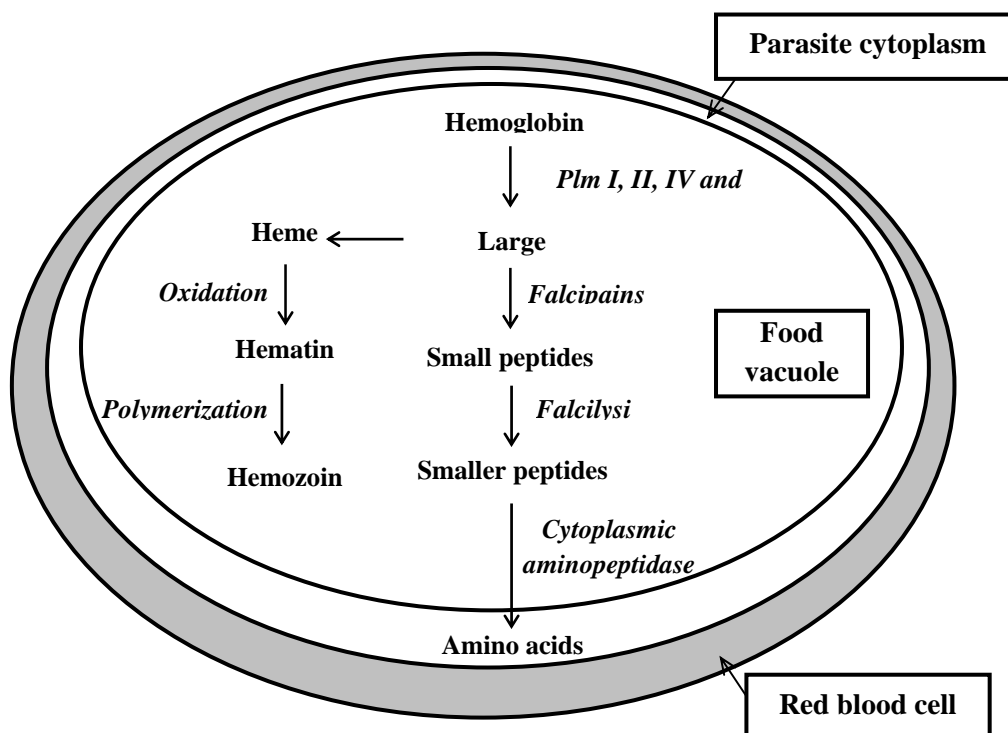


Figure 2.3 Degradation of hemoglobin by Plms and associated proteases.

2.2 Plasmepsins

Plasmepsins (Plms) are groups of aspartic proteases inside the parasite food vacuole. There are ten different isoforms of these enzymes in *P. falciparum*, i.e., Plm I, II, IV, V, VI, VII, VIII, IX, X and HAP. The expression of Plm I, II, IV, V, IX, X and HAP occurs in the erythrocytic stage, whereas Plm VI, VII and VIII are expressed in the exo-erythrocytic stages (36). Only four of them, i.e., Plm I, II, IV and HAP are the most extensively studied Plms those are involved in the human hemoglobin degradation inside the parasite digestive food vacuole. The expression of four aspartic protease Plms varies during the erythrocytic stage. Plm I is transcribed in the early ring stage followed by Plm II which is appropriately expressed in the trophozoite stage (37). HAP and Plm IV are detectable from the trophozoite stage and all four of them persist to schizogony (the term of division of trophozoite into schizonts). Among of these enzymes, Plm II is the most thoroughly studied enzyme to

discover the novel antimalarial agents, most likely because it is the easiest enzyme to crystallize (4).

1) Crystal structure of Plm II

The X-ray crystal structure of Plm II has the typical bilobal shape and topology of eukaryotic aspartic proteases. The mature enzyme, molecular weight 37 kDa, is formed by a single chain of 329 amino acids residues folded into two topologically similar N- and C-terminal domains. The binding cavity contains Asp34 and Asp214 which together represent the catalytic dyad. The N-terminal domain contains a β -hairpin structure, known as flap, which covers the substrate-binding cavity (Figure 2.4) (38).

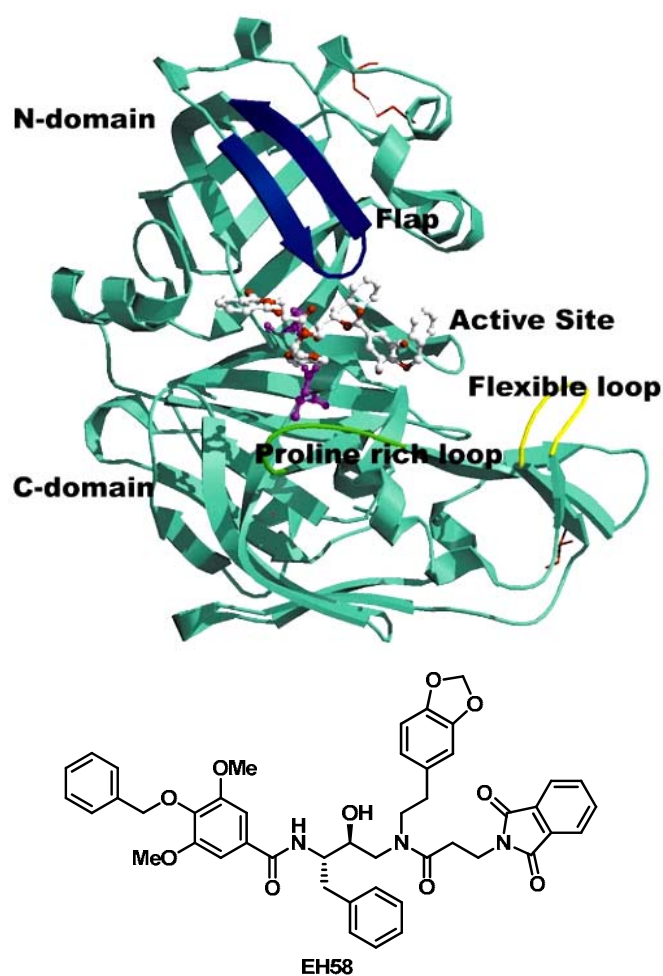


Figure 2.4 Ribbon structure of Plm II complexed with EH58 ligand (PDB code 1LF3).

The catalytic mechanism of Plm II is an acid-base hydrolysis (Figure 2.5). The Asp34 and Asp214 residue coordinate a water molecule which is activated by Asp214 for nucleophilic attack the Phe33-Leu34 peptide bond and generating a tetrahedral intermediate. Hydrolysis of the C-N bond in the transition state then affords two peptides and regenerates the aspartates in the catalytic dyad. As products leave the active binding cleft, Asp34 and Asp214 are coordinated with water molecule again (5).

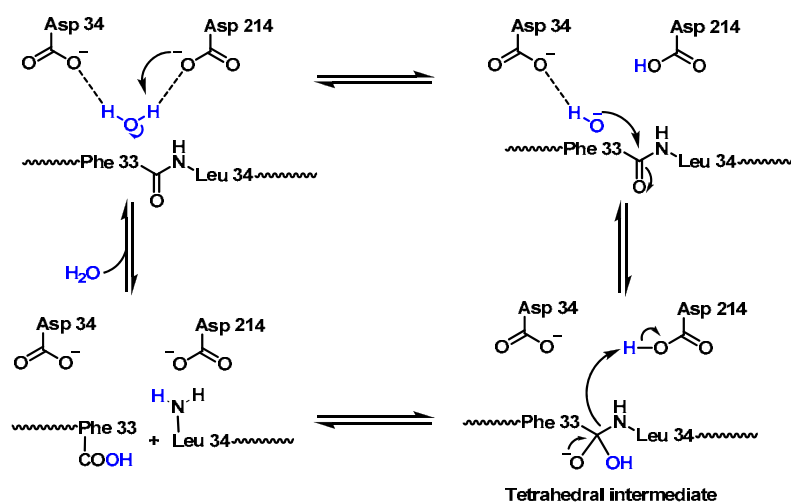


Figure 2.5 Catalytic mechanisms for Plm II-mediated hydrolysis of hemoglobin.

The active binding site of Plm II consist eight subsites from S4 to S4' derived from substrate mimic residue (pepstatin A) as shown in Figure 2.6. The amino acid residues of each subsite are shown in Table 2.2 (4).

Table 2.2 The amino acid residues of each subsite of the active binding site of Plm II.

Subsite	Amino acids
S4	Ser218, Ala219, Pro243, Met286, Asn288, Ile290
S3	Met15, Thr114
S2	Val 78, Thr217, Thr221, Ile290, Leu292,Ile300
S1	Ile32, Tyr77,Ser79 Phe111, Ile123, Gly216
S1'	Ser37, Met75, Tyr77
S2'	Asn76, Tyr77, Val78, Tyr192
S3'-S4'	Leu131, Ile133, Leu191

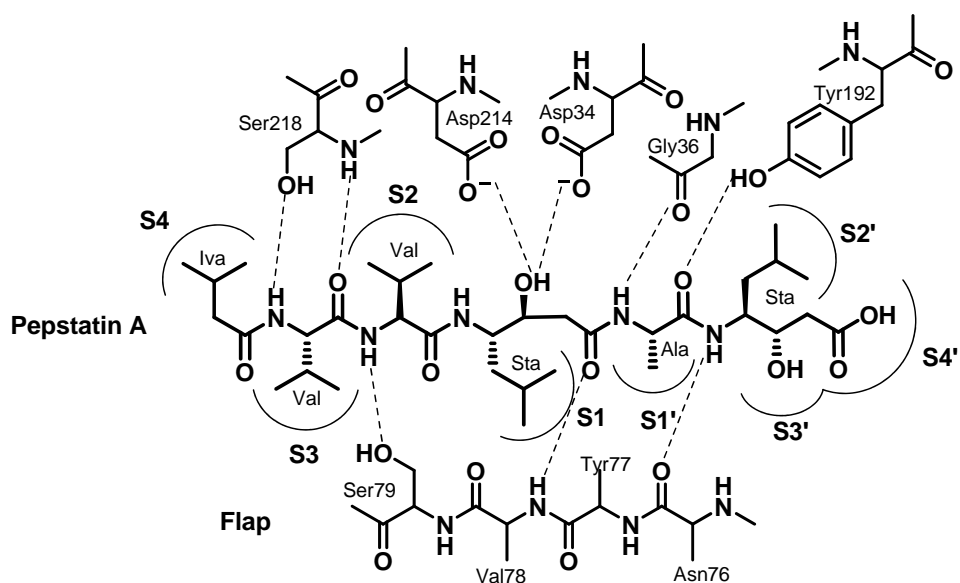
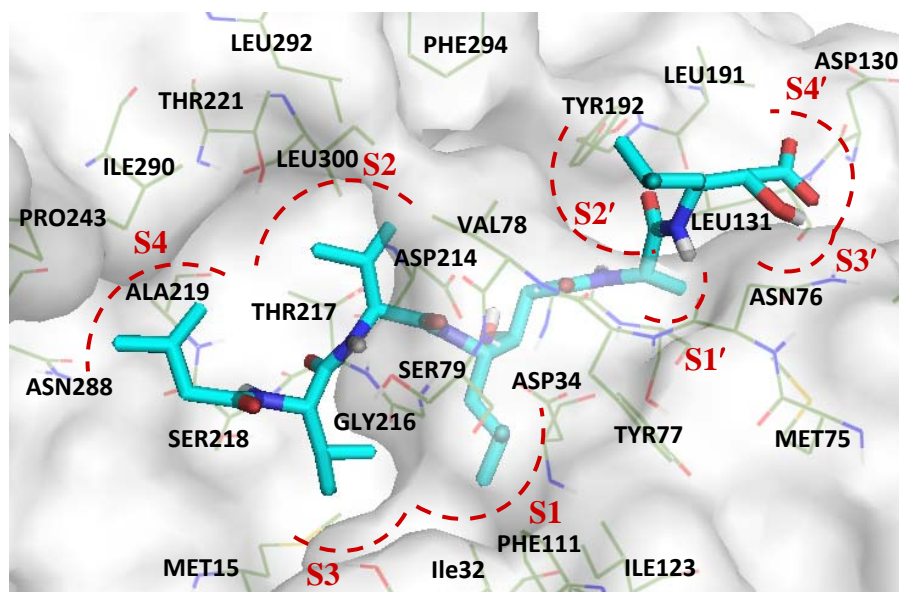


Figure 2.6 The active site of Plm II from S4 to S4' derived from substrate mimic (pepstatin A) (39).

The binding cavity size of the X-ray crystal structure of Plm II depends on the inhibitors that bound with the enzyme. The relative opening of the binding cavity can be measured by the distance between α -C of Val78, which is the tip of flap, to α -C of Leu292, which lying opposite to Val78 at the hydrophobic edge of the binding cavity. The distance between these atoms is 12.6 Å in the unbounded structure, 12.0 Å

in the EH58 complex and 9.9 Å in the pepstatin A complex (39). The molecular surfaces of uncomplexed Plm II and Plm II in complex with EH58 and pepstatin A shown in Figure 2.7 illustrate how tight the embrace is in the presence of each inhibitor. The different conformation of the binding cavity of Plm II crystal structure likely affects the interaction between the crystal structure and inhibitors from the docking study. The unbounded structure of Plm II shows the most open conformation with subsites that can readily accept bulkier than predicted from the Plm II-pepstatin A complex structure. The study of interaction between crystal structure of Plm II and inhibitor should be considering the conformation of the binding cavity of the crystal structure to design and discover the new potent Plm II inhibitors (39).

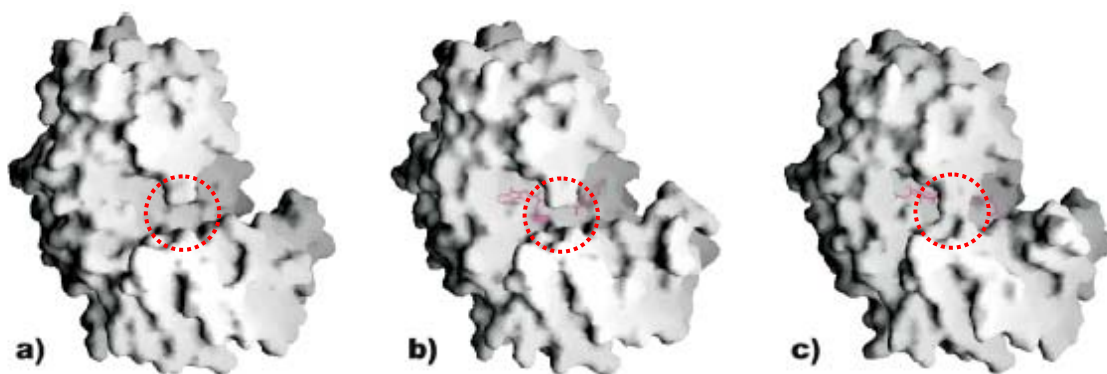


Figure 2.7 Surface representations of a monomer of uncomplexed Plm II (a) and Plm II complexed with EH58 (b) and pepstatin A (c). The binding cavity of the complex with pepstatin A reveals a much tighter embrace of the inhibitor.

2) Aspartic protease inhibitors

Aspartic protease inhibitors are classified in two groups that are peptidomimetic inhibitors and non-peptidomimetic inhibitors. A key structural element in peptidomimetic aspartic protease inhibitors is a hydroxyl or hydroxyl-like moiety that mimics the transition state of amide hydrolysis. A number of chemical functionalities and structural units have been employed as noncleavable transition-state isosteres in aspartic protease inhibitors, e.g., statines, reversed statines, norstatines, reduced amide, hydroxyethylenes, hydroxyethylamines, hydroxyethyl-

piperazine, hydroxypropylamines, and dihydroxyethylene (N-duplicated and C-duplicated) (Figure 2.8).

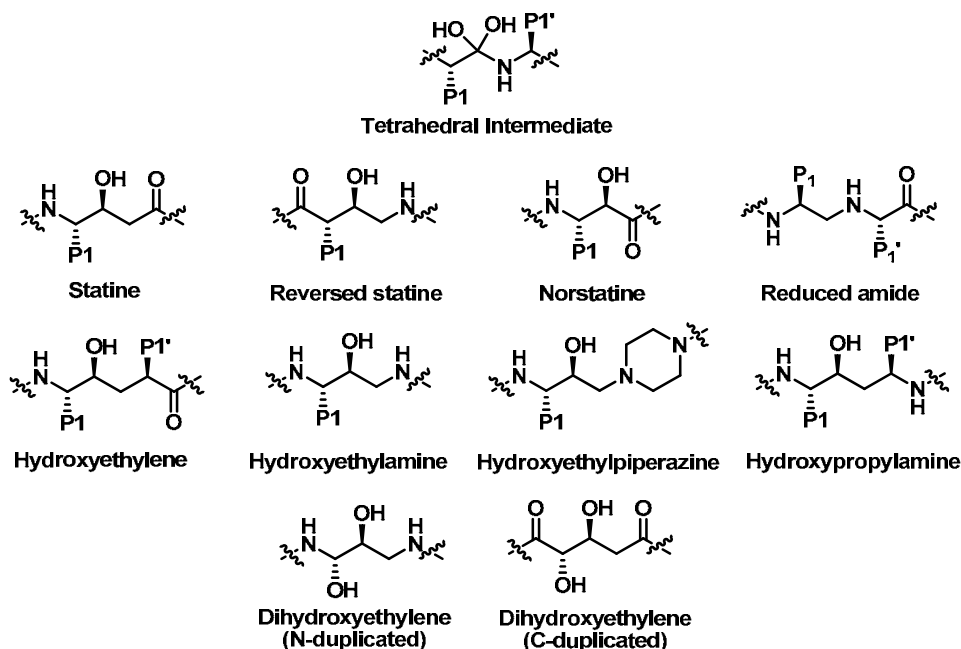


Figure 2.8 Transition-state analog units (TSA) in peptidomimetic inhibitors.

Since HIV-1 protease (HIV-1 PR) is also an aspartic protease enzyme, several HIV-1 PR inhibitors are designed by using the transition-state analog units (TSA) as a core structure. Pepstatin A, hexa-peptide containing statine as a core structure (Figure 2.9), is a known potent peptidomimetic aspartic proteases inhibitor. It can inhibit HIV-1 PR, several Plms and also exhibits activity against cultured malaria parasites (2, 6). The binding inhibition constant, K_i , for HIV-1 PR, Plm I, II and IV have been reported to be 22 ± 1.6 nM, 0.39 nM, 0.006 nM and 0.020 nM, respectively (3, 38, 40, 41). The IC_{50} of pepstatin A for inhibition of parasite growth against *P. falciparum*-infected erythrocytes is 4.00 μ M. Some HIV-1 PR inhibitors, currently used in AIDS patients, i.e., saquinavir, ritonavir and lopinavir (Figure 2.9) have demonstrated activity against Plm II and can directly inhibit the *in vitro* growth of both drug-sensitive and drug-resistant *P. falciparum* parasites (7, 8). Lopinavir is the most active against *P. falciparum* and also inhibits Plm II with IC_{50} value in range 0.9-2.1 μ M and 2.7 μ M, respectively (7). These findings indicate that HIV-1 PR inhibitors may aid in the removal of Plasmodium parasite and used as antimalarial drugs (7, 8).

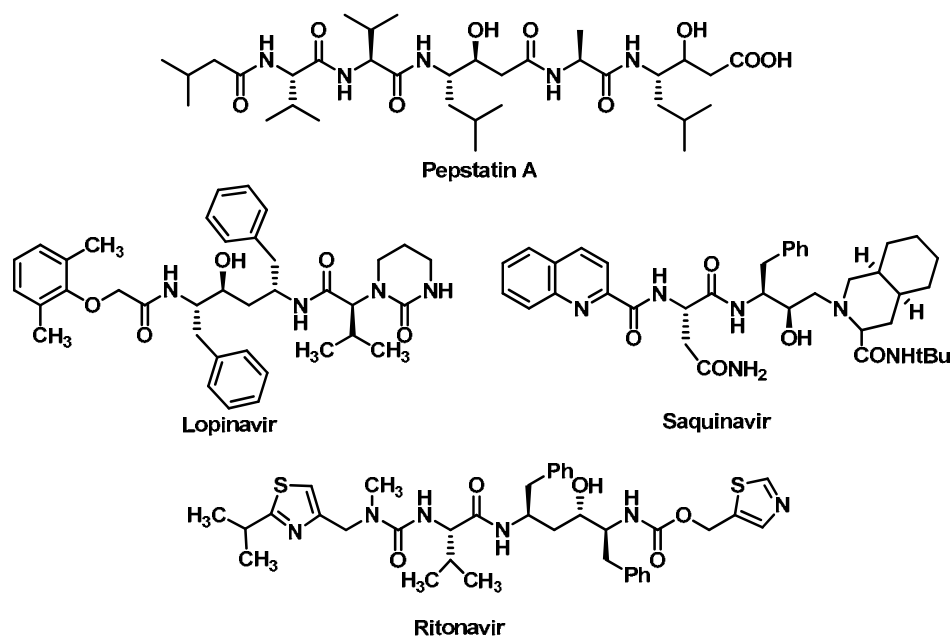


Figure 2.9 Peptidomimetic aspartic protease inhibitors, pepstatin A, lopinavir, saquinavir and ritonavir.

However, peptidomimetic inhibitors normally exhibit low bioavailability due to their high molecular weight, poor solubility and synthetic difficulties. Therefore, the non-peptidomimetic inhibitors are more interesting for developing as the new aspartic protease inhibitors. In our search for new potent non-peptidomimetic aspartic protease inhibitors, we concentrate on flavonoids or chromone compounds (Figure 2.10). Flavonoids are natural phenyl-substituted chromones that produce a wide range of biological activities beneficial for human health (9).

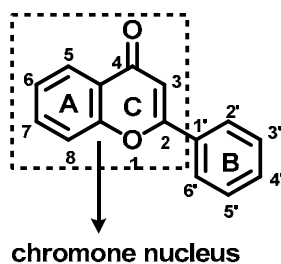


Figure 2.10 General flavonoid structure.

3) Flavonoids as aspartic protease inhibitors and antimalarial agents

Flavonoids are a ubiquitous group of secondary metabolites compounds with a wide distribution in fruits and vegetables (42, 43). They exert a number of biological activities such as antiviral, antibacterial, antiprotozoal, antioxidant, antiinflammatory and antimutagenic activities, and are also capable of inhibiting many types of enzymes (44). Furthermore, some naturally flavonoids have been reported that they can exhibit the antimalarial activity against *P. falciparum* (10). Compounds from four classes of flavonoids (flavanone, isoflavone, flavonols and flavones) were tested against a chloroquine-sensitive (3D7) and a chloroquine-resistant (7G8) *P. falciparum* strains (Figure 2.11). From this investigation, eight compounds (except acacetin, naringenin and genistein) showed antimalarial activity against the 3D7 strain, with IC₅₀ values in the range of 11-66 µM (10). All of them showed measurable activity against the 7G8 strain, with IC₅₀ values between 12 and 76 µM (10). The most active compound in both strains was luteolin with IC₅₀ values of 11 ± 1 µM and 12 ± 1 µM for 3D7 and 7G8 respectively (10). Moreover, luteolin was investigated which stage of the parasite's intraerythrocytic life cycle was inhibited. The result showed that luteolin did not inhibit the ring stage of the parasite but prevented the progression of parasite growth beyond the young trophozoite stage as shown in Figure 2.12. As a consequence the parasites were unable to complete a full intraerythrocytic cycle (10).

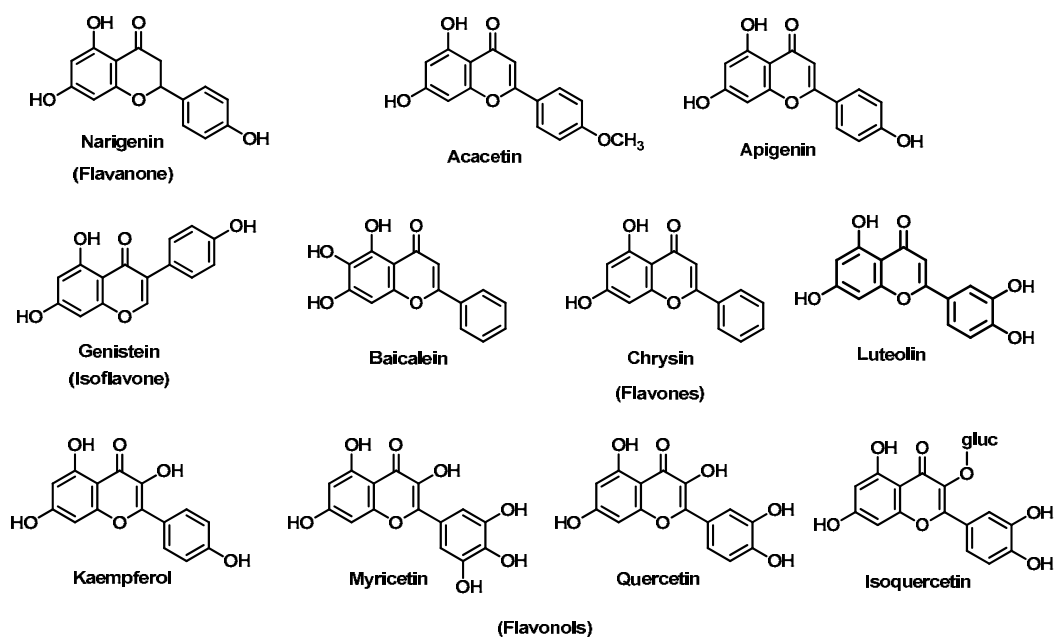


Figure 2.11 Structure of flavonoid compounds with antimalarial activity (10).

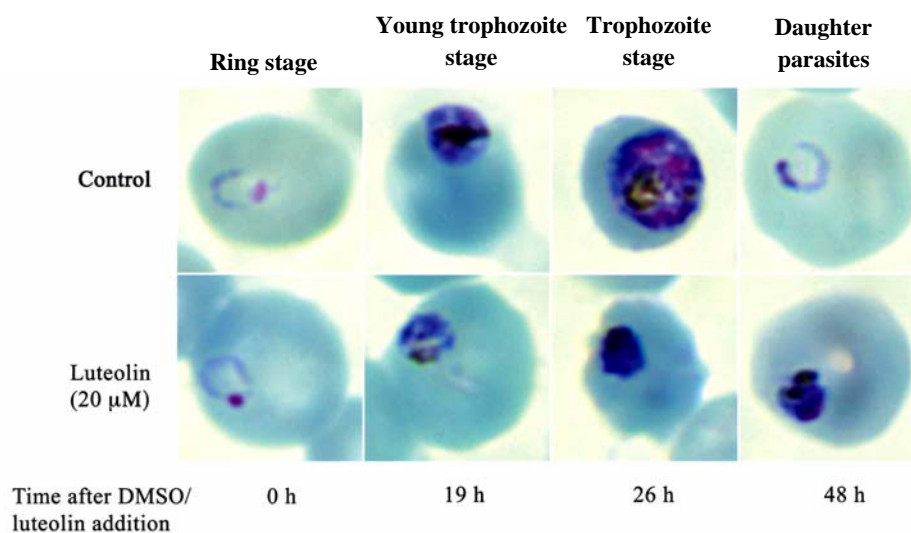


Figure 2.12 The effect of luteolin of the intraerythrocytic growth of *P. falciparum* (10).

Two flavones, 5,7,4'-trimethoxyflavone and 5,7,3',4'-tetramethoxyflavone (Figure 2.13) isolated from the rhizome of *Kaempferia parviflora* in the northeast of Thailand, exhibited antimalarial activity against *P. falciparum* K1 multidrug resistant strain. The assay was performed with the microdilution radioisotope technique with IC_{50} values of 3.70 and 4.06 $\mu\text{g/ml}$ for 5,7,4'-trimethoxyflavone and 5,7,3',4'-tetramethoxyflavone respectively (11). The *in vitro* antimalarial activity of dehydrosilybin and 8-(1;1)-dimethylallyl-kaempferide has been evaluated by real time PCR for five *P. falciparum* strains. Both flavonoids revealed significant antimalarial activity against the different strains with IC_{50} values ranging from 1.7-23.9 μM and 2.1-10.1 μM for dehydrosilybin and 8-(1;1)-dimethylallyl-kaempferide respectively (12) (Figure 2.13).

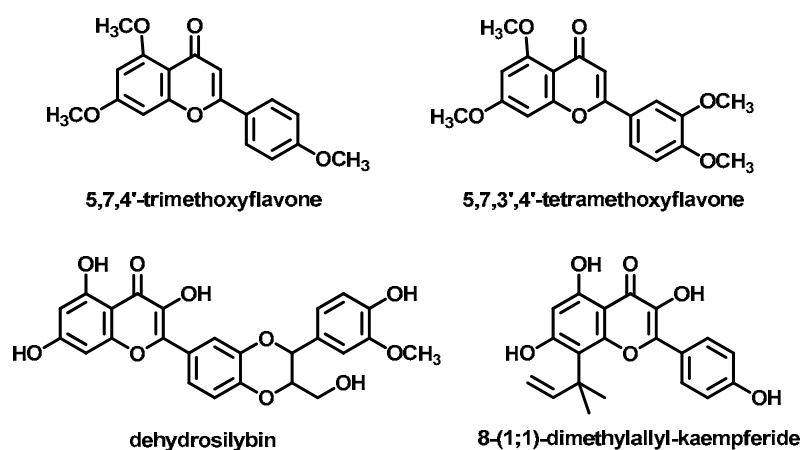


Figure 2.13 Some naturally flavonoids which exhibited antimalarial activity.

A series of flavonoid derivatives containing a piperazinyl chain have been synthesized and tested for their antiplasmodial activity against chloroquine-sensitive (Thai strain) and chloroquine-resistant (FcB1, K1 strains) *P. falciparum* strains. The three most active compounds (compounds 1, 31, 36) which had a N-(2,3,4-trimethoxybenzyl)-N-ethanoyl-piperazine chain attached to the flavone at the 7-phenol group (Figure 2.14), showed the IC_{50} values in micromolar to submicromolar range and showed non-cytotoxicity upon the mammalian cells MCR5 (13).

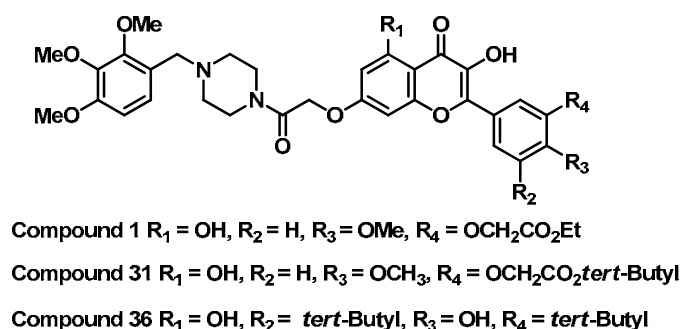


Figure 2.14 Structure of flavonoid derivatives containing a piperazinyl chain (13).

From the previous study of chromone derivatives as HIV-1 PR inhibitors, forty-six chromone derivatives with a benzopyran-4-one scaffold have been synthesized and evaluated the *in vitro* inhibitory activity against HIV-1 PR using stop time HPLC method as the preliminary screening (9). The inhibitory activity of these compounds was in range of 10-97 % inhibition. The three most potent inhibitors were chromones **31**, **35** and **26** with $\text{IC}_{50} = 0.34$, 0.65 and $2.53 \mu\text{M}$, respectively (Figure 2.15). It was found that IC_{50} of the most active chromone compound (chromone **31**) is 4-fold lower potency than amprenavir ($\text{IC}_{50} = 0.084 \mu\text{M}$) (14). Therefore, these forty-six chromone derivatives were selected to investigate their inhibitory activity against Plm II in this study.

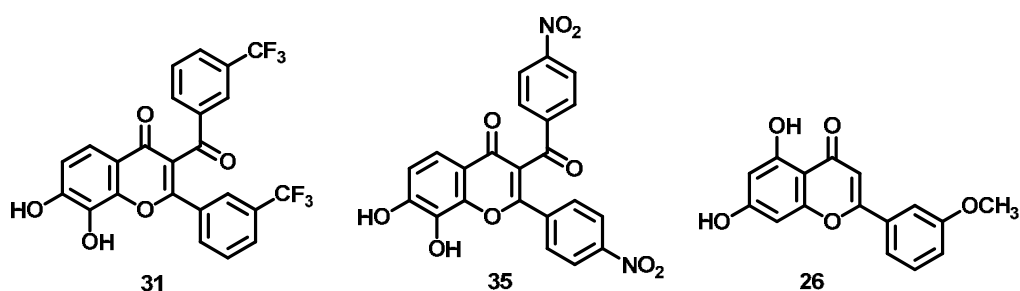


Figure 2.15 The three most active HIV-1 PR inhibitors in chromone series.

2.3 Antimalarial activity assay

All several antimalarial activity *in vitro* assays are based on the measurement of the effect of drugs or testing compounds on the growth and multiplication of malaria parasites. The assay systems can be classified into three groups according to the methods used to quantify malaria parasite growth in relation to drug concentrations. First method is direct, visual counting of the schizonts stage of malaria parasites against the total number of parasites under a microscope. This assay is a simple method to evaluate the parasites growth inhibition. However, microscopic or visual examination method is generally not popular due to it requires highly trained personnel to limit individual variability in counting and assessing the developmental stages of the parasites. Second method is incorporation of radioisotope precursors into the parasites for determination of the level of malaria parasites growth inhibition. The last one is non-radioactive methods, i.e., parasite lactate dehydrogenase (pLDH) enzymatic assay and histidine-rich protein II (HRP2) assay. The common *in vitro* assays for evaluation the inhibition of the parasites growth and their development are summarized in Table 2.3 (45). Among these assays, the radioisotope assay is a well suited method to screen the antimalarial candidate compounds. Due to the radioisotope assay use the fewer periods for culture and drug incubation and the results are assessed by the automatic equipment, this assay is one of rapid, suitable, sensitive and precise method (15, 45).

The radioisotope assay is an *in vitro* assay based on the incorporation of [³H]-hypoxanthine to determine the level of *P. falciparum* growth. [³H]-hypoxanthine is taken up by malaria parasite for purine salvage and DNA synthesis. The uptake amounts of radiolabeled hypoxanthine are an indicator of parasites growth and their multiplication. Incorporation of [³H]-hypoxanthine is quantified with a liquid β -scintillation counter as the signal count per minute (CPM). The percentage of inhibition of parasite growth is calculated using the signal count per minute of treated (CPM_T) and untreated conditions (CPM_U), as the following formula.

$$\% \text{ inhibition of parasite growth} = 100 \times (\text{CPM}_U - \text{CPM}_T) / \text{CPM}_U$$

The percentage of inhibition of parasite growth is used to plot as a function of drug concentration. The inhibition concentration which killed 50% of parasites (IC₅₀ value) is usually determined by linear regression analyses on the linear segments of dose response curve (46).

Table 2.3 The commonly used *in vitro* antimalarial activity assay.

<i>In vitro</i> assays	Equipment	The activity assessment
Microscopic or visual examination method	Microscope	Counting the schizonts stage of the malaria parasite against the total number of parasites.
Radioisotope method	Scintillation counter	Measuring the uptake amounts of [³ H]-hypoxanthine, which correspond with the malaria parasite growth.
pLDH ^a enzymatic assay	Spectrophotometry micro plate reader	Measuring the enzymatic activities of pLDH that correspond to the parasite viability.
HRP2 ^a assay	ELISA plate reader	Measuring the production of HRP2 that is related with the parasite growth and development.

^apLDH (parasite lactate dehydrogenase), HRP2 (histidine-rich protein II)

CHAPTER III

MOLECULAR MODELING EXPERIMENTAL

3.1 Materials

1) Computers

Internet network, silicon graphics SGI Iris R800

Silicon graphic SGI O2 Webforce R5000 SC

Personal computer (PC) Intel core 2 duo

2) Softwares

AutoDock 4.0 for Windows (The Scripps Research Institute, USA)

SYBYL software version 8.0

EditPlus Text Editor version 2.30 (ES-computing, South Korea)

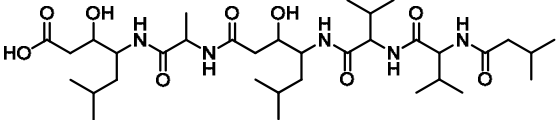
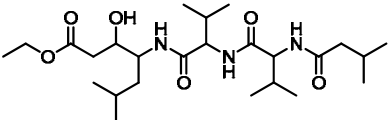
PyMol Molecular Graphics System version 1.3 (Schrodinger, USA)

3.2 Methods

1) Preparation and Validation of Plm II template

Two x-ray crystal structures of Plm II bound to inhibitors (PDB code 1SME and 1ME6) were obtained from the Brookhaven Protein Database (<http://www.rcsb.org>) for using as the protein template (Table 3.1). The protein templates were prepared for docking study by removing all the native ligand structures and all water molecules from the complex structures. The polar hydrogen atoms were added and Gasteiger charges were assigned to protein atoms.

Table 3.1 The structure of ligands complexed in the crystal structures of Plm II.

PDB code	Ligand	Structure	Resolution
1SME	IHN		2.7 Å
1ME6	IVS		2.7 Å

To ensure that the ligand orientations and positions obtained from the docking studies were likely to represent valid and reasonable potential binding modes of the inhibitors, the Plm II template was validated by re-docking and cross-docking experiments. First, each ligand (IHN and IVS) was docked into the orientation and position of the ligand observed in the crystal structures. Second, cross-docking of each ligand into the nonnative protein was undertaken. The grid maps for each atom type in the ligands (A, C, HD, N, NA, OA, S, SA, F, and Cl)¹ and docking parameters were set and calculated with AutoGrid 4 and AutoDock 4 respectively. All of parameters used in template validation were shown in Table 3.2. These grid map parameters and docking parameters were used for further Plm II docking experiment. The root mean square deviation (RMSD) values were obtained from the best cluster conformation of the re-docking and cross-docking validation of Plm II. The Plm II protein template which showed the lowest RMSD values, was selected for further docking studies of chromone derivatives against Plm II.

¹Atom type: A (aromatic); C (carbon); HD (hydrogen donor); N (nitrogen); NA (nitrogen acceptor); OA (oxygen acceptor); S (sulfur); SA (sulfur acceptor); F (fluorine); Cl (chlorine)

Table 3.2 Grid parameters and docking parameters.

Parameter	
Number of point in x, y, z dimensions	40:54:40
Spacing (Å)	0.375
Grid center	center on ligand
Number of GA run	100
Population size	150
Maximum number of energy evaluations	2500000
Rate of gene mutation	0.02
Rate of crossover	0.8

2) Ligand preparation

The 3D molecular structures of all chromone compounds were modeled with SYBYL 8.0 molecular modeling program (Tripos Associates, Saint Louis, MO) on an Indigo Elan workstation (Silicon Graphics Inc., Mountain View, CA) using the sketch approach. Each structure was energy minimized using the standard Tripos force field (Powell method and 0.05 kcal/mole Å energy gradient convergence criteria) and electrostatic charge was assigned by the Gasteiger-Hückel method. These conformations were used as starting conformations to perform docking simulation.

3) Docking studies of chromone derivatives with Plm II

The preliminary screening of Plm II inhibitory activity of the previously synthesized forty-six chromone derivatives which have been evaluated for HIV-1 PR inhibitory activity was performed by AutoDock 4.0 on Garibaldi platform at The Scripps Research Institute. The docking results of each series of the chromone derivatives were ranked by their binding energy against Plm II and were filtered with % inhibition against HIV-1 PR. Twenty chromone compounds which showed good binding energy with Plm II from docking study and high inhibitory activity against HIV-1 PR (more than 70 % inhibition) were selected from 3-rings system (R_2 = substituted phenyl, R_3 = H, CH₃; chromones **1-30**) and 4-rings system (R_2 = substituted phenyl, R_3 = substituted benzoyl; chromones **31-46**). The entire twenty

compounds were evaluated for antimalarial activity against *P. falciparum* by microculture radioisotope technique.

4) Structural modification of chromone derivatives as Plm II inhibitors

The new chromone structures were designed to obtain better binding energy. The new chromone derivatives with hydroxyl groups at positions 6 and 7 of chromone structure were designed and performed docking with Plm II. The docking study was performed to find out whether these compounds exhibited better binding energy than the chromone compounds in the 3-rings system series (chromones **1-30**). Subsequently, the structures of chromone derivatives were modified by adding the steric groups at both of hydroxyl group of the chromone structure. Seventy-two modified chromone structures were docked to preliminary evaluate their Plm II inhibitory activity. The binding energy and binding mode of each chromone compound were analyzed to explore the interaction between the chromone structure and amino acid residues in the active binding site of Plm II. Finally, nine modified chromone derivatives were identified from the docking study and were selected to synthesize and evaluate for antimalarial activity against *P. falciparum*.

CHAPTER IV

CHEMICAL EXPERIMENTAL

4.1 Equipment and chemicals

1) Equipments

Analytical balance model 2842	Sartorius, Germany
FTIR (FTIR 6700)	Nicolet, USA
Magnetic stirrer (MR 3001K)	Heidolph, Germany
Mass spectrometer (ESI, microTOF)	Bruker, Switzerland
Mass spectrometer (ESI, LCQ Fleet)	Thermo, USA
Melting point apparatus (Model 9100)	Electrothermal, UK
Nuclear Magnetic Resonance (NMR) spectrometer	Bruker, Switzerland
Rotary evaporator	Buchi, Switzerland

2) Chemicals

Acetic acid	Labscan, Thailand
Acetone	Honeywell B&J, USA
Aluminium chloride	Fluka, USA
Benzyl bromide	Aldrich, USA
Chlorobenzene	Carlo Erba, Italy
3-Chlorobenzoyl chloride	Aldrich, USA
4-Chlorobenzoyl chloride	Aldrich, USA
DBU (1,8-diazabicyclo[5,4,0]undec-7-ene)	Fluka, Switzerland
3,4-Dichlorobenzoyl chloride	Aldrich, USA
Dichloromethane	Labscan, Thailand
Dimethylformamide	Labscan, Thailand
3,4-Dimethoxybenzoic acid	TCI, Japan
3,5-Dinitrobenzoyl chloride	Aldrich, China

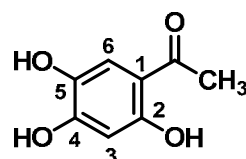
EDAC.HCl [1-Ethyl-3-(3'-dimethylaminopropyl) carbodiimide.HCl]	AK Scientific, USA
Ethyl acetate	Honeywell B&J, USA
Hexane	Honeywell B&J, USA
HOBt (Hydroxylbenzotriazole)	AK Scientific, USA
Hydrochloric acid	E. Merck, Germany
Methanol	Honeywell B&J, USA
3-Methoxybenzoyl chloride	Aldrich, USA
4-Methoxybenzoyl chloride	Aldrich, USA
3-Nitrobenzoyl chloride	Aldrich, USA
4-Nitrobenzoyl chloride	Aldrich, USA
Potassium carbonate anhydrous	Carlo Erba, France
Sea sand	Panreac, Barcelona
Silica gel F ₂₅₄ (0.2 mm)	Merck, Germany
Silica gel 60 No. 1.07734	Merck, Germany
Sodium sulfate anhydrous	Merck, Germany
Sulfuric acid	Merck, Germany
TEA (Triethylamine)	Fisher Scientific, UK
2,4,5-Trimethoxyacetophenone	Aldrich, India

4.2 Methods

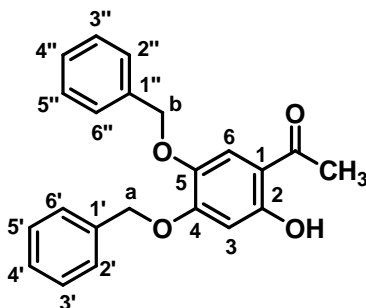
The structures of intermediates, chromone **49** and chromone **49a-49i** were elucidated by melting point, infrared (IR), nuclear magnetic resonance (¹H-NMR) and mass spectrometry (MS). Melting points of these compounds were determined on an Electrothermal model 9100 capillary melting point apparatus. Infrared (IR) spectra were run on FTIR Nicolet 6700 in 4000-400 cm⁻¹ using the potassium bromide pellet (KBr) technique. Proton nuclear magnetic resonance (¹H-NMR) spectra were obtained on an Advance 300 MHz NMR Spectroscopy (Bruker Switzerland). The NMR solvents used were deuterated dimethylsulfoxide (DMSO-d₆, δ (CH₃)₂SO = 2.50 ppm, absorbed water H₂O = 3.33 ppm), deuterated methanol (CD₃OD, δ CH₃OH = 3.31, 4.78 ppm, absorbed water H₂O = 4.90 ppm) and deuterated chloroform (CDCl₃, δ

$\text{CHCl}_3 = 7.25$ ppm, absorbed water $\text{H}_2\text{O} = 1.50$ ppm) (47). Low resolution mass spectrometer (LRMS, LCQ Fleet, Thermo) and high resolution mass spectrometer (HRMS, microTOF, Bruker) was applied to verify molecular weights of the synthesized compounds.

1) 2,4,5-Trihydroxyacetophenone

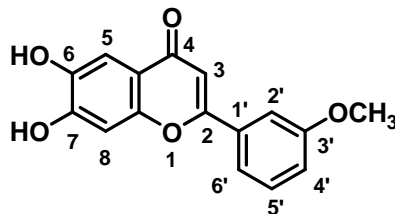


A solution of 2,4,5-trimethoxyacetophenone (4.00 g, 19.03 mmol) in chlorobenzene (20 mL) was treated with AlCl_3 (6.60 g, 49.47 mmol) at room temperature and then refluxed for 12 hours. Afterwards the solvent was evaporated. The residue was carefully hydrolyzed with cooled 1 M HCl (50 mL) and extracted with ethyl acetate (3 x 50 mL). The organic layer was washed with water (2 x 50 mL), dried over with sodium sulfate anhydrous, and filtered. After evaporation, the crude product was purified by column chromatography (methanol/dichloromethane [0.5:9.5]) to provide 2,4,5-trihydroxyacetophenone as the pale yellow solid (2.42 g, 75.87 %); m.p. 206-207 °C; FTIR (KBr) (cm^{-1}): 3405, 3238 (O-H st.), 1634 (C=O st.) 1589, 1536 (C=C st.), 1300, 1211, 1135 (C-O st.); $^1\text{H-NMR}$ 300 MHz (CD_3OD): δ 2.46 (s, 3H, CH_3), 6.27 (s, 1H, H3), 7.14 (s, 1H, H6); HRMS (ESI) m/z calcd. for $\text{C}_8\text{H}_8\text{O}_4$, 168.0428 $[\text{M}]^+$, 167.0350 $[\text{M-H}]^+$; found 167.0356 $[\text{M-H}]^+$; TLC (silica gel GF 254, methanol/dichloromethane [0.5:9.5]). R_f of 2,4,5-trimethoxyacetophenone = 0.82, 2,4,5-trihydroxyacetophenone = 0.29.

2) 4,5-Bisbenzyloxy-2-hydroxyacetophenone

To a solution of 2,4,5-trihydroxyacetophenone (1.50 g, 8.93 mmol) in acetone (24 mL) was added anhydrous potassium carbonate (2.22 g, 16.07 mmol), and the mixture was stirred at room temperature for 10 min. Then benzyl bromide was added and the mixture was refluxed for 5 hours. After cooling to room temperature, the solvent was evaporated and water was added to the residue. The aqueous mixture was extracted with ethyl acetate (3 x 40 mL). The combine organic layer was washed with water (2 x 40 mL), dried over with sodium sulfate anhydrous, and filtered. After removing the solvent, the crude product was purified by column chromatography (ethyl acetate/hexane [1:4]) to provide 4,5-bisbenzyloxy-2-hydroxy-acetophenone as the white solid (2.18 g, 70.19 %); m.p. 99-100 °C; FTIR (KBr) (cm^{-1}): 3065, 3037 (aromatic C-H st.), 2867 (aliphatic C-H st.), 1633 (C=O st.), 1510, 1455 (C=C st.), 1370 (C-H bending), 1263, 1210, 1166 (C-O st.); $^1\text{H-NMR}$ 300 MHz (CDCl_3): δ 2.48 (s, 3H, CH_3), 5.10 (s, 2H, Hb), 5.21 (s, 2H, Ha), 6.54 (s, 1H, H3), 7.19 (s, 1H, H6), 7.34-7.48 (m, 10H, H2', H3', H4', H5', H6', H2'', H3'', H4'', H5'', H6''); LRMS (ESI) m/z $[\text{M}+\text{Na}]^+$ 371.29 (46.0), 280.20 (100.0), 189.29 (10.0); TLC (silica gel GF 254, ethyl acetate/hexane [1:1]). R_f of 2,4,5-trihydroxy acetophenone = 0.23, 4,5-bisbenzyloxy-2-hydroxyacetophenone = 0.62.

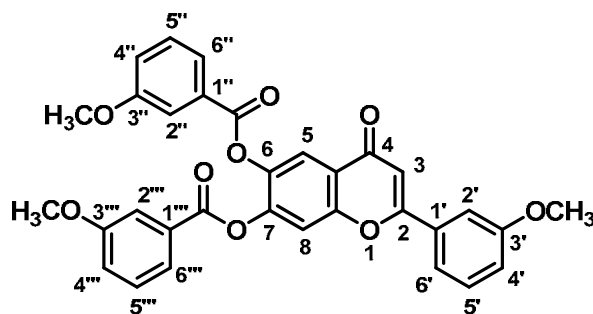
3) 6,7-Dihydroxy-2-(3'-methoxyphenyl) chromone, **49**.



The Baker-Venkataraman rearrangement was performed by added potassium carbonate anhydrous (1.90 g, 13.79 mmol) to a solution of 4,5-bisbenzyloxy-2-hydroxyacetophenone (1.20 g, 3.45 mmol) in acetone (25 mL), and the mixture was stirred at room temperature for 20 min. Then 3-methoxybenzoyl chloride (0.56 mL, 4.14 mmol) was added dropwise, and the mixture was refluxed for 24 hours. Afterward the reaction mixture was allowed to room temperature, the solvent was evaporated and water was added to the residue. The aqueous mixture was extracted with ethyl acetate (3 x 40 mL). The organic layer was washed with water (2 x 40 mL), dried over anhydrous sodium sulfate, and filtered. After removing the solvent, the yellow residue of 1,3-diketone was obtained.

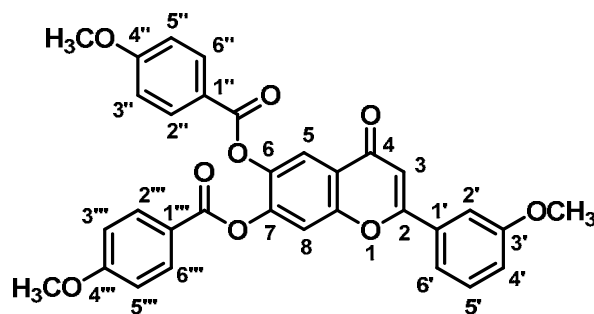
To a mixture of 1,3-diketone in glacial acetic acid (20 mL) was added concentration sulfuric acid (0.28 mL), and the mixture was refluxed at 120 °C for 4 hours. Subsequently, the reaction mixture was poured into cool water and extracted with ethyl acetate (3 x 40 mL). The organic layer was washed with water (2 x 40 mL), dried over with sodium sulfate anhydrous, filtered and solvent was evaporated. The crude product was purified by column chromatography (ethyl acetate/hexane [3:2]) to provide pure compound as the pale yellow solid (547.4 mg, 55.89 %); m.p. 246-247 °C; FTIR (KBr) (cm⁻¹): 3495 (O-H st.), 3092 (aromatic C-H st.), 1630 (C=O st.), 1602, 1590, 1471 (C=C st.), 1346 (C-H bending), 1293, 1145 (C-O st.); ¹H-NMR 300 MHz (DMSO-d₆): δ 3.84 (s, 3H, OCH₃), 6.85 (s, 1H, H₃), 7.03 (s, 1H, H₈), 7.12 (dd, *J* = 8.00, 2.35 Hz, 1H, H_{4'}), 7.28 (s, 1H, H₅), 7.45 (t, *J* = 8.00 Hz, 1H, H_{5'}), 7.52 (s, 1H, H_{2'}), 7.59 (d, *J* = 8.00 Hz, 1H, H_{6'}); HRMS (ESI) *m/z* calcd. for C₁₆H₁₂O₅, 284.0681 [M]⁺, 285.0759 [M+H]⁺; found 285.0755 [M+H]⁺; TLC (silica gel GF 254, ethyl acetate/hexane [3.5:1.5]). R_f of 4,5-bisbenzyloxy-2-hydroxyacetophenone = 0.75, chromone **49** = 0.19.

4) 6-(3''-Methoxybenzoate)-7-(3'''-methoxybenzoate)-2-(3'-methoxy-phenyl) chromone, 49a.



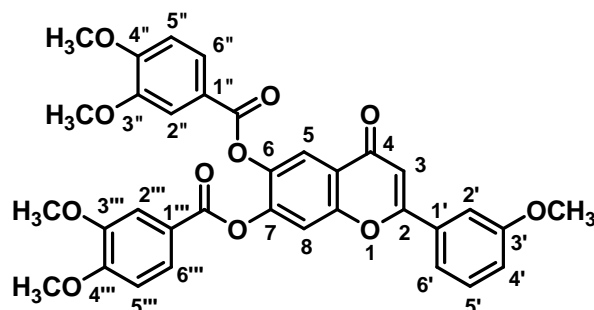
To a solution of chromone **49** (80.0 mg, 0.28 mmol) in 5 mL of dry dimethylformamide (DMF) was added DBU (0.12 mL, 0.77 mmol), and the mixture was stirred at room temperature for 15 min. Then 3-methoxybenzoyl chloride (0.09 mL, 0.63 mmol) was added dropwise, and the reaction mixture was stirred at room temperature for 1 hour and then poured into water (25 mL). The aqueous mixture was filtered. The residue was washed with water (100 mL) and ethylacetate (20 mL) to afford white solid. The white solid residue was purified by column chromatography (ethyl acetate/dichloromethane [0.5:9.5]) to provide pure chromone **49a** as the white powder (90.7 mg, 57.26 %); m.p. 197-198 °C; FTIR (KBr) (cm⁻¹) : 3076 (aromatic C-H st.), 2962, 2835 (aliphatic C-H st.), 1742, 1654 (C=O st.), 1604, 1489 (C=C st.), 1449, 1347 (C-H bending), 1274, 1221, 1147 (C-O st.); ¹H NMR 300 MHz (CDCl₃): δ 3.73 (s, 3H, OCH₃), 3.84 (s, 3H, OCH₃), 3.93 (s, 3H, OCH₃), 6.86 (s, 1H, H₃), 7.12-7.18 (m, 3H, H_{4'}, H_{4''}, H_{4'''}), 7.26-7.38 (m, 2H, H_{5''}, H_{5'''}), 7.45-7.60 (m, 5H, H_{2'}, H_{5'}, H_{6'}, H_{2''}, H_{2'''}), 7.69 (d, *J* = 7.61 Hz, 1H, H_{6''}), 7.74 (d, *J* = 7.61 Hz, 1H, H_{6'''}) 7.81 (s, 1H, H₈), 8.23 (s, 1H, H₅); LRMS (ESI) *m/z* (relative intensity): [M+H]⁺ 553.36 (100.0), 510.01 (51.0), 401.15 (95.0), 269.10 (62.0); HRMS (ESI) *m/z* calcd. for C₃₂H₂₄O₉, 552.1413 [M]⁺, 575.1311 [M+Na]⁺; found 575.1323 [M+Na]⁺; TLC (silica gel GF 254, ethyl acetate/hexane [3.5:1.5]). R_f of chromone **49** = 0.19, chromone **49a** = 0.60.

5) 6-(4''-Methoxybenzoate)-7-(4'''-methoxybenzoate)-2-(3'-methoxy-phenyl) chromone, 49b.



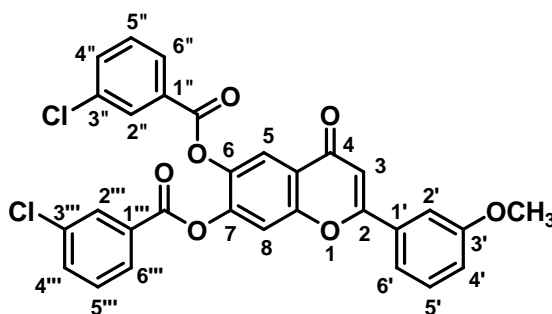
Chromone **49b** was synthesized using the same procedure as described for chromone **49a** from 4-methoxybenzoyl chloride (0.09 mL, 0.68 mmol), DBU (0.10 mL, 0.70 mmol) and chromone **49** (80.0 mg, 0.28 mmol). After the reaction and purification by column chromatography (ethyl acetate/dichloromethane [0.5:9.5]), the desired chromone **49b** was obtained as a white powder (84.5 mg, 54.35 %); m.p. 201-202 °C; FTIR (KBr) (cm^{-1}): 3068 (aromatic C-H st.), 2945, 2831 (aliphatic C-H st.), 1733, 1655 (C=O st.), 1607, 1511 (C=C st.), 1451, 1370 (C-H bending), 1256, 1175, 1161, 1063 (C-O st.); $^1\text{H-NMR}$ 300 MHz (CDCl_3): δ 3.84 (s, 3H, OCH_3), 3.86 (s, 3H, OCH_3), 3.90 (s, 3H, OCH_3), 6.83 (s, 1H, H3), 6.83-6.86 (m, 2H, H3'', H5''), 6.89 (d, J = 8.97 Hz, 2H, H3''', H5'''), 7.07-7.10 (m, 1H, H4'), 7.41-7.46 (m, 2H, H2', H5'), 7.50 (d, J = 7.92 Hz, 1H, H6'), 7.74 (s, 1H, H8), 8.00 (d, J = 8.97 Hz, 2H, H2'', H6''), 8.05 (d, J = 8.96 Hz, 2H, H2''', H6'''), 8.17 (s, 1H, H5); LRMS (ESI) m/z (relative intensity): $[\text{M}+\text{H}]^+$ 553.18 (100.0), 510.35 (16.0), 401.45 (46.0); HRMS (ESI) m/z calcd. for $\text{C}_{32}\text{H}_{24}\text{O}_9$, 552.1413 $[\text{M}]^+$, 575.1311 $[\text{M}+\text{Na}]^+$; found 575.1334 $[\text{M}+\text{Na}]^+$; TLC (silica gel GF 254, ethyl acetate/hexane [3.5:1.5]). R_f of chromone **49** = 0.19, chromone **49b** = 0.57.

6) 6-(3'',4''-Dimethoxybenzoate)-7-(3''',4'''-dimethoxybenzoate)-2-(3'-methoxyphenyl) chromone, 49c.



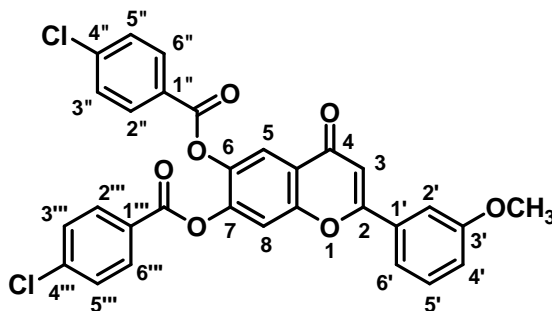
The mixture of 3,4-dimethoxybenzoic acid (0.12 g, 0.68 mmol), EDAC.HCl (0.13 g, 0.68 mmol), HOBt (0.08 g, 0.56 mmol) was stirred in dichloromethane (3 mL) at room temperature for 15-30 min. To this mixture, chromone **49** (80 mg, 0.28 mmol) in dry dimethylformamide (3 mL) was added. Then, TEA (0.09 mL, 0.68 mmol) was added as a catalyst and the reaction mixture was allowed to stir at room temperature for 4 hours. Afterward, the reaction mixture was poured into water and extracted with dichloromethane (3 x 20 mL). The combined organic layers were washed with water (2 x 20 mL), dried over with sodium sulfate anhydrous, filtered and removed organic solvent. The crude product was purified by column chromatography (ethyl acetate/dichloromethane [0.5:9.5]) to yield chromone **49c** as the white powder (95.5 mg, 55.42 %); m.p. 188-189 °C; FTIR (KBr) (cm⁻¹): 3076 (aromatic C-H st.), 2925, 2831 (aliphatic C-H st.), 1742, 1654 (C=O st.), 1602, 1517 (C=C st.), 1453, 1347 (C-H bending), 1295, 1271, 1218, 1172, 1145, 1084 (C-O st.); ¹H-NMR 300 MHz (CDCl₃): δ 3.78 (s, 3H, OCH₃), 3.86 (s, 3H, OCH₃), 3.92 (s, 3H, OCH₃), 3.94 (s, 3H, OCH₃), 3.96 (s, 3H, OCH₃), 6.83-6.86 (m, 1H, H5''), 6.86 (s, 1H, H3) 6.88 (d, *J* = 8.50 Hz, 1H, H5'''), 7.10-7.13 (m, 1H, H4'), 7.44-7.49 (m, 2H, H2', H5'), 7.52-7.54 (m, 2H, H6', H2''), 7.58 (d, *J* = 2.00 Hz, 1H, H2'''), 7.75 (dd, *J* = 8.48, 1.97 Hz, 1H, H6''), 7.79 (s, 1H, H8), 7.80 (dd, *J* = 8.50, 2.00 Hz, 1H, H6'''), 8.21 (s, 1H, H5); LRMS (ESI) *m/z* (relative intensity): [M+H]⁺ 613.35 (100.0), 583.57 (50.0), 307 (59.0), 305 (74.0); HRMS (ESI) *m/z* calcd. for C₃₄H₂₈O₁₁, 612.1623 [M]⁺, 635.1521 [M+Na]⁺; found 635.1557 [M+Na]⁺; TLC (silica gel GF 254, ethyl acetate/hexane [3.5:1.5]). R_f of chromone **49** = 0.19, chromone **49c** = 0.49.

7) 6-(3''-Chlorobenzoate)-7-(3'''-chlorobenzoate)-2-(3'-methoxyphenyl) chromone, 49d.



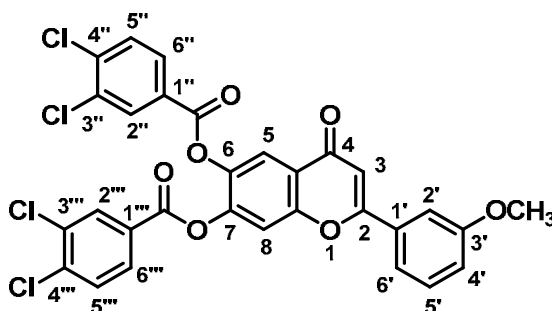
Chromone **49d** was synthesized using the same procedure as described for chromone **49a** from 3-chlorobenzoyl chloride (0.09 mL, 0.68 mmol), DBU (0.10 mL, 0.70 mmol) and chromone **49** (80.0 mg, 0.28 mmol). After the reaction and purification by column chromatography (ethyl acetate/dichloromethane [0.5:9.5]), the desired chromone **49d** was obtained as a white powder (64.8 mg, 41.00 %); m.p. 211-212 °C; FTIR (KBr) (cm^{-1}): 3071 (aromatic C-H st.), 2834 (aliphatic C-H st.), 1747, 1633 (C=O st.), 1608, 1572, 1486 (C=C st.), 1450, 1343 (C-H bending), 1255, 1242, 1146 (C-O st.); $^1\text{H-NMR}$ 300 MHz (CDCl_3): δ 3.91 (s, 3H, OCH_3), 6.85 (s, 1H, H3), 7.10 (ddd, $J = 7.96, 2.52, 1.22$ Hz, 1H, H4'), 7.33-7.42 (m, 2H, H5'', H5'''), 7.43-7.48 (m, 2H, H2', H5'), 7.51 (dt, $J = 7.86, 1.39$ Hz, 1H, H6'), 7.54-7.60 (m, 2H, H4'', H4'''), 7.79 (s, 1H, H8), 7.93-8.01 (m, 3H, H2'', H6'', H6'''), 8.06 (t, $J = 1.72$ Hz, 1H, H2'''), 8.22 (s, 1H, H5); LRMS (ESI) m/z (relative intensity): $[\text{M}+\text{H}]^+$ 561.73 (100.0), 405.39 (49.0); HRMS (ESI) m/z calcd. for $\text{C}_{30}\text{H}_{18}\text{O}_7\text{Cl}_2$, 560.0423 $[\text{M}]^+$, 583.0321 $[\text{M}+\text{Na}]^+$; found 583.0348 $[\text{M}+\text{Na}]^+$; TLC (silica gel GF 254, ethyl acetate/hexane [3.5:1.5]). R_f of chromone **49** = 0.19, chromone **49d** = 0.63.

8) 6-(4''-Chlorobenzoate)-7-(4'''-chlorobenzoate)-2-(3'-methoxyphenyl) chromone, 49e.



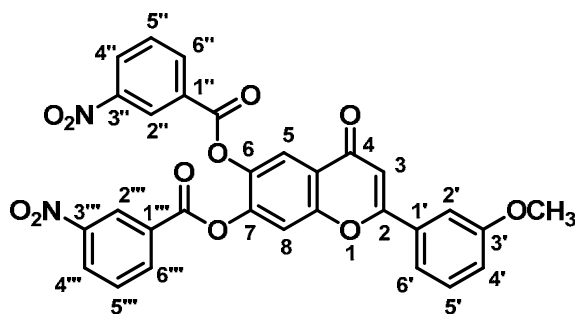
Chromone **49e** was synthesized using the same procedure as described for chromone **49a** from 4-chlorobenzoyl chloride (0.09 mL, 0.68 mmol), DBU (0.10 mL, 0.7042 mmol) and chromone **49** (80.0 mg, 0.28 mmol). After the reaction and purification by column chromatography (ethyl acetate/dichloromethane [0.5:9.5]), the desired chromone **49e** was obtained as a white powder (62.4 mg, 39.48 %); m.p. 251-252 °C; FTIR (KBr) (cm^{-1}): 3064 (aromatic C-H st.), 2925, 2834 (aliphatic C-H st.), 1749, 1650 (C=O st.), 1593, 1489 (C=C st.), 1450 (C-H bending), 1258, 1069 (C-O st.); $^1\text{H-NMR}$ 300 MHz (CDCl_3): δ 3.90 (s, 3H, OCH_3), 6.84 (s, 1H, H3), 7.10 (ddd, J = 7.91, 2.51, 1.23 Hz, 1H, H4'), 7.36-7.47 (m, 6H, H2', H5', H3'', H5'', H3''', H5'''), 7.51 (dt, J = 7.90, 1.40 Hz, 1H, H6'), 7.75 (s, 1H, H8), 7.98 (d, J = 8.67 Hz, 2H, H2'', H6''), 8.02 (d, J = 8.67 Hz, 2H, H2''', H6''') 8.19 (s, 1H, H5); LRMS (ESI) m/z (relative intensity): $[\text{M}+\text{H}]^+$ 561.68 (83.0), $[\text{M}]^+$ 560 (100.0) 405.29 (93.0); HRMS (ESI) m/z calcd. for $\text{C}_{30}\text{H}_{18}\text{O}_7\text{Cl}_2$, 560.0423 $[\text{M}]^+$, 583.0321 $[\text{M}+\text{Na}]^+$; found 583.0342 $[\text{M}+\text{Na}]^+$; TLC (silica gel GF 254, ethyl acetate/hexane [3.5:1.5]). R_f of chromone **49** = 0.19, chromone **49e** = 0.63.

9) 6-(3'',4''-Dichlorobenzoate)-7-(3''',4'''-dichlorobenzoate)-2-(3'-methoxy-phenyl) chromone, 49f.



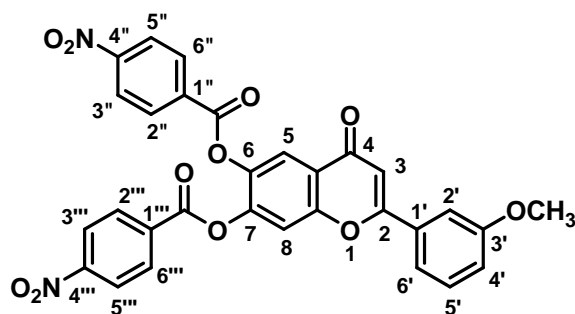
Chromone **49f** was synthesized using the same procedure as described for chromone **49a** from 3,4-dichlorobenzoyl chloride in dry dimethylformamide (0.14 g, 0.68 mmol), DBU (0.10 mL, 0.70mmol) and chromone **49** (80.0 mg, 0.28 mmol). After purification by column chromatography (ethyl acetate/dichloromethane [0.5:9.5]), the desired chromone **49f** was obtained as a white powder (66.7 mg, 37.58 %); m.p. 254-255 °C; FTIR (KBr) (cm⁻¹): 3072 (aromatic C-H st.), 2941, 2834 (aliphatic C-H st.), 1752, 1662 (C=O st.), 1625, 1491 (C=C st.), 1451, 1342 (C-H bending), 1270, 1238, 1077 (C-O st.); ¹H-NMR 300 MHz (CDCl₃): δ 3.84 (s, 3H, OCH₃), 6.78 (s, 1H, H₃), 7.02-7.06 (m, 1H, H_{4'}), 7.36-7.50 (m, 5H, H_{2'}, H_{5'}, H_{6'}, H_{5''}, H_{5'''}) 7.70 (s, 1H, H₈), 7.82 (dd, *J* = 8.40, 2.02 Hz, 1H, H_{6''}), 7.86 (dd, *J* = 8.40, 2.01 Hz, 1H, H_{6'''}), 8.03 (d, *J* = 2.02 Hz, 1H, H_{2''}), 8.09 (d, *J* = 2.01 Hz, 1H, H_{2'''}), 8.14 (s, 1H, H₅); LRMS (ESI) *m/z* (relative intensity): [M+H]⁺ 628 (100.0), 516.46 (79.0), 404.43 (10.0); HRMS (ESI) *m/z* calcd. for C₃₀H₁₆O₇Cl₄, 627.9643 [M]⁺, 650.9541 [M+Na]⁺; found 650.9589 [M+Na]⁺; TLC (silica gel GF 254, ethyl acetate/hexane [3.5:1.5]). R_f of chromone **49** = 0.19, chromone **49f** = 0.66.

10) 6-(3''-Nitrobenzoate)-7-(3'''-nitrobenzoate)-2-(3'-methoxyphenyl) chromone, 49g.



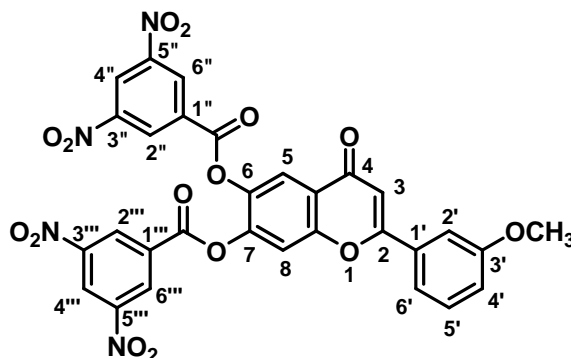
Chromone **49g** was synthesized using the same procedure as described for chromone **49a** from 3-nitrobenzoyl chloride in dry dimethylformamide (0.13 g, 0.70 mmol), DBU (0.10 mL, 0.70 mmol) and chromone **49** (80.0 mg, 0.28 mmol). After the reaction and purification by column chromatography (ethyl acetate/dichloromethane [0.5:9.5]), the desired chromone **49g** was obtained as a white powder (37.9 mg, 23.12 %); m.p. 225-226 °C; FTIR (KBr) (cm^{-1}): 3080 (aromatic C-H st.), 2941, 2834 (aliphatic C-H st.), 1754, 1660 (C=O st.), 1619, 1533 (C=C st.), 1451 (C-H bending), 1351 (C-N st.), 1255, 1145, 1109 (C-O st.); $^1\text{H-NMR}$ 300 MHz (CDCl_3): δ 3.91 (s, 3H, OCH_3), 6.86 (s, 1H, H3), 7.10-7.13 (m, 1H, H4'), 7.44-7.53 (m, 3H, H2', H5', H6'), 7.68 (t, $J = 7.66$ Hz, 1H, H5''), 7.70 (t, $J = 7.58$ Hz, 1H, H5'''), 7.85 (s, 1H, H8), 8.28 (s, 1H, H5), 8.42-8.49 (m, 4H, H4'', H4''', H6'', H6'''), 8.84 (t, $J = 1.86$ Hz, 1H, H2''), 8.90 (t, $J = 1.86$ Hz, 1H, H2'''); LRMS (ESI) m/z (relative intensity): $[\text{M}+\text{H}]^+$ 583.59 (98.0), $[\text{M}]^+$ 582.55 (100.0), 416.18 (48.0); HRMS (ESI) m/z calcd. for $\text{C}_{30}\text{H}_{18}\text{O}_{11}\text{N}_2$, 582.0905 $[\text{M}]^+$, 605.0803 $[\text{M}+\text{Na}]^+$; found 605.0852 $[\text{M}+\text{Na}]^+$; TLC (silica gel GF 254, ethyl acetate/hexane [3.5:1.5]). R_f of chromone **49** = 0.19, chromone **49g** = 0.60.

11) 6-(4''-Nitrobenzoate)-7-(4'''-nitrobenzoate)-2-(3'-methoxyphenyl) chromone, 49h.



Chromone **49h** was synthesized using the same procedure as described for chromone **49a** from 4-nitrobenzoyl chloride in dry dimethylformamide (0.13 g, 0.70 mmol), DBU (0.10 mL, 0.70 mmol) and chromone **49** (80.0 mg, 0.28 mmol). After the reaction and purification by column chromatography (ethyl acetate/dichloromethane [0.5:9.5]), the desired chromone **49h** was obtained as a white powder (45.3 mg, 27.63 %); m.p. 259-260 °C; FTIR (KBr) (cm⁻¹): 3108, 3071 (aromatic C-H st.), 2834 (aliphatic C-H st.), 1750, 1657 (C=O st.), 1608, 1523 (C=C st.), 1450 (C-H bending), 1348 (C-N st.), 1263, 1143, 1083 (C-O st.); ¹H-NMR 300 MHz (CDCl₃): δ 3.91 (s, 3H, OCH₃), 6.86 (s, 1H, H₃), 7.12 (ddd, *J* = 7.83, 2.50, 1.34 Hz, 1H, H_{4'}), 7.44-7.53 (m, 3H, H_{2'}, H_{5'}, H_{6'}), 7.77 (s, 1H, H₈), 8.24 (s, 1H, H₅), 8.26-8.29 (m, 8H, H_{2''}, H_{2'''}, H_{3''}, H_{3'''}, H_{5''}, H_{5'''}, H_{6''}, H_{6'''}); LRMS (ESI) *m/z* (relative intensity): [M+H]⁺ 583.16 (100.0), 536.26 (37.0), 416.23 (75.0), 388.26 (44.0); HRMS (ESI) *m/z* calcd. for C₃₀H₁₈O₁₁N₂, 582.0905 [M]⁺, 605.0803 [M+Na]⁺; found 605.0848 [M+Na]⁺; TLC (silica gel GF 254, ethyl acetate/hexane [3.5:1.5]). R_f of chromone **49** = 0.19, chromone **49h** = 0.64.

12) 6-(3'',5''-Dinitrobenzoate)-7-(3''',5'''-dinitrobenzoate)-2-(3'-methoxy-phenyl) chromone, 49i.



Chromone **49i** was synthesized using the same procedure as described for chromone **49a** from 3,5-dinitrobenzoyl chloride in dry dimethylformamide (0.16 g, 0.68 mmol), DBU (0.10 mL, 0.70 mmol) and chromone **49** (80.0 mg, 0.28 mmol). After purification by column chromatography (ethylacetate/dichloromethane [0.5:9.5]), the desired chromone **49i** was obtained as a yellow powder in the small amount and was not pure which might be due to hydrolysis of **49i** during purification step.

CHAPTER V

BIOLOGICAL EXPERIMENTAL

5.1 Equipment and chemicals

1) Equipments

Analytical balance model CP225D	Sartorius, Germany
Flat bottom 96-well plate	Corning, USA
Micropipettes 2-20 µL	Biologix oyj, Finland
Micropipettes 20-200 µL	Biologix oyj, Finland
TopCount NXT Microplate Scintillation and Luminescence Counters	Perkin Elmer, USA

2) Chemicals

Dihydroartemisinin	BIOTEC, Thailand
DMSO (Dimethyl sulfoxide)	RCI Labscan, Thailand
HEPES	Sigma, USA
[³ H]-hypoxanthine monohydrochloride	Perkin Elmer, USA
Mefloquine	Sigma, USA
RPMI-1640 medium (Roswell Park Memorial Institute medium)	Gibco, USA
Sodium bicarbonate	Fluka, USA

5.2 Method

The antimalarial activity test was performed by microculture radioisotope method. The malaria parasite, *P. falciparum* (K1, multi-drug resistant strain), was cultivated *in vitro* conditions, according to Trager and Jensen (48), in RPMI 1640 medium containing 20 mM HEPES (N-2-hydroethylpiperazine-N'-2-ethanesulfonic acid), 32 mM NaHCO₃ and 10% heat activated human serum with 3% erythrocytes, in

humidified 37°C incubator with 3% CO₂. The culture was passaged with fresh mixture of erythrocytes and medium for every day to maintain cell growth.

Quantitative assessment of antimalarial activity *in vitro* was determined by microculture radioisotope technique based upon the methods described by Desjardins *et al* (16). In brief, a mixture of 200 µL of 1.5% erythrocytes with 1% parasitemia at the early ring stage was pre-exposed to 25 µL of the medium containing a test sample dissolved in 1 % DMSO (0.1% final concentration) for 24 hours. Subsequently, 25 µL of [³H]-hypoxanthine in culture medium (0.5 µCi) was added to each well and the plates were incubated for an additional 24 hours. Levels of incorporated radioactive labeled hypoxanthine, indicating parasite growth, were determined using the TopCount NXT Microplate Scintillation and Luminescence Counters (Perkin Elmer, USA). The percentage of parasite growth was calculated using the signal count per minute of treated (CPM_T) and untreated conditions (CPM_U), by this formula.

$$\% \text{ parasite growth} = \text{CPM}_T / \text{CPM}_U \times 100$$

The inhibition concentration which killed the parasite was obtained from the calculation by the following equation:

$$\text{IC}_{50} = 10^{\left[\left\{ \log \left(\frac{C_1}{C_2} \right) \times \left(\frac{G_1 - 50}{G_2 - G_1} \right) \right\} + \log (C_2) \right]}$$

C1 is concentration of sample with % parasite growth < 50

C2 is concentration of sample with % parasite growth ≥ 50

G1 is the percentage of parasite growth at C1

G2 is the percentage of parasite growth at C2

Dihydroartemisinin (DHA) and mefloquine (MEF) were used as the positive controls. The negative control was 0.1% DMSO. All of chromone compounds were dissolved in 100 % of DMSO as the stock solution at concentration 10 mg/mL. The tested concentrations of chromone compounds were 10, 1 and 0.1 µg/mL in duplicate experiment for evaluating the % parasite growth.

CHAPTER VI

RESULTS AND DISCUSSION

The aim of this study is to design and synthesize the chromone derivatives as non-peptidomimetic Plm II inhibitors. The research study was initiated from the preliminary screening of the Plm II inhibitory activity of forty-six chromone derivatives that have been previously synthesized and evaluated as HIV-1 PR inhibitors. The screening study was performed by using docking simulation technique with AutoDock 4.0 program. Chromone derivatives which showed good binding energy with Plm II and high HIV-1 PR inhibitory activity (more than 70 % inhibition) were selected to evaluate for their antimalarial activity against *P. falciparum* (K1 multi-drug resistant strain) by using the microculture radioisotope method. Based on the docking study of chromone core structure, a new series of chromone derivatives which have the hydroxyl groups at positions 6 and 7 of the chromone structure were designed and performed docking study with the Plm II. The results of docking simulation of the six new chromone derivatives showed the slightly better binding energy than the selected chromone derivatives from the 3-rings system series. These compounds were further structure modified by adding the steric groups at positions 6 and 7. Seventy-two modified chromone structures were docked and screened to find the new potent chromone derivatives as Plm II inhibitors. From the screening results, nine modified chromone derivatives (chromones **49a-49i**) were identified and selected for synthesis. The synthesis route of these nine modified chromone derivatives was mainly divided into two parts. Firstly, the chromone core structure was prepared by Baker-Venkataraman rearrangement and subsequent intramolecular cyclization with a catalytic amount of strong acid. Secondly, the esterification at positions 6 and 7 of the chromone structure was performed to provide the designed chromone derivatives. Finally, the synthesized chromones were also evaluated their antimalarial activity against *P. falciparum*. The scope of this research study was summarized in Figure 6.1.

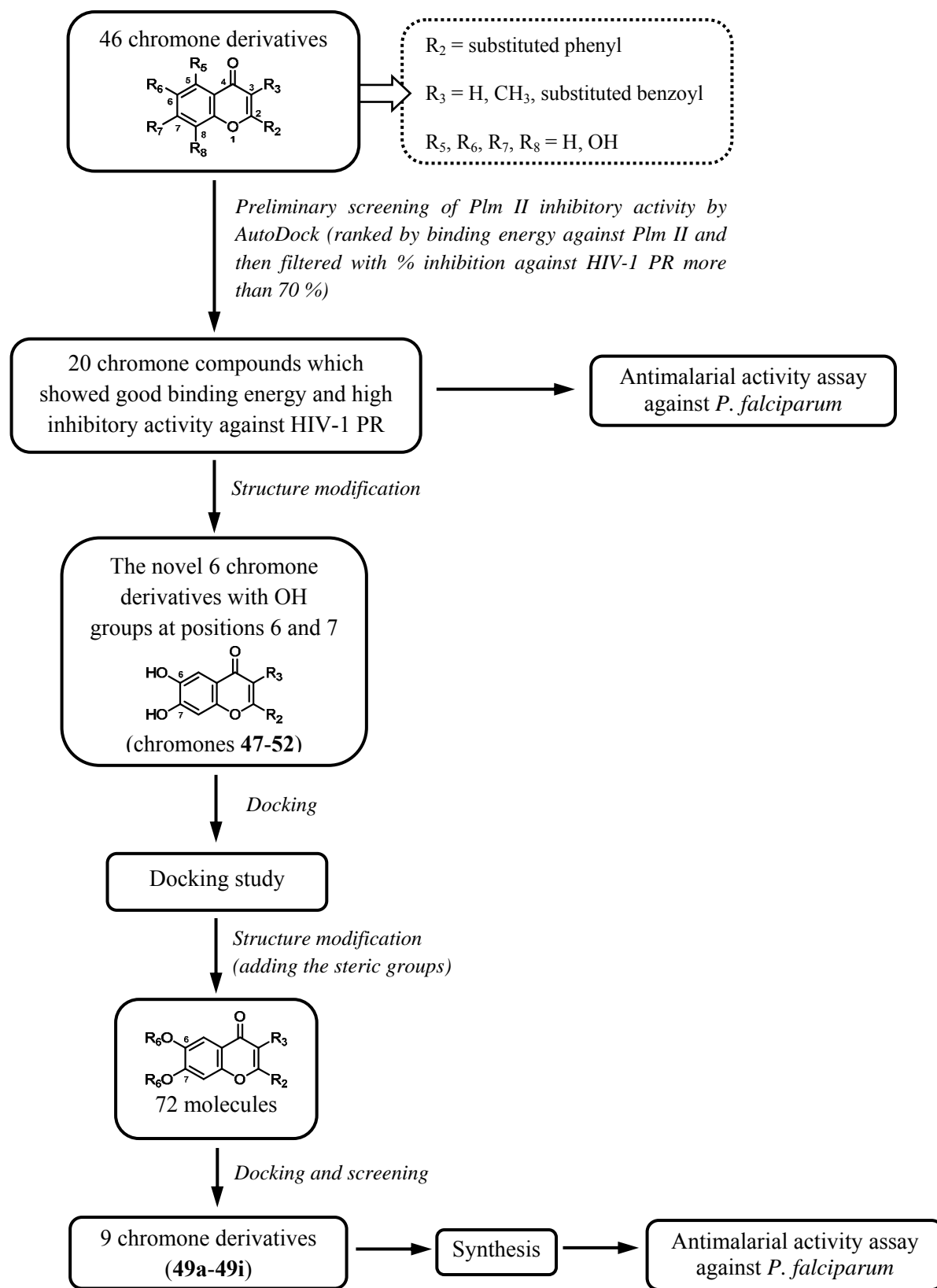


Figure 6.1 The summary diagram of screening process.

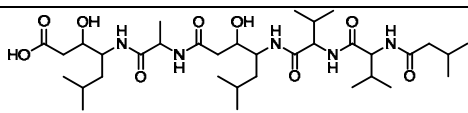
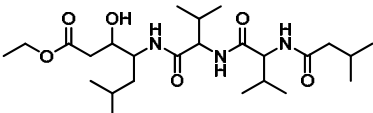
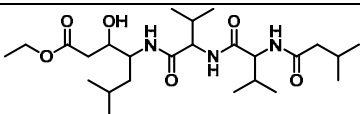
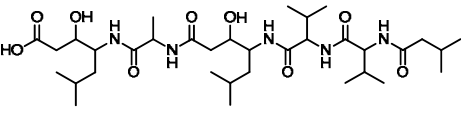
6.1 Molecular modeling

The docking simulation study was performed by using AutoDock 4.0 software (The Scripps Research Institute) to assess the interaction between the designed chromone structures and macromolecular targets (Plm II crystal structure). Conformations of the ligands evaluated with AutoDock program were allowed to be flexible while the macromolecular target was fixed.

1) Preparation and Validation of Plm II template

The Plm II template was prepared and validated by re-docking and cross-docking experiments. Two X-ray crystal structures of Plm II PDB code 1SME and 1ME6 were selected to study. The validation results of re-docking and cross-docking were shown in Table 6.1.

Table 6.1 Validation results of Plm II template.

PDB code	Ligand	AutoDock 4.0*		
		Ligand cluster number	%Member in cluster	RMSD (Å)
1SME	 IHN (re-docking)	1	81	0.35
	 IVS (cross-docking)	1	13	0.64
1ME6	 IVS (re-docking)	1	56	0.49
	 IHN (cross-docking)	2	29	2.58

*GA run = 100, population = 150, max num. of energy evaluation = 2500000 per run

The results of validation of Plm II as a protein template showed the template with PDB code 1SME was the good model with the RMSD values of re-docking and cross-docking less than 2.0 Å and lower than the RMSD values from the re-docking and cross-docking of 1ME6. Therefore the X-ray crystal structure of Plm II with PDB code 1SME was used as a protein template in the further docking studies.

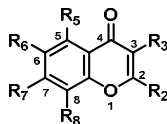
2) Docking studies of chromone derivatives with Plm II

The preliminary screening of the Plm II inhibitory activity of the forty-six previously synthesized chromone derivatives were performed by using AutoDock 4.0 program on Garibaldi platform at The Scripps Research Institute. The studied chromone derivatives were classified into 2 series; 3-rings system (R_2 = substituted phenyl, R_3 = H, CH_3 ; chromones **1-30**) and 4-rings system (R_2 = substituted phenyl, R_3 = substituted benzoyl; chromones **31-46**). The structures of the chromone derivatives and their binding energy docking with Plm II (PDB code 1SME) were shown in Table 6.2. The results of docking study of the chromones in 3-rings system (chromones **1-30**) and 4-rings system (chromones **31-46**) showed the binding energy between -6.13 to -10.36 kcal/mole and -10.56 to -13.24 kcal/mole, respectively.

The docking results of each series of the chromone derivatives were ranked by their binding energy against Plm II and were filtered with % inhibition against HIV-1 PR. Twenty chromone compounds which showed good binding energy with Plm II from docking study and high inhibitory activity against HIV-1 PR (more than 70 % inhibition) were selected from the two series (Table 6.3) for evaluating the antimalarial activity against *P. falciparum*.

Table 6.2 Structures and binding energy of chromone derivatives with Plm II (1SME).

[illegible]

Table 6.3 Twenty chromone compounds which showed good binding energy and high inhibitory activity against HIV-1 PR (more than 70 % inhibition).

Chromone	R ₂	R ₃	R ₅	R ₆	R ₇	R ₈	Binding Energy (kcal/mole)
3	Benzyl	H	H	H	OH	OH	-8.86
4	Phenyl	H	H	H	OH	OH	-8.16
16	4'-(<i>t</i> -butyl)-Phenyl	H	H	H	OH	H	-8.37
17	3'-(CF ₃)-Phenyl	H	OH	H	OH	H	-8.60
18	4'-(F)-Phenyl	H	OH	H	OH	H	-8.32
19	3',4'-(diF)-Phenyl	H	OH	H	OH	H	-8.54
20	4'-(<i>t</i> -butyl)-Phenyl	H	OH	H	OH	H	-8.87
23	3'-(Cl)-Phenyl	H	OH	H	OH	H	-8.27
24	3',4'-(diCl)-Phenyl	H	OH	H	OH	H	-8.89
25	4'-(OCH ₃)-Phenyl	H	OH	H	OH	H	-8.70
26	3'-(OCH ₃)-Phenyl	H	OH	H	OH	H	-8.93
27	3'-(OCH ₃)-Phenyl	H	H	OH	H	H	-7.95
31	3'-(CF ₃)-Phenyl	3''-(CF ₃)-Benzoyl	H	H	OH	OH	-12.53
34	4'-(F)-Phenyl	4''-(F)-Benzoyl	H	H	OH	OH	-10.83
35	4'-(NO ₂)-Phenyl	4''-(NO ₂)-Benzoyl	H	H	OH	OH	-13.24
37	3',4'-(diF)-Phenyl	3'',4''-(diF)-Benzoyl	H	H	OH	H	-10.56
38	3'-(CF ₃)-Phenyl	3''-(CF ₃)-Benzoyl	H	H	OH	H	-11.84
42	4'-(NO ₂)-Phenyl	4''-(NO ₂)-Benzoyl	H	H	OH	H	-11.79
44	4'-(<i>t</i> -butyl)-Phenyl	4''-(<i>t</i> -butyl)-Benzoyl	H	H	OH	H	-12.21
46	4'-(NO ₂)-Phenyl	4''-(NO ₂)-Benzoyl	OH	H	OH	H	-13.03

3) Structural modification of chromone derivatives as Plm II inhibitors

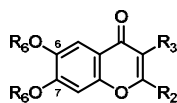
Based on the previous docking study, new chromone derivatives, which have hydroxyl groups at positions 6 and 7 of chromone structure, were designed and performed docking against Plm II. The docking study was performed to find out whether these compounds exhibit better binding energy than the chromone compounds in the 3-rings system series (chromones **1-30**). The results of these compounds were shown in Table 6.4.

Table 6.4 Structures of the chromone derivatives (**47-52**) and their binding energy.

Chromone	R ₂	R ₃	Binding Energy (kcal/mole)
47	4'-(NO ₂)-Phenyl	H	-9.40
48	4'-(<i>t</i> -butyl)-Phenyl	H	-8.84
49	3'-(OCH ₃)-Phenyl	H	-8.89
50	3'-(CF ₃)-Phenyl	H	-8.77
51	Benzyl	H	-8.75
52	3'-(NO ₂)-Phenyl	H	-9.31

The results of docking simulation of chromones **47-52** showed the slightly better binding energy than the chromone compounds in the 3-rings system series. Therefore, chromones **47-52** were subjected to structural modification by adding the steric groups at the both hydroxyl groups to gain the better binding energy (Table 6.5).

The structural modifications of unmodified chromones **47**, **49**, **50** and **52** led to the better binding energy than the unmodified chromones and pepstatin A. However, the binding energies of modified chromones were slightly different. Although chromones **47** and **47a-47i** (R₂ = 4'-(NO₂)-phenyl) exhibited the best binding energy with Plm II, chromones **47** and **47a-47i** were not selected to synthesize and evaluate because the synthesis of chromones with R₂ = 4'-(NO₂)-phenyl usually gave low % yield of the desired product. Therefore, only nine modified chromone derivatives (**49a-49i**) were chosen to synthesize due to the modified chromones **49** (R₂ = 3'-(OCH₃)-phenyl) were easier and less cost for synthesis.

Table 6.5 Structures of the modified chromone derivatives and their binding energy.

Compound	R ₂	R ₃	R ₆	Binding Energy (kcal/mole)
47a	4'-(NO ₂)-Phenyl	H	3'''-(OCH ₃)-benzoyl	-14.43
47b	4'-(NO ₂)-Phenyl	H	4'''-(OCH ₃)-benzoyl	-14.31
47c	4'-(NO ₂)-Phenyl	H	3''',4'''-(diOCH ₃)-benzoyl	-15.52
47d	4'-(NO ₂)-Phenyl	H	3'''-(Cl)-benzoyl	-14.34
47e	4'-(NO ₂)-Phenyl	H	4'''-(Cl)-benzoyl	-14.16
47f	4'-(NO ₂)-Phenyl	H	3''',4'''-(diCl)-benzoyl	-14.71
47g	4'-(NO ₂)-Phenyl	H	3'''-(NO ₂)-benzoyl	-15.65
47h	4'-(NO ₂)-Phenyl	H	4'''-(NO ₂)-benzoyl	-15.09
47i	4'-(NO ₂)-Phenyl	H	3''',5'''-(diNO ₂)-benzoyl	-15.11
48a	4'-(<i>t</i> -butyl)-Phenyl	H	3'''-(OCH ₃)-benzoyl	-12.32
48b	4'-(<i>t</i> -butyl)-Phenyl	H	4'''-(OCH ₃)-benzoyl	-11.35
48c	4'-(<i>t</i> -butyl)-Phenyl	H	3''',4'''-(diOCH ₃)-benzoyl	-12.51
48d	4'-(<i>t</i> -butyl)-Phenyl	H	3'''-(Cl)-benzoyl	-11.54
48e	4'-(<i>t</i> -butyl)-Phenyl	H	4'''-(Cl)-benzoyl	-11.36
48f	4'-(<i>t</i> -butyl)-Phenyl	H	3''',4'''-(diCl)-benzoyl	-12.04
48g	4'-(<i>t</i> -butyl)-Phenyl	H	3'''-(NO ₂)-benzoyl	-12.74
48h	4'-(<i>t</i> -butyl)-Phenyl	H	4'''-(NO ₂)-benzoyl	-12.07
48i	4'-(<i>t</i> -butyl)-Phenyl	H	3''',5'''-(diNO ₂)-benzoyl	-12.63
49a	3'-(OCH ₃)-Phenyl	H	3'''-(OCH ₃)-benzoyl	-13.96
49b	3'-(OCH ₃)-Phenyl	H	4'''-(OCH ₃)-benzoyl	-13.88
49c	3'-(OCH ₃)-Phenyl	H	3''',4'''-(diOCH ₃)-benzoyl	-15.08
49d	3'-(OCH ₃)-Phenyl	H	3'''-(Cl)-benzoyl	-13.91
49e	3'-(OCH ₃)-Phenyl	H	4'''-(Cl)-benzoyl	-13.80
49f	3'-(OCH ₃)-Phenyl	H	3''',4'''-(diCl)-benzoyl	-14.51
49g	3'-(OCH ₃)-Phenyl	H	3'''-(NO ₂)-benzoyl	-15.22
49h	3'-(OCH ₃)-Phenyl	H	4'''-(NO ₂)-benzoyl	-14.76
49i	3'-(OCH ₃)-Phenyl	H	3''',5'''-(diNO ₂)-benzoyl	-15.06
50a	3'-(CF ₃)-Phenyl	H	3'''-(OCH ₃)-benzoyl	-14.04
50b	3'-(CF ₃)-Phenyl	H	4'''-(OCH ₃)-benzoyl	-14.00
50c	3'-(CF ₃)-Phenyl	H	3''',4'''-(diOCH ₃)-benzoyl	-15.13
50d	3'-(CF ₃)-Phenyl	H	3'''-(Cl)-benzoyl	-14.00
50e	3'-(CF ₃)-Phenyl	H	4'''-(Cl)-benzoyl	-14.61
50f	3'-(CF ₃)-Phenyl	H	3''',4'''-(diCl)-benzoyl	-13.90
50g	3'-(CF ₃)-Phenyl	H	3'''-(NO ₂)-benzoyl	-15.29
50h	3'-(CF ₃)-Phenyl	H	4'''-(NO ₂)-benzoyl	-14.82
50i	3'-(CF ₃)-Phenyl	H	3''',5'''-(diNO ₂)-benzoyl	-15.31
51a	Benzyl	H	3'''-(OCH ₃)-benzoyl	-13.13
51b	Benzyl	H	4'''-(OCH ₃)-benzoyl	-13.01
51c	Benzyl	H	3''',4'''-(diOCH ₃)-benzoyl	-14.21
51d	Benzyl	H	3'''-(Cl)-benzoyl	-13.24

Table 6.5 Structures of the modified chromone derivatives and their binding energy (cont.).

Compound	R ₂	R ₃	R ₆	Binding Energy (kcal/mole)
51e	Benzyl	H	4'''-(Cl)-benzoyl	-12.93
51f	Benzyl	H	3''',4'''-(diCl)-benzoyl	-13.82
51g	Benzyl	H	3'''-(NO ₂)-benzoyl	-14.38
51h	Benzyl	H	4'''-(NO ₂)-benzoyl	-13.86
51i	Benzyl	H	3''',5'''-(diNO ₂)-benzoyl	-14.70
52a	3'-(NO ₂)-Phenyl	H	3'''-(OCH ₃)-benzoyl	-14.13
52b	3'-(NO ₂)-Phenyl	H	4'''-(OCH ₃)-benzoyl	-14.04
52c	3'-(NO ₂)-Phenyl	H	3''',4'''-(diOCH ₃)-benzoyl	-15.25
52d	3'-(NO ₂)-Phenyl	H	3'''-(Cl)-benzoyl	-14.05
52e	3'-(NO ₂)-Phenyl	H	4'''-(Cl)-benzoyl	-13.95
52f	3'-(NO ₂)-Phenyl	H	3''',4'''-(diCl)-benzoyl	-14.72
52g	3'-(NO ₂)-Phenyl	H	3'''-(NO ₂)-benzoyl	-15.24
52h	3'-(NO ₂)-Phenyl	H	4'''-(NO ₂)-benzoyl	-14.88
52i	3'-(NO ₂)-Phenyl	H	3''',5'''-(diNO ₂)-benzoyl	-15.09

The binding modes of nine modified chromone derivatives (**49a-49i**) were analyzed. It was found that the alignments of all chromones were fit in the pocket of Plm II template and aligned in the same orientation as shown in Figure 6.2. The docked poses showed the 3'-(OCH₃)-phenyl group at the position 2 of chromone ring lied in the S1' and S3'-S4' subsites and was in close contract with hydrophobic side chains of Met75, Leu131 and Ile133 residues. The substituted benzoate groups (R₆) at the positions 6 and 7 were located in the S2-S4 subsites and S1-S3 subsites, respectively. The phenyl ring of the R₆ at position 6 formed hydrophobic interaction with Ala219, Leu290 Leu292 and Ile300 residues in S2-S4 subsites. The other phenyl ring (R₆ at position 7) was surrounded by hydrophobic amino acid residues, Met15, Ile32, Phe111 and Ile123 residues in the S1-S3 subsites (Figure 6.3). The H-bond interactions of chromones **49a-49i** with Plm II were listed in Table 6.6. All of modified chromone compounds (**49a-49i**) could form H-bond interaction with the amino group of Ser79 and hydroxyl group of Thr217. These H-bond interactions explained the good binding energies of compounds in this series.

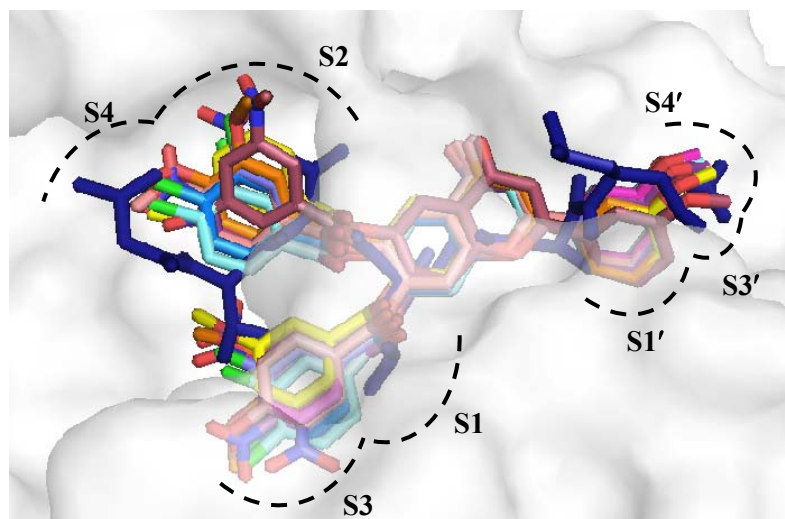


Figure 6.2 The binding mode of nine modified chromone derivatives (**49a-49i**) comparing with the pepstatin A (navy blue color).

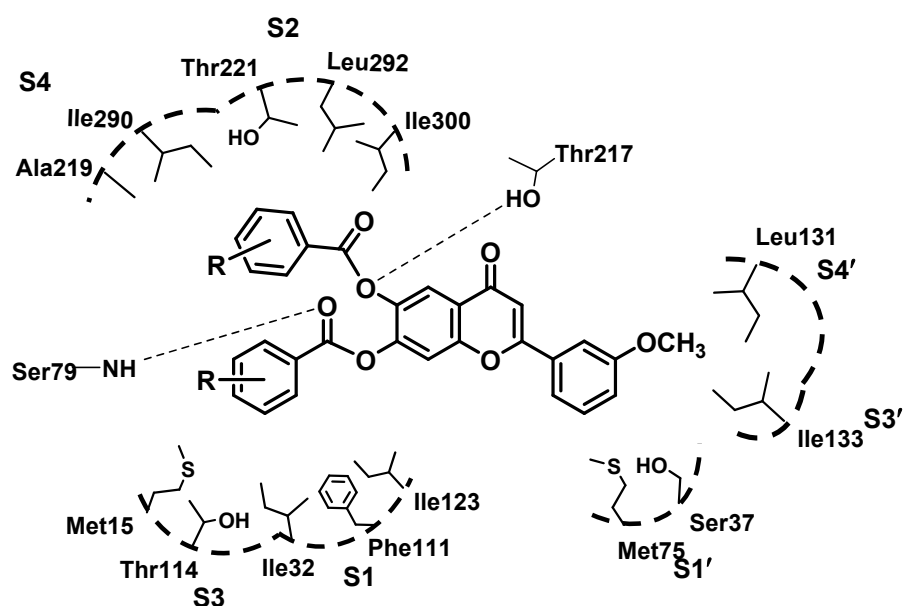


Figure 6.3 Schematic picture of binding interactions between modified chromones (**49a-49i**) and Plm II.

Table 6.6 The binding interactions of modified chromone derivatives (**49a-49i**) with Plm II.

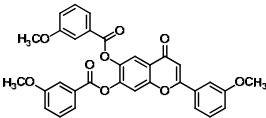
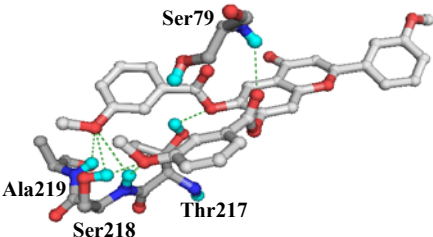
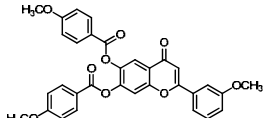
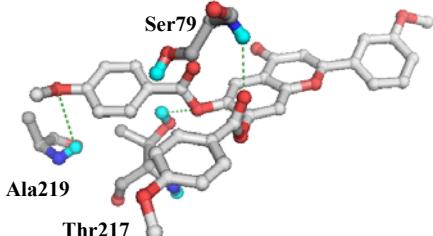
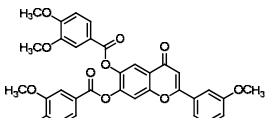
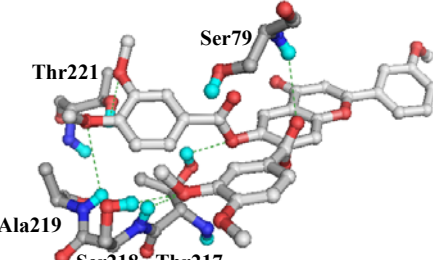
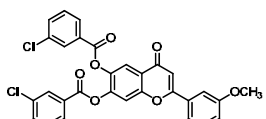
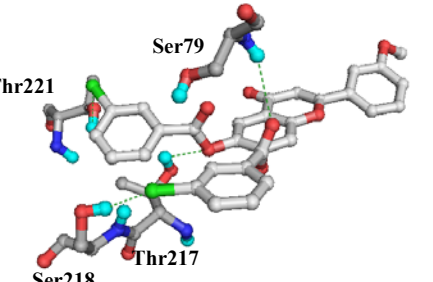
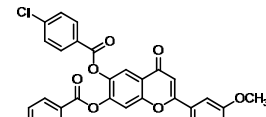
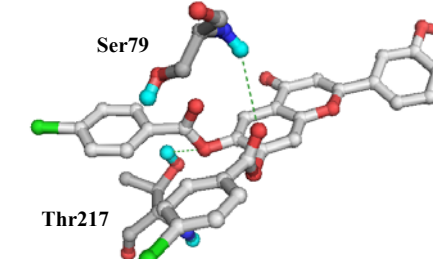
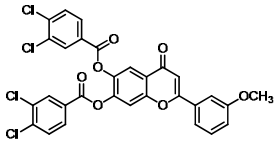
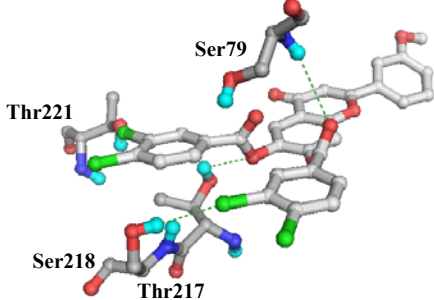
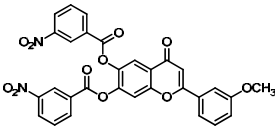
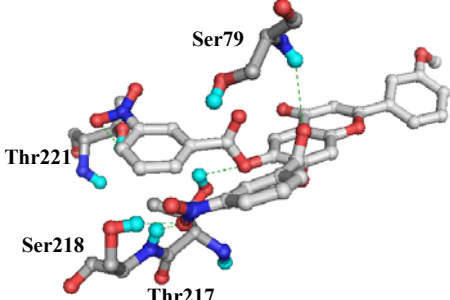
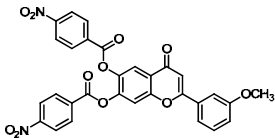
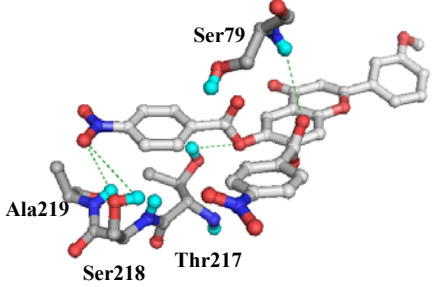
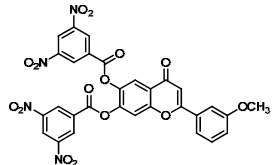
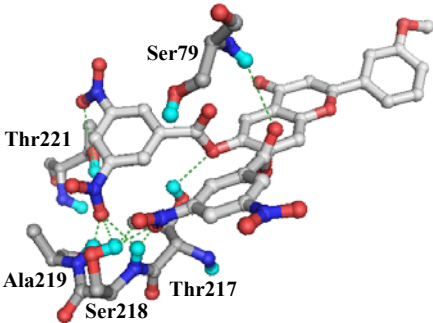
Chromone structure (Binding energy kcal/mole)	Ligand-protein template interactions (H-bond interaction [*])	H-bond interaction residues (distance Å)
 <p>49a (-13.96)</p>	 <p>Ser79 Ala219 Ser218 Thr217</p>	<p>Ser79-NH (2.597) Thr217-OH (2.232) Ser218-NH (2.996, 2.836) Ser218-OH (2.160, 2.865) Ala219-NH (2.571)</p>
 <p>49b (-13.88)</p>	 <p>Ser79 Ala219 Thr217</p>	<p>Ser79-NH (2.574) Thr217-OH (2.514) Ala219-NH (3.125)</p>
 <p>49c (-15.08)</p>	 <p>Ser79 Thr221 Ala219 Ser218 Thr217</p>	<p>Ser79-NH (2.962) Thr217-OH (2.354) Ser218-NH (3.173) Ser218-OH (2.405) Ala219-NH (3.327) Thr221-OH (3.457)</p>
 <p>49d (-13.91)</p>	 <p>Ser79 Thr221 Ser218 Thr217</p>	<p>Ser79-NH (3.016) Thr217-OH (2.458) Ser218-OH (2.834) Thr221-OH (3.226)</p>
 <p>49e (-13.80)</p>	 <p>Ser79 Thr217</p>	<p>Ser79-NH (3.186) Thr217-OH (2.516)</p>

Table 6.6 The binding interactions of modified chromone derivatives (**49a-49i**) with Plm II (cont.).

Chromone structure (Binding energy kcal/mole)	Ligand-protein template interactions (H-bond interaction *)	H-bond interaction residues (distance Å)
 <p>49f (-14.51)</p>		Ser79-NH (3.287) Thr217-OH (2.643) Ser218-OH (3.487) Thr221-OH (2.682)
 <p>49g (-15.22)</p>		Ser79-NH (2.872) Thr217-OH (2.413) Ser218-NH (2.375) Ser218-OH (1.908) Thr221-OH (2.601)
 <p>49h (-14.79)</p>		Ser79-NH (3.270) Thr217-OH (2.584) Ser218-OH (3.594) Ala219-NH (3.280)
 <p>49i (-15.06)</p>		Ser79-NH (3.027) Thr217-OH (2.544) Ser218-NH (1.845, 2.211) Ser218-OH (1.827, 2.294, 2.753) Ala219-NH (1.744) Thr221-OH (3.528)

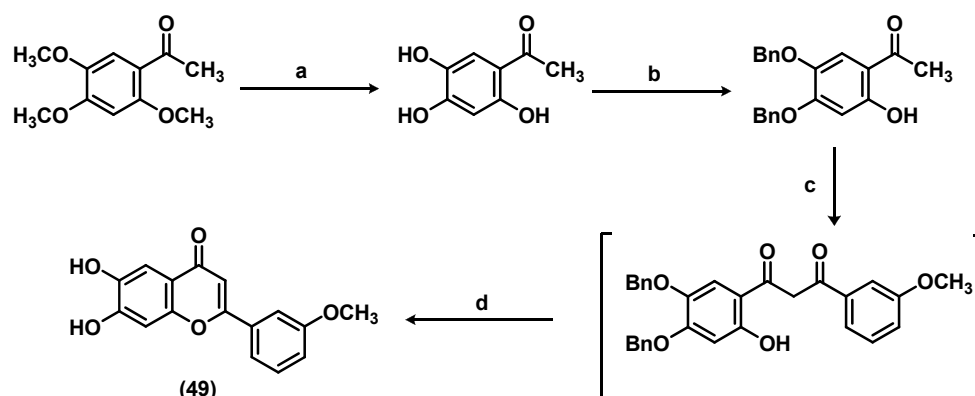
* Hydrogen bond in green dotted line

6.2 Synthesis

The designed chromone derivatives were synthesized using the commercially available 2,4,5-trimethoxyacetophenone as starting material. The synthesis of nine modified chromone derivatives (**49a-49i**) was divided into two major parts, i.e., (i) the preparation of 6,7-dihydroxy-2-(3'-methoxyphenyl) chromone (**49**) as a core structure and (ii) the addition of the steric groups at positions 6 and 7 of the core structure.

1) Preparation of 6,7-dihydroxy-2-(3'-methoxyphenyl) chromone (**49**)

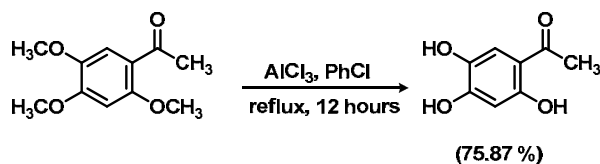
The synthesis route of chromone **49** was composed of 4 steps as shown in Scheme 6.1. The crucial steps for constructing the chromone structure was Baker-Venkataraman rearrangement (c) and subsequent intramolecular cyclization with strong acid as catalyst (d).



Scheme 6.1 Synthesis route of 6,7-dihydroxy-2-(3'-methoxyphenyl) chromone (**49**) preparation (a) AlCl_3 , PhCl , reflux, 12 hours (49, 50); (b) BnBr , K_2CO_3 , acetone, reflux, 5 hours (51); (c) 3-methoxybenzoyl chloride, K_2CO_3 , acetone, reflux, 24 hours (17); (d) conc. H_2SO_4 , glacial acetic acid, 120°C , 3 hours (18).

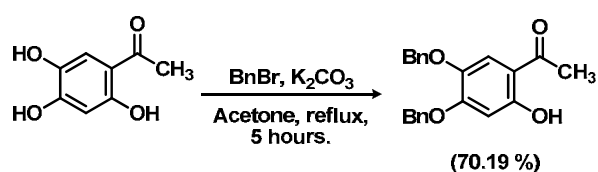
The first step was the demethylation reaction. The commercially available 2,4,5-trimethoxyacetophenone was demethylated by anhydrous AlCl_3 in

chlorobenzene to yield the 2,4,5-trihydroxyacetophenone (75.87 %) which was the starting material for constructing the novel chromone derivatives (Scheme 6.2).



Scheme 6.2 The demethylation reaction of 2,4,5-trimethoxyacetophenone.

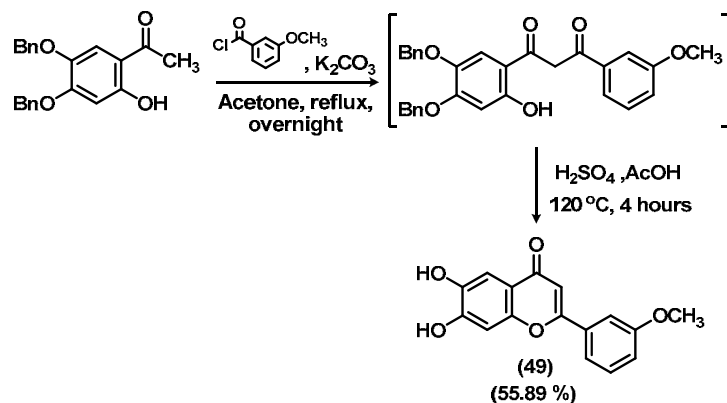
The second step was the selective protection of hydroxyl group. The hydroxyl groups at positions 4 and 5 of 2,4,5-trihydroxyacetophenone were selectively protected with benzyl groups to afford 4,5-bisbenzyloxy-2-hydroxyacetophenone. These two hydroxyl groups were protected to prevent the by products that could occur in the next steps. It resulted in only one free hydroxyl group at position 2, which was an essential for cyclization to construct the chromone structure (Scheme 6.3). The hydroxyl group at position 2 was not protected because it could form H-bond with the oxygen atom of acetyl group. Therefore the acidity of hydroxyl proton at position 2 was less than hydroxyl protons at positions 4 and 5.



Scheme 6.3 The selective protection of 2,4,5-trihydroxyacetophenone.

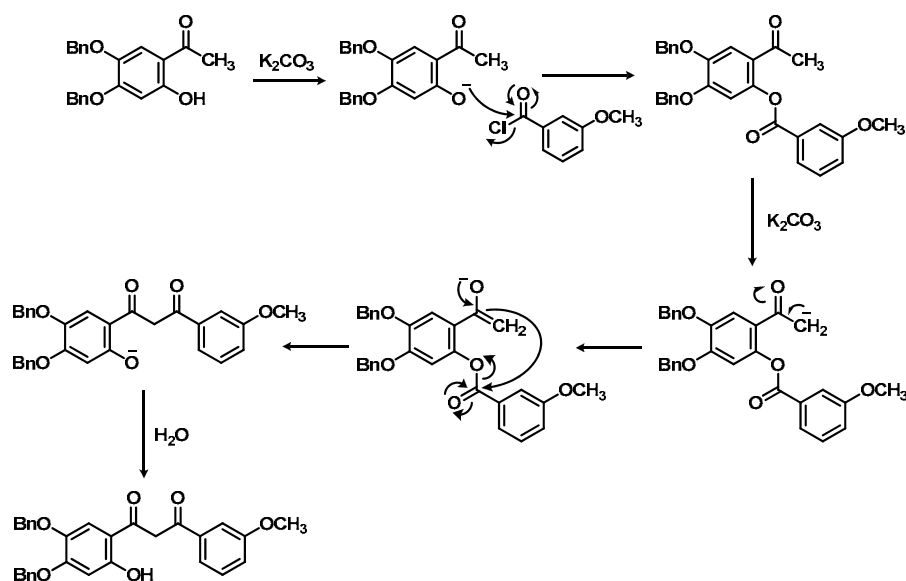
The third step was Baker-Venkataraman rearrangement reaction. The Baker-Venkataraman rearrangement reaction was the first crucial step to prepare the chromone structure from the protected hydroxyacetophenone. The protected hydroxyacetophenone was reacted with the 3-methoxybenzoyl chloride in the present of potassium carbonate anhydrous to produce the crude product of 1,3-diketone. The last step for constructing the chromone core structure was intramolecular cyclization and simultaneous deprotection of benzyl groups. The intramolecular cyclization of

1,3-diketone and removal of benzyl groups were carried out under strong acid condition to provide chromone **49** (55.89 %) (Scheme 6.4).



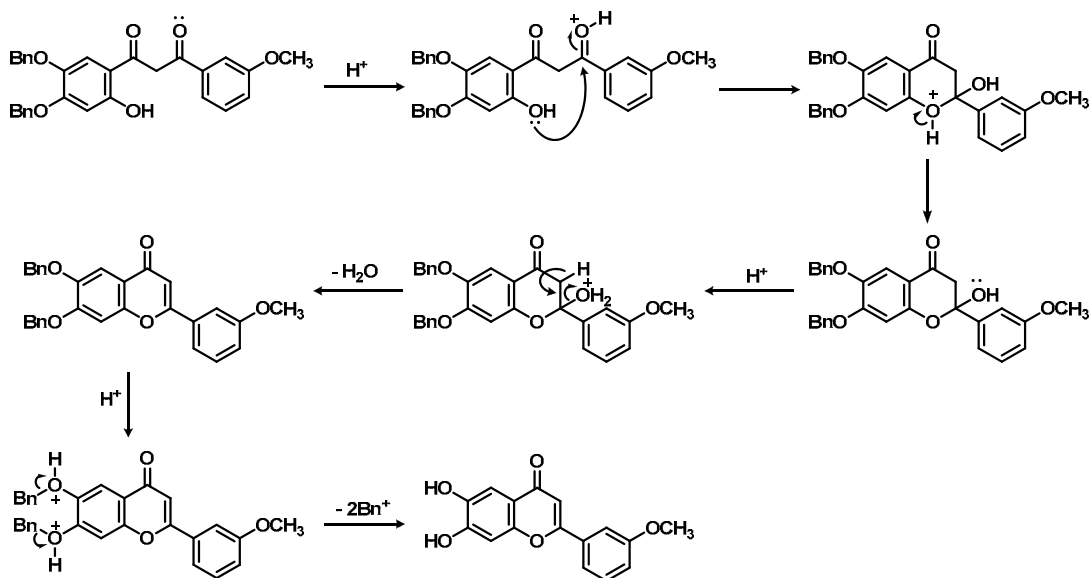
Scheme 6.4 Baker-Venkataraman rearrangement, intramolecular cyclization and debenzylaton reactions.

The proposed mechanism of Baker-Venkataraman rearrangement was shown in Scheme 6.5. The protected hydroxyacetophenone was stirred with potassium carbonate anhydrous to generate phenolate anion. Then phenolate anion reacted with the 3-methoxybenzoyl chloride to form phenolic ester. The formation of the phenolic ester was followed by rearrangement to provide the crude product of 1,3-diketone.



Scheme 6.5 The proposed mechanism of Baker-Venkataraman rearrangement.

The crude product of 1,3-diketone was cyclized to the chromone structure by stirring at 120°C with conc. H₂SO₄ in glacial AcOH. The proposed mechanism of intramolecular cyclization was shown in Scheme 6.6. The hydroxyl group at position 2 attacked the protonated ketone to close the ring. Afterward, water molecule was condensed to yield the chromone ring structure. During the cyclization process, the protecting benzyl groups were removed in the strong acidic condition. The benzyl groups were cleaved out in the benzyl cation form and provided chromone **49** was provide (52).

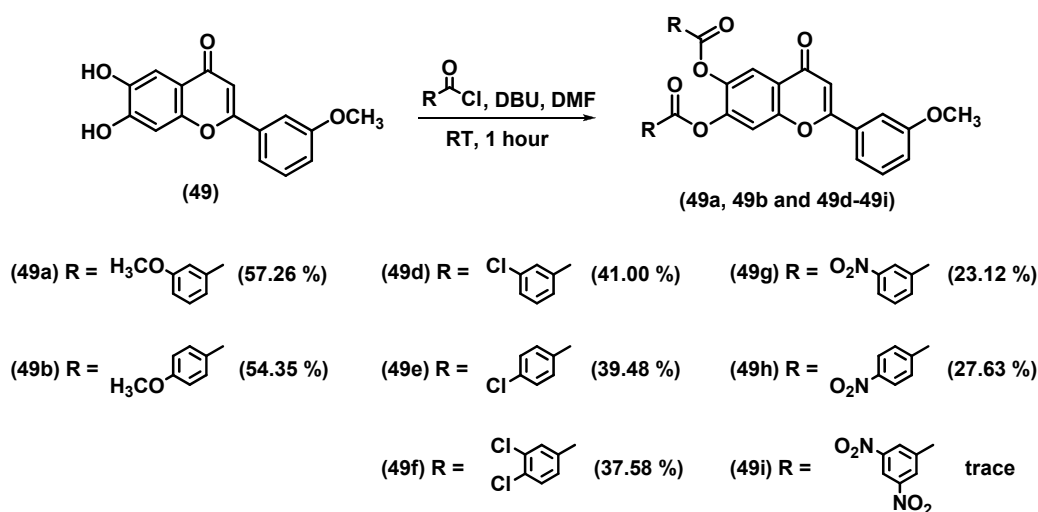


Scheme 6.6 The proposed mechanism of intramolecular cyclization and debenzylation of chromone **49**.

As seen from the preparation of chromone core structure, all steps of the synthesis pathway were practical and economical methods for the synthesis. The Baker-Venkataraman rearrangement and subsequent intramolecular cyclization with strong acids as catalyst were used because only simple reagents and solvent were required and the desired chromone (**49**) was provided as the major product with % yield more than 50 %.

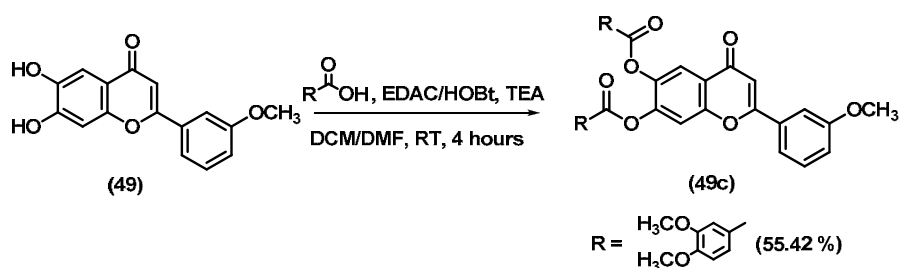
2) Synthesis of the modified chromone derivatives (49a-49i)

The esterification reaction was preformed to yield nine modified chromone derivatives. Eight of them (**49a**, **49b** and **49d-49i**) were synthesized via alcoholysis of chromone **49** and substituted benzoyl chloride under basic condition (Scheme 6.7). The synthesis of chromone **49i** was unsuccessful due to only trace amount of impure compound was obtained.

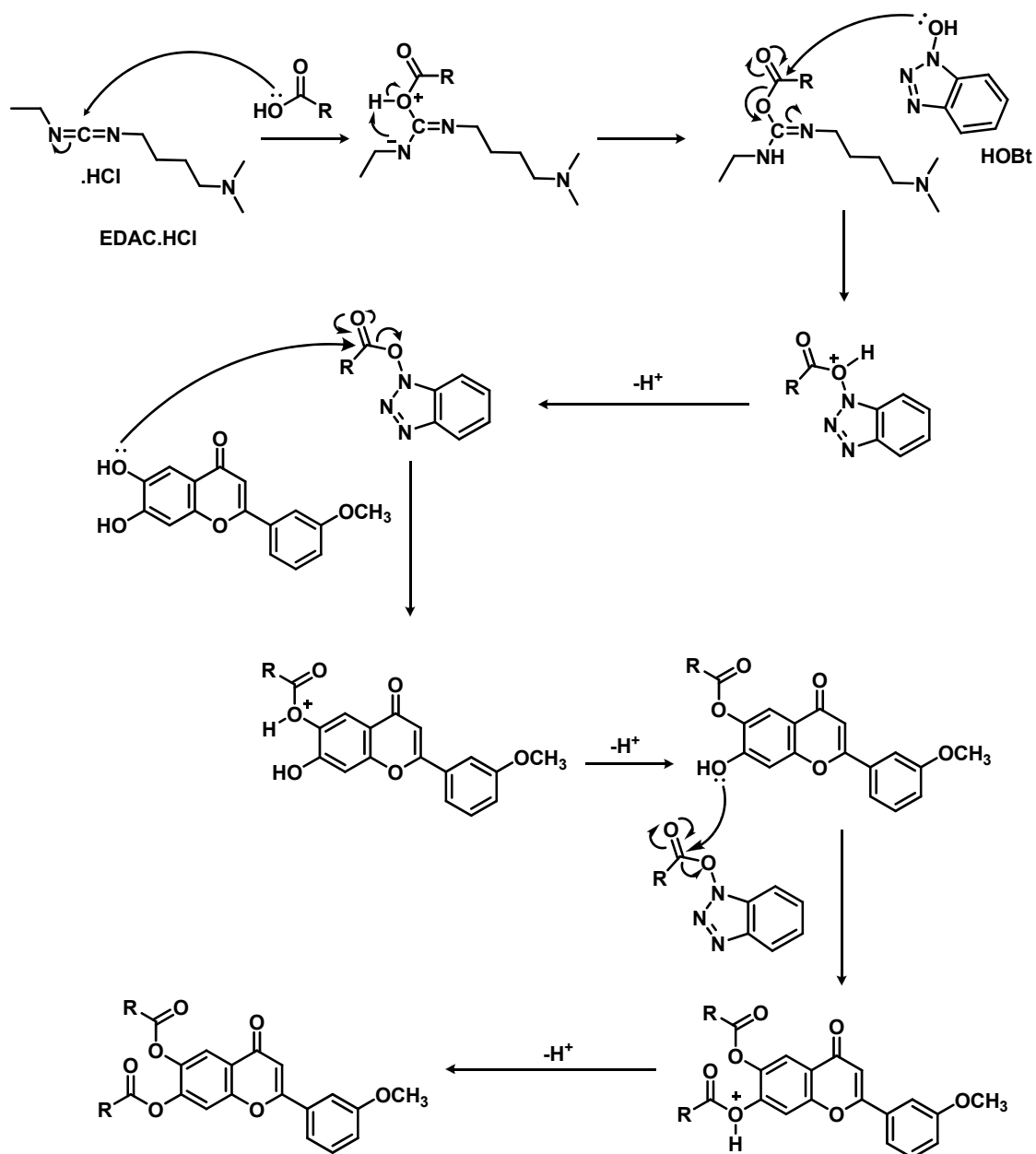


Scheme 6.7 The esterification of chromone **49a**, **49b** and **49d-49i**.

Chromone **49c** was synthesized via esterification of chromone **49** and substituted benzoic acid using 1-ethyl-3-(3'-dimethylaminopropyl)carbodiimide.HCl (EDAC.HCl) and hydroxybenzotriazole (HOBt) as coupling reagents (Scheme 6.8). Triethylamine should be added as catalyst into the reaction to increase rate of the reaction. The proposed mechanism of esterification of chromone **49c** was shown in Scheme 6.9.

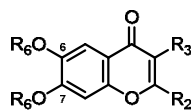


Scheme 6.8 The esterification of chromone **49c** (53).



Scheme 6.9 The proposed mechanism of esterification of chromone **49c**.

Melting point and % yield of the synthesized chromone compounds were summarized in Table 6.7.

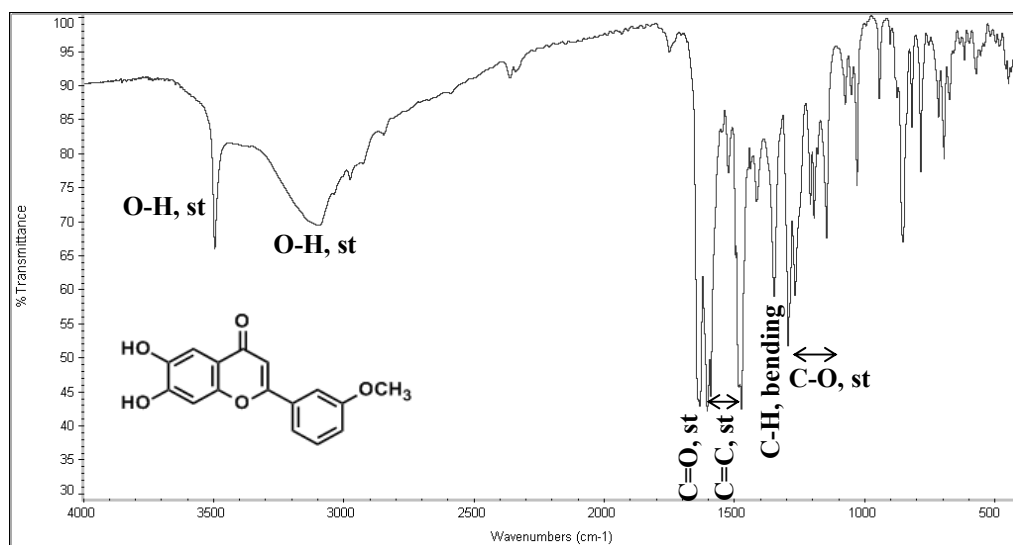
Table 6.7 Melting point (m.p.) and % yield of chromones **49** and **49a-49i**.

Chromone	R ₂	R ₃	R ₆	m.p. (°C)	% yield (%)
49	3'-(OCH ₃)-Phenyl	H	H	246-247	55.89
49a	3'-(OCH ₃)-Phenyl	H	3'''-(OCH ₃)-benzoyl	197-198	57.26
49b	3'-(OCH ₃)-Phenyl	H	4'''-(OCH ₃)-benzoyl	201-202	54.35
49c	3'-(OCH ₃)-Phenyl	H	3''',4'''-(diOCH ₃)-benzoyl	188-189	55.42
49d	3'-(OCH ₃)-Phenyl	H	3'''-(Cl)-benzoyl	211-212	41.00
49e	3'-(OCH ₃)-Phenyl	H	4'''-(Cl)-benzoyl	251-252	39.48
49f	3'-(OCH ₃)-Phenyl	H	3''',4'''-(diCl)-benzoyl	254-255	37.58
49g	3'-(OCH ₃)-Phenyl	H	3'''-(NO ₂)-benzoyl	225-226	23.12
49h	3'-(OCH ₃)-Phenyl	H	4'''-(NO ₂)-benzoyl	259-260	27.63
49i	3'-(OCH ₃)-Phenyl	H	3''',5'''-(diNO ₂)-benzoyl	-	-

3) Structure elucidation

The structures of intermediates and chromones **49**, **49a-49h** were elucidated by infrared (IR), proton nuclear magnetic resonance (¹H-NMR), low resolution mass spectrometry (LRMS) and high resolution mass spectrometry (HRMS). The results were in agreement with the assigned structures in all cases (Appendix section).

IR spectrum of chromone **49** showed the frequency of O-H stretching at 3495 and 3092 cm⁻¹, C=O stretching at 1630 cm⁻¹, C=C stretching at 1602, 1590 and 1471 cm⁻¹, C-H bending at 1346 cm⁻¹, C-O stretching at 1293, 1266, 1145 and 1027 cm⁻¹ (Figure 6.4). The ¹H-NMR spectrum of chromone **49** was shown in Figure 6.5.

**Figure 6.4** IR spectrum of chromone **49**.

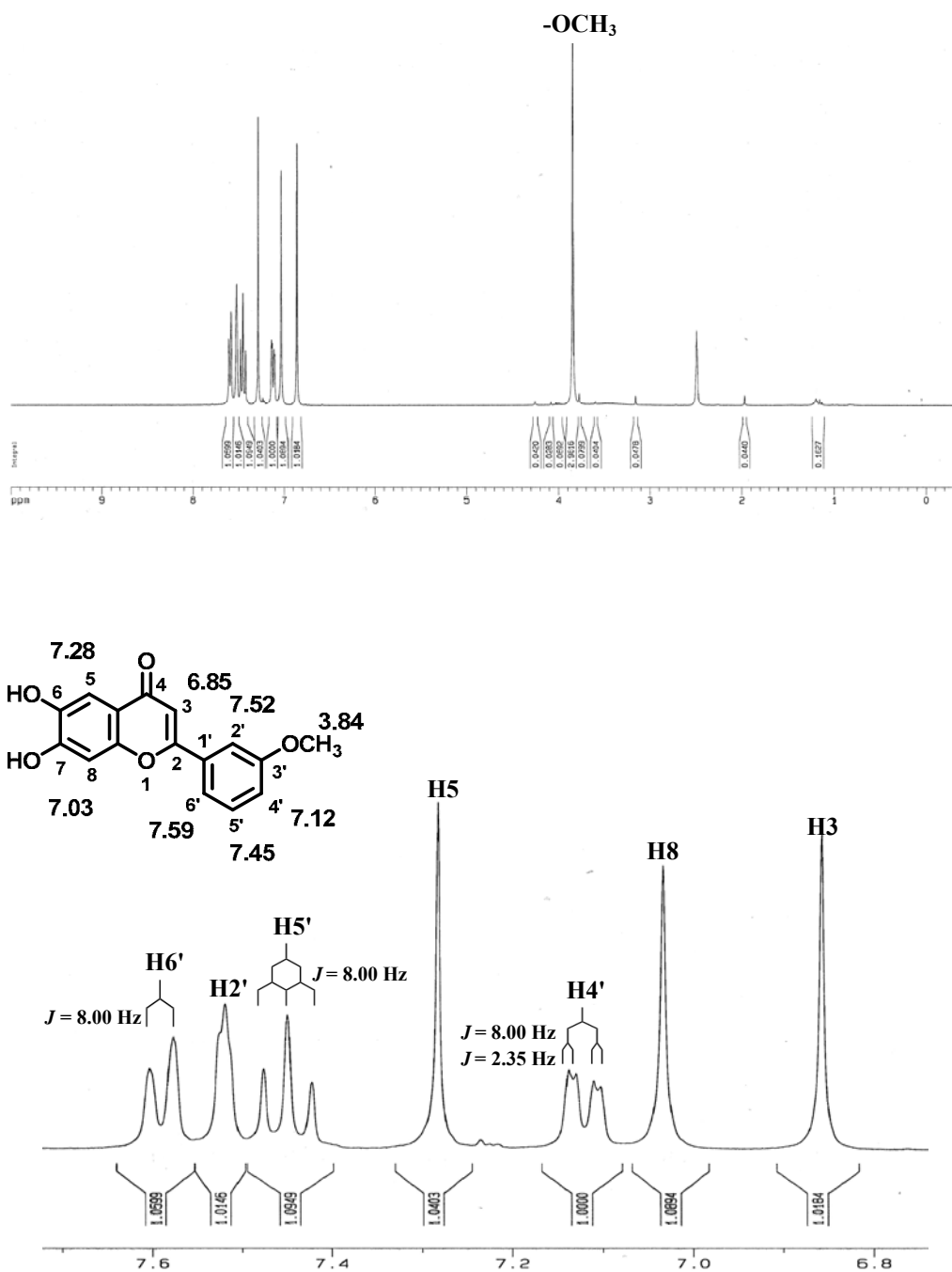


Figure 6.5 ^1H -NMR spectra (300 MHz, DMSO-d_6) of chromone **49**.

The modified chromone derivatives (**49a-49h**) showed the similar pattern of IR spectrum, e.g., IR spectrum of chromone **49c** (Figure 6.6) showed the frequency of aromatic C-H stretching at 3076 cm^{-1} , aliphatic C-H stretching at 2925 and 2831 cm^{-1} , carbonyl C=O stretching at 1742 and 1654 cm^{-1} , C=C stretching at 1602 and 1517 cm^{-1} , C-H bending at 1453 and 1347 cm^{-1} , C-O stretching at 1295, 1271, 1218, 1172, 1145 and 1084 cm^{-1} .

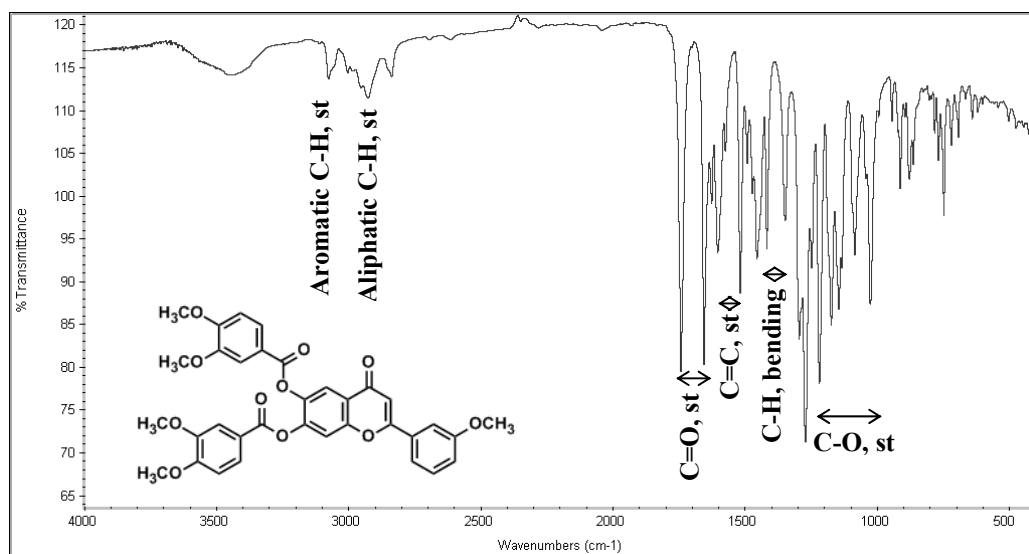


Figure 6.6 IR spectrum of chromone **49c**.

The ^1H -NMR and ^1H - ^1H COSY spectrum of chromone **49c** were shown in Figure 6.7 and Figure 6.8 respectively. The details of ^1H -NMR data and ^1H - ^1H correlation of chromone **49c** were summarized in Table 6.8.

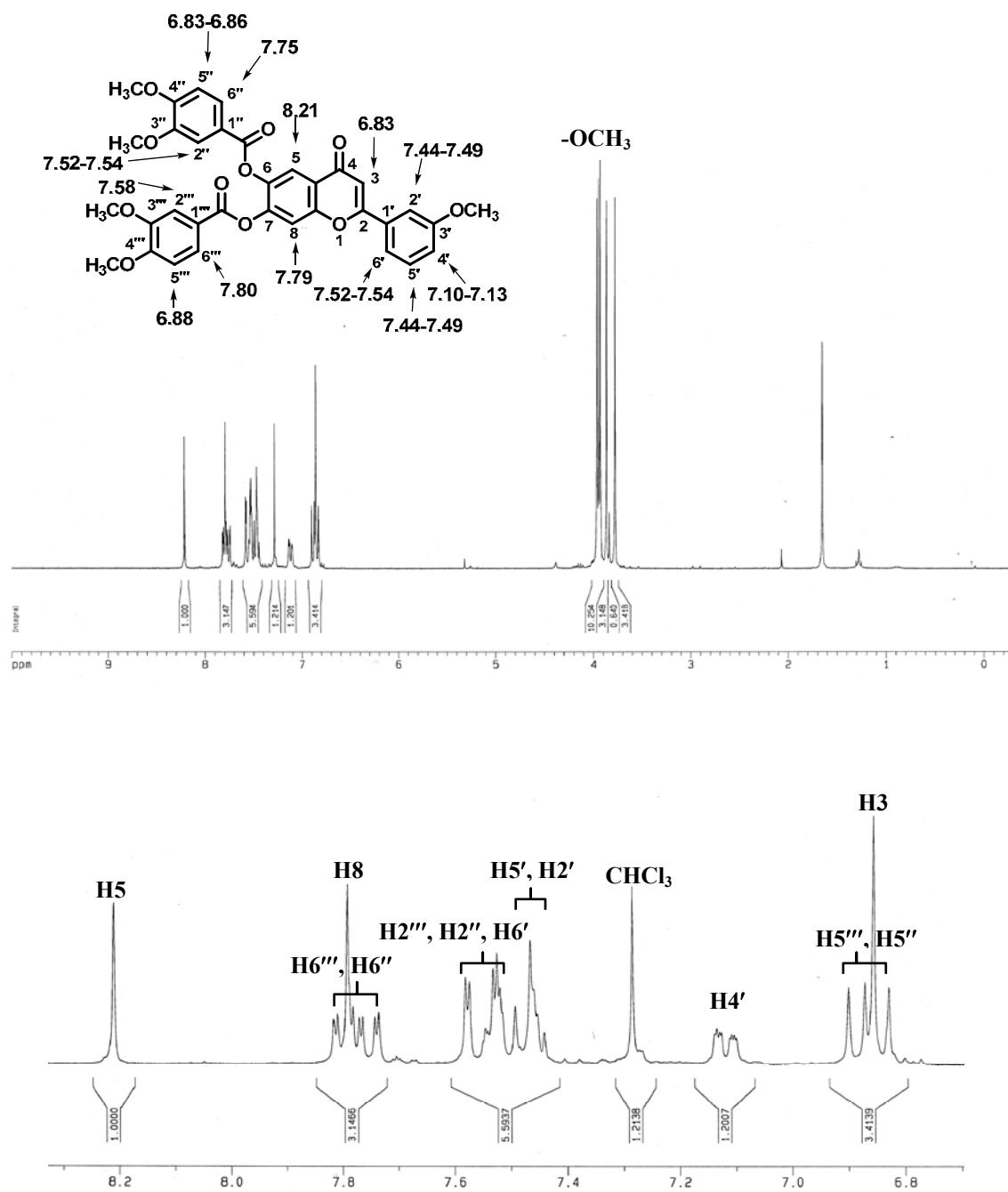


Figure 6.7 ^1H -NMR spectra (300 MHz, CDCl_3) of chromone **49c**.

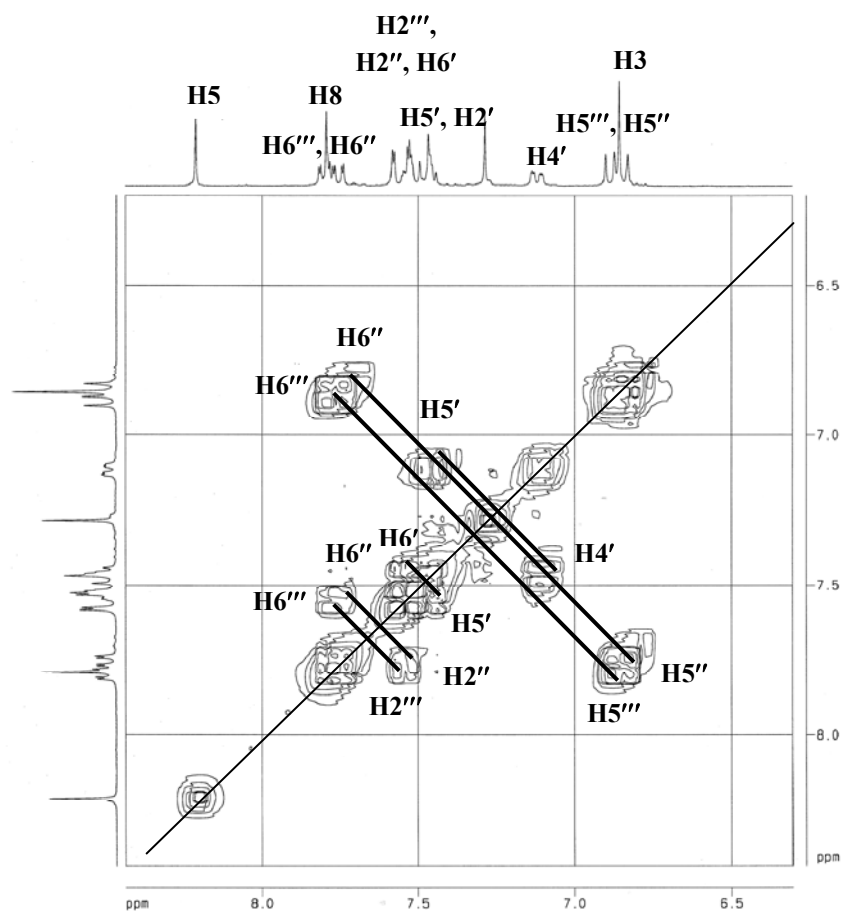


Figure 6.8 ^1H - ^1H COSY spectra (300 MHz, CDCl_3) of chromone **49c**.

Table 6.8 ^1H -NMR data and ^1H - ^1H correlation of chromone **49c**.

H	δ (ppm)	Multiplicity (coupling protons)	J (Hz)	^1H - ^1H COSY
OCH_3	3.78, 3.86, 3.92, 3.94, 3.96	s	-	-
$\text{H5}''$	6.83-6.86	m	-	$\text{H6}''$
H3	6.86	s	-	-
$\text{H5}'''$	6.88	d ($\text{H6}'''$)	8.50	$\text{H6}'''$
$\text{H4}'$	7.10-7.13	m	-	$\text{H5}'$
$\text{H2}', \text{H5}'$	7.44-7.49	m	-	$\text{H4}', \text{H6}'$
$\text{H6}', \text{H2}''$	7.52-7.54	m	-	$\text{H5}'/ \text{H6}''$
$\text{H2}'''$	7.58	d ($\text{H6}'''$)	1.95	$\text{H6}'''$
$\text{H6}''$	7.75	dd ($\text{H5}'', \text{H2}''$)	8.48, 1.97	$\text{H5}'', \text{H2}''$
H8	7.79	s	-	-
$\text{H6}'''$	7.80	dd ($\text{H5}''', \text{H2}'''$)	8.50, 2.00	$\text{H5}''', \text{H2}'''$
H5	8.21	s	-	-

The ^1H -NMR and ^1H - ^1H COSY spectrum of chromone **49d** were shown in Figure 6.9 and Figure 6.10, respectively. The details of ^1H -NMR data and ^1H - ^1H correlation of chromone **49d** were summarized in Table 6.9. The high resolution mass spectrometry of chromone **49** and chromones **49a-49h** were listed in Table 6.10.

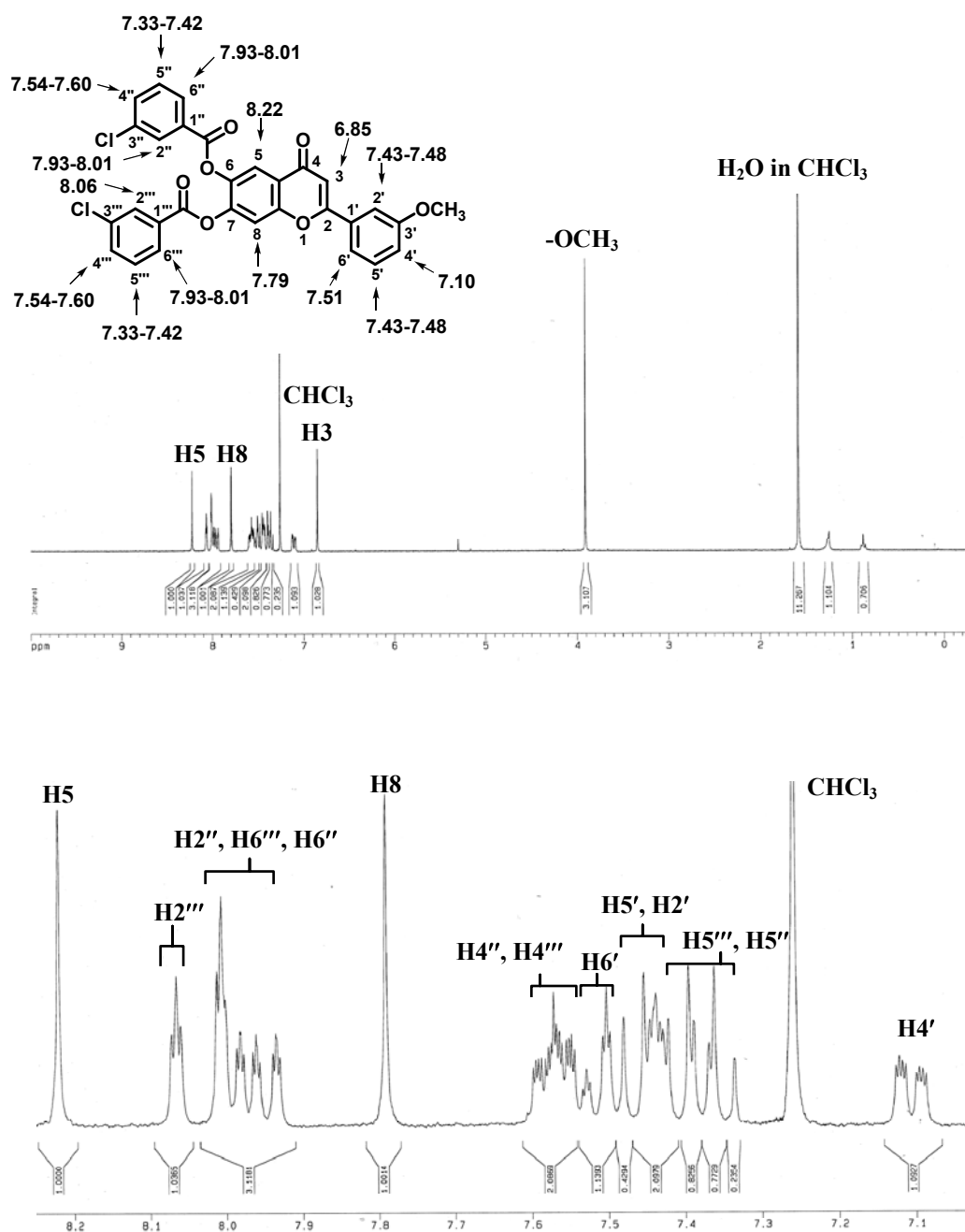


Figure 6.9 ^1H -NMR spectra (300 MHz, CDCl_3) of chromone **49d**.

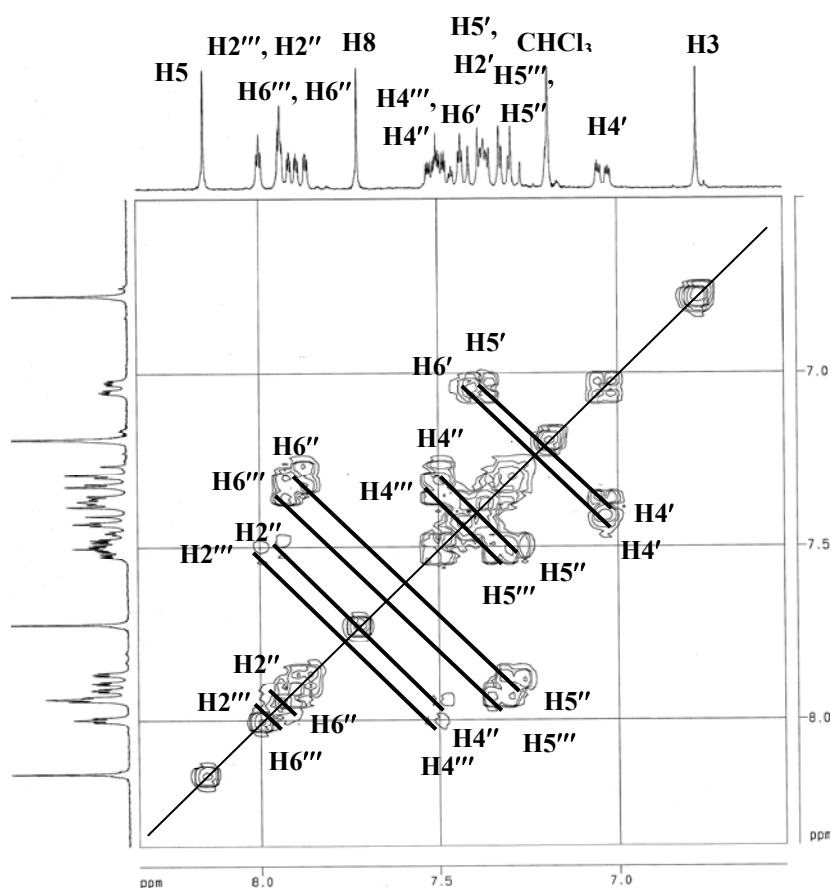
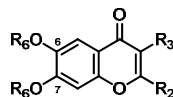


Figure 6.10 ^1H - ^1H COSY spectra (300 MHz, CDCl_3) of chromone **49d**.

Table 6.9 ^1H -NMR data and ^1H - ^1H correlation of chromone **49d**.

H	δ (ppm)	Multiplicity (coupling protons)	J (Hz)	^1H - ^1H COSY
OCH_3	3.91	s	-	-
H3	6.85	s	-	-
H4'	7.10	ddd (H5', H6', H2')	7.96, 2.52, 1.22	H5', H6'
H5'', H5'''	7.33-7.42	m	-	H4'', H6''/ H4''', H6'''
H2', H5'	7.43-7.48	m	-	H4', H6'
H6'	7.51	dt (H5', H4', H2')	7.86, 1.39	H5', H4'
H4'', H4'''	7.54-7.60	m	-	H5'', H2''/ H5''', H2'''
H8	7.79	s	-	-
H2'', H6'', H6'''	7.93-8.01	m	-	H5'', H2''/ H5''', H2'''/ H6'', H4''
H2'''	8.06	t	1.72	H6''', H4'''
H5	8.22	s	-	-

Table 6.10 The high resolution mass spectrometry (ESI technique) of chromone **49** and chromones **49a-49h**.

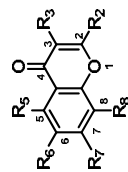
Chromone	R ₂	R ₃	R ₆	HRMS (ESI) Calculation	HRMS (ESI) Observe
49	3'-(OCH ₃)-Phenyl	H	H	285.0759 [*]	285.0755 [*]
49a	3'-(OCH ₃)-Phenyl	H	3'''-(OCH ₃)-benzoyl	575.1311 ^{**}	575.1323 ^{**}
49b	3'-(OCH ₃)-Phenyl	H	4'''-(OCH ₃)-benzoyl	575.1311 ^{**}	575.1334 ^{**}
49c	3'-(OCH ₃)-Phenyl	H	3''',4'''-(diOCH ₃)-benzoyl	653.1521 ^{**}	653.1557 ^{**}
49d	3'-(OCH ₃)-Phenyl	H	3'''-(Cl)-benzoyl	583.0321 ^{**}	583.0348 ^{**}
49e	3'-(OCH ₃)-Phenyl	H	4'''-(Cl)-benzoyl	583.0321 ^{**}	583.0342 ^{**}
49f	3'-(OCH ₃)-Phenyl	H	3''',4'''-(diCl)-benzoyl	650.9541 ^{**}	650.9589 ^{**}
49g	3'-(OCH ₃)-Phenyl	H	3'''-(NO ₂)-benzoyl	605.0803 ^{**}	605.0852 ^{**}
49h	3'-(OCH ₃)-Phenyl	H	4'''-(NO ₂)-benzoyl	605.0803 ^{**}	605.0848 ^{**}

^{*} [M+H]⁺^{**} [M+Na]⁺

6.3 Antimalarial activity assay against *P. falciparum*

As discussed earlier, the preliminary activity screening of chromone derivatives was carried out using docking study against Plm II. However the direct Plm II inhibitory activity test is unavailable during this study period, the antimalarial against *P. falciparum* was evaluated *in vitro* by microculture radioisotope method. The uptake amounts of radiolabeled hypoxanthine were quantified as the signal count per minute (CPM) by the liquid scintillation counter to determine the level of parasites growth. Twenty chromones compounds from the docking study and the newly designed chromone **49** were evaluated against *P. falciparum* (K1 multi-drug resistant strain). The results of the antimalarial activity of these chromone compounds were shown in Table 6.11. Most of the tested compounds (except chromones **18**, **19**, **25**, **26**, **31** and **34**) exhibited the antimalarial activity with IC₅₀ values in the range of 0.95-19.66 μM. The three most potent compounds were chromones **35**, **38** and **44** with IC₅₀ = 0.95, 4.87, 5.46 μM, respectively whereas the well known antimalarial drugs currently used in patients, i.e., primaquine, tafenoquine and chloroquine possessed IC₅₀ 2.41 ± 0.10, 1.95 ± 0.06 and 0.42 ± 0.10 μM, respectively (54).

Table 6.11 The antimalarial activity of twenty selected chromone compounds and chromone **49**.



Cpd	R ₂	R ₃	R ₅	R ₆	R ₇	R ₈	Final Conc. (μg/mL)	Radioactivity (counts per minute: CPM _T)			% Parasite growth ^a	Activity ^b	IC ₅₀ (μg/mL)	IC ₅₀ (μM)
								CPM1	CPM2	Average				
3	Benzyl	H	H	H	OH	OH	10	426	505	466	3.1	Active	2.53	9.43
							1	11586	10419	11003	81.8			
4	Phenyl	H	H	H	OH	OH	10	5084	5581	5333	28.1	Active	5.00	19.66
							1	18119	19349	19147	100.8			
16	4'-(<i>t</i> -butyl)-Phenyl	H	H	H	OH	H	10	3262	3479	3371	17.7	Active	3.41	11.41
							1	16411	16567	16489	86.8			
17	3'-(CF ₃)-Phenyl	H	OH	H	OH	H	10	2702	3328	3015	15.9	Active	3.57	11.07
							1	17638	17351	17495	92.1			
18	4'-(F)-Phenyl	H	OH	H	OH	H	10	11536	12183	11860	62.5	Inactive	-	-
							1	17292	17143	17218	90.7			
19	3',4'-(diF)-Phenyl	H	OH	H	OH	H	10	14326	14406	14366	75.7	Inactive	-	-
							1	16570	16656	16613	87.5			
20	4'-(<i>t</i> -butyl)-Phenyl	H	OH	H	OH	H	10	832	979	906	4.8	Active	2.88	9.15
							1	16965	16654	16810	88.5			
23	3'-(Cl)-Phenyl	H	OH	H	OH	H	10	4200	4849	4525	23.8	Active	4.11	13.83
							1	17631	17181	17406	91.7			
24	3',4'-(diCl)-Phenyl	H	OH	H	OH	H	10	1844	109	106	0.5	Active	2.65	11.25
							1	17525	18129	17059	86.4			

Table 6.11 The antimalarial activity of twenty selected chromone compounds and chromone **49** (cont.).

Cpd	R ₂	R ₃	R ₅	R ₆	R ₇	R ₈	Final Conc. (μg/mL)	Radioactivity (counts per minute: CPM _T)			% Parasite growth ^a	Activity ^b	IC ₅₀ (μg/mL)	IC ₅₀ (μM)
								CPM1	CPM2	Average				
25	4'-(OCH ₃)-Phenyl	H	OH	H	OH	H	10	11672	13162	12417	72.5	Inactive	-	-
							1	13929	12741	13335	87.9			
26	3'-(OCH ₃)-Phenyl	H	OH	H	OH	H	10	13476	13880	13678	72.0	Inactive	-	-
							1	17737	18314	18026	94.9			
27	3'-(OCH ₃)-Phenyl	H	H	OH	H	H	10	5998	6138	6068	32.0	Active	3.55	13.23
							1	12901	14476	13689	72.1			
31	3'-(CF ₃)-Phenyl	3''-(CF ₃)-Benzoyl	H	H	OH	OH	10	17434	17354	17394	91.6	Inactive	-	-
							1	18303	17965	18134	95.5			
34	4'-(F)-Phenyl	4''-(F)-Benzoyl	H	H	OH	OH	10	17610	17507	17559	92.5	Inactive	-	-
							1	18485	18133	18309	96.4			
35	4'-(NO ₂)-Phenyl	4''-(NO ₂)-Benzoyl	H	H	OH	OH	1	4475	4108	4292	22.5	Active	0.429	0.95
							0.1	18124	18909	18517	97.2			
37	3',4'-(diF)-Phenyl	3'',4''-(diF)-Benzoyl	H	H	OH	H	10	6649	6629	6639	34.9	Active	5.14	12.40
							1	17445	15769	16607	87.2			
38	3'-(CF ₃)-Phenyl	3''-(CF ₃)-Benzoyl	H	H	OH	H	10	258	255	257	1.3	Active	2.33	4.87
							1	15221	14597	14909	78.3			
42	4'-(NO ₂)-Phenyl	4''-(NO ₂)-Benzoyl	H	H	OH	H	10	5154	5767	5461	28.7	Active	4.26	9.85
							1	17295	15539	14909	86.2			
44	4'-(<i>t</i> -butyl)-Phenyl	4''-(<i>t</i> -butyl)-Benzoyl	H	H	OH	H	10	272	304	288	1.5	Active	2.50	5.46
							1	16171	15074	15623	82.0			

Table 6.11 The antimalarial activity of twenty selected chromone compounds and chromone **49** (cont.).

Cpd	R ₂	R ₃	R ₅	R ₆	R ₇	R ₈	Final Conc. (µg/mL)	Radioactivity (counts per minute: CPM _T)			% Parasite growth ^a	Activity ^b	IC ₅₀ (µg/mL)	IC ₅₀ (µM)
								CPM1	CPM2	Average				
46	4'-(NO ₂)-Phenyl	4''-(NO ₂)-Benzoyl	OH	H	OH	H	10	103	109	106	0.5	Active	2.65	5.91
							1	17267	16851	17059	86.4			
49	3'-(OCH ₃)-Phenyl	H	H	OH	OH	H	10	2195	2543	2369	15.3	Active	3.96	13.94
							1	15821	15540	15681	101.4			
DHA [*]							5.0 nM	187	225	206	1.3	Active	-	2.02 nM
							1.67 nM	9099	10220	9660	60.1			
MEF [*]							0.1 µM	502	376	439	2.7	Active	-	0.0301
							0.01 µM	15312	14698	15005	93.4			
Negative control							0.1 % DMSO	15846	16277	16062 ^a	100.0	-	-	-
PQ ^{**}													2.41 ± 0.10	
TQ ^{**}													1.95 ± 0.06	
CQ ^{**}													0.42 ± 0.10	

^{*}Positive control: DHA (dihydroartemisinin), MEF (mefloquine)^{**}PQ (primaquine), TQ (tafenoquine) and CQ (chloroquine) (54)^a% Parasite growth = CPM_T/CPM_U x 100^b% Inhibition: < 50% = Inactive; ≥ 50% = Active^cCPM_U

Chromone **35** did not only exhibit the most potent antimalarial activity against *P. falciparum*, but also showed the best binding energy (-13.24 kcal/mole, Table 6.2) from the docking study with Plm II. However, the Plm II binding energy and antimalarial activity were not correlated for the whole chromone series, data as shown in Tables 6.2 and 6.11. This result referred that the mechanism of antimalarial activity might not involve in inhibiting enzyme Plm II. Due to the types of substituents were not diverse, the structure-activity relationship (SAR) of chromone derivatives as antimalarial agents could not be clearly concluded. However, almost all of the 3-substituted chromone (R_3 = substituted benzoyl), except chromones **31** and **34**, were active as antimalarial agents.

Apart from being the most potent antimalarials in this study ($IC_{50} = 0.95 \mu M$), results from previous study showed that chromone **35** was also potent HIV-1 PR inhibitor with 92.24 % inhibition (9).

Both HIV-1 PR and Plm II are aspartic protease enzymes. HIV-1 PR is a symmetrical homodimer, with each subunits and two Asp25 residues of each subunits act as the catalytic dyad. This enzyme has two flaps which cover the active binding cleft and move to allow substrates or inhibitors to the binding cleft (Figure 6.11). Plm II is a monomer which is formed by single chain of 329 amino acids residues folded into two topologically similar N- and C-terminal domains. The binding cavity contains Asp34 and Asp214 which together represent the catalytic dyad. This enzyme has only one β -hairpin structure (flap) with the ability to interact with substrates and inhibitors cover the binding cavity (Figure 2.4).

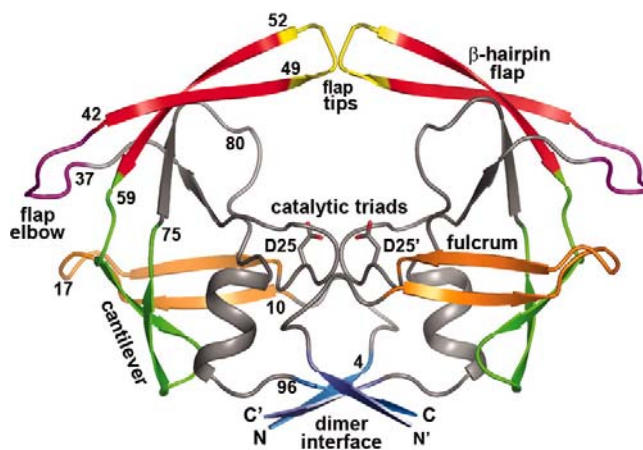


Figure 6.11 Structure of HIV-1 PR enzyme.

The binding interactions of chromone derivatives with HIV-1 PR and Plm II were compared (Figures 6.12 and 6.13). From the previous docking study of chromone derivatives against HIV-1 PR using FlexiDock option in SYBYL/Bio-polymer program, the binding interaction of chromone **31** was used as the representative molecule for discussion (Figure 6.12) (9). The 3-trifluoro-methyl-benzoyl ring bound to S1 subsite (Val32, Ile50', Pro81 and Val82) via hydrophobic interaction with the hydrophobic amino acid residues. The 3-trifluoro-methyl-phenyl ring also formed hydrophobic interaction with the hydrophobic residues in S2 subsite (Leu23, Val32, Val82 and Ile84). The hydroxyl groups at positions 7 and 8 of the chromone formed hydrogen bonds with the carbonyl oxygen of Asp25 and Asp25' (9).

The binding interaction of chromone **35** with Plm II from AutoDock 4.0 program showed the 4-nitro-phenyl ring and 4-nitro-benzoyl ring bind to the S1 (Ile32, Phe111, Ile123 and Gly216) and S2 subsites (Val78, Ile290 Leu292 and Ile300) via hydrophobic interaction with the hydrophobic amino acid residues similar to HIV-1 PR. The hydroxyl groups at positions 7 and 8 of chromone **35** did not form H-bond with the Asp catalytic dyad, but instead hydroxyl group at position 7 formed H-bond with the carbonyl oxygen of Asn76 (Figure 6.13).

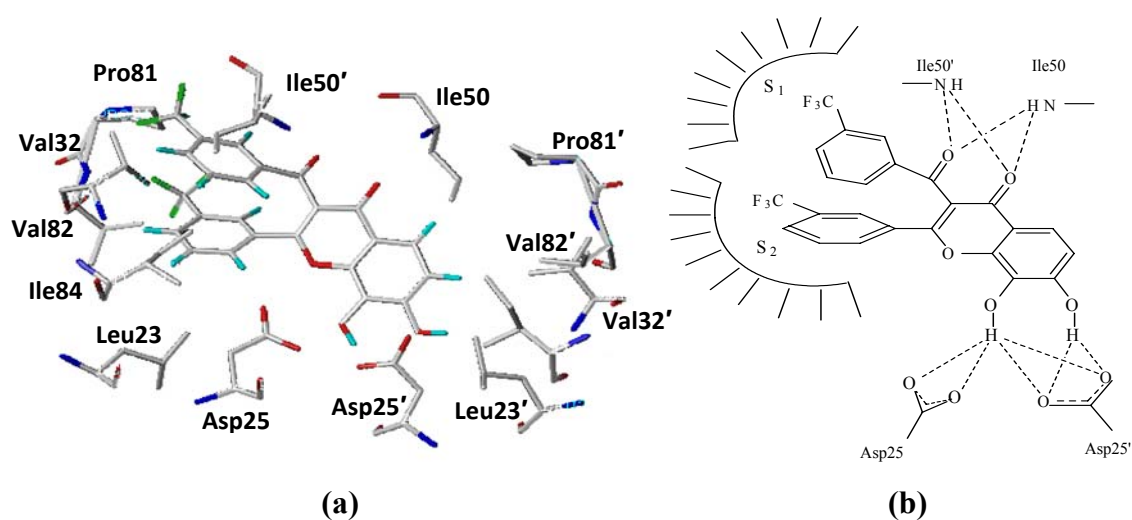


Figure 6.12 Hydrophobic interaction of chromone **31** in the active site of HIV-1 PR (a) and schematic view of the protease active site pockets binding with chromone **31** (b) (9).

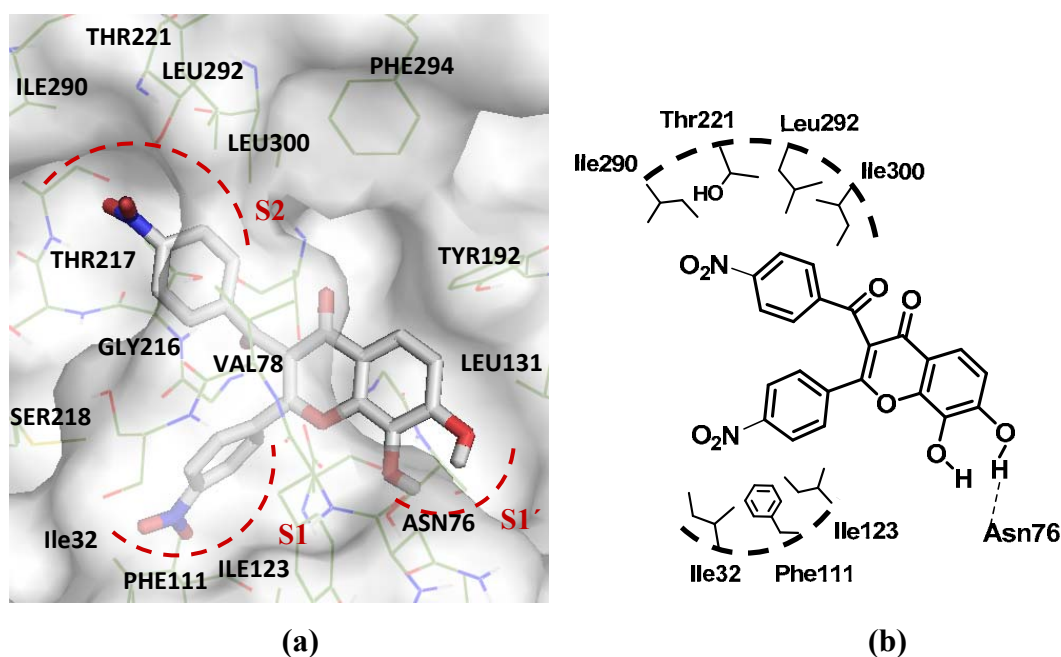
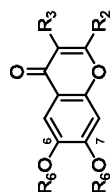
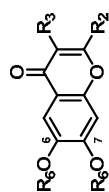


Figure 6.13 The binding interaction of chromone **35** with Plm II from AutoDock 4.0 program (a) and schematic picture showing the interactions between binding pocket of Plm II and chromone **35** (b).

The modified compounds (chromones **49a-49h**) were also evaluated for the antimalarial activity against *P. falciparum*. The results of the antimalarial activity of chromones **49a-49h** were shown in Table 6.12. Unfortunately, chromones **49a-49h** were all inactive against *P. falciparum*. The high molecular weights of these chromones resulting from adding more steric substituents at positions 6 and 7 accounted for the poor solubility of these compounds in DMSO (solvent used in the assay). The poor DMSO solubility might be responsible for the dissatisfactory result of the activity testing. Therefore, for the further design of non-peptidomimetic compounds in chromone series, the appropriate structure should be the 4-rings system without bulky substituents at positions 7 and 8.

Table 6.12 The antimalarial activity of chromones **49a-49h**.

Cpd	R ₂	R ₃	R ₆	Final Conc. (μg/mL)	Radioactivity			% Parasite growth ^a	Activity ^b	IC ₅₀ (μg/mL)	IC ₅₀ (μM)
					CPM1	CPM2	Average				
49a[*]	3'-(OCH ₃)-Phenyl	H	3'''-(OCH ₃)-benzoyl	10	14722	14476	14599	94.9	Inactive	-	-
				1	15734	15547	15641	101.2			
49b[*]	3'-(OCH ₃)-Phenyl	H	4'''-(OCH ₃)-benzoyl	10	13814	14241	14028	90.7	Inactive	-	-
				1	15799	14725	15262	98.7			
49c[*]	3'-(OCH ₃)-Phenyl	H	3''',4'''-(diOCH ₃)-benzoyl	10	9234	9212	9223	59.7	Inactive	-	-
				1	14365	13399	13882	89.8			
49d[*]	3'-(OCH ₃)-Phenyl	H	3'''-(Cl)-benzoyl	10	14945	14796	14871	96.2	Inactive	-	-
				1	14279	14747	14513	93.9			
49e[*]	3'-(OCH ₃)-Phenyl	H	4'''-(Cl)-benzoyl	10	14492	15072	14782	95.6	Inactive	-	-
				1	14255	15240	14748	95.4			
49f[*]	3'-(OCH ₃)-Phenyl	H	3''',4'''-(diCl)-benzoyl	10	15153	14995	15117	97.5	Inactive	-	-
				1	15988	15139	15564	99.8			
49g[*]	3'-(OCH ₃)-Phenyl	H	3'''-(NO ₂)-benzoyl	10	15239	14995	15117	97.8	Inactive	-	-
				1	15988	15153	15564	100.7			

Table 6.12 The antimalarial activity of chromones **49a-49h** (cont.).

Cpd	R ₂	R ₃	R ₆	Final Conc. (μg/mL)	Radioactivity (counts per minute: CPM _T)			Parasite growth ^a	Activity ^b	IC ₅₀ (μg/mL)	IC ₅₀ (μM)
					CPM1	CPM2	Average				
49h [*]	3'-(OCH ₃)-Phenyl	H	4'''-(NO ₂)-benzoyl	10	14793	14787	14790	95.7	Inactive	-	-
				1	15728	15907	15818	102.3			
DHA ^{**}	-	-	-	5.0 nM	187	225	206	1.3	Active	-	2.02 nM
				1.67 nM	9099	10220	9660	60.1			
MEF ^{**}	-	-	-	0.1 μM	502	376	439	2.7	Active	-	0.0301
				0.01 μM	15312	14698	15005	93.4			
Negative control	-	-	-	0.1 %	15846	16277	16062 ^c	100.0	-	-	-
				DMSO							

^{*}Partially soluble in 100% DMSO^{**}Positive control: DHA (dihydroartemisinin), MEF (mefloquine)^a% Parasite growth = CPM_T/CPM_U x 100^b% Inhibition: < 50% = Inactive; ≥ 50% = Active^cCPM_U

CHAPTER VII

CONCLUSION

In this study chromone derivatives were designed and synthesized as the non-peptidomimetic Plm II inhibitors. The preliminary screening of Plm II inhibitory activity of the previous forty-six synthesized chromones with HIV-1 PR inhibitory activities were performed by docking study using AutoDock program. Chromone compounds which showed good binding energy with Plm II and high HIV-1 PR inhibitory activity (more than 70 % inhibition) were selected to evaluate for their antimalarial activity against *P. falciparum* (K1 multi-drug resistant strain) using the microculture radioisotope technique. Most of the tested compounds (except chromones **18**, **19**, **25**, **26**, **31** and **34**) exhibited the antimalarial activity with IC_{50} values in the range of 0.95-19.66 μ M. The three most potent compounds were chromones **35**, **38** and **44** with IC_{50} = 0.95, 4.87, 5.46 μ M, respectively. The most active chromone **35**, which exhibited high potency against HIV-1 PR, showed better antimalarial activity than the currently used drugs, i.e., primaquine (IC_{50} = 2.41 ± 0.10 μ M) and tafenoquine (IC_{50} = 1.95 ± 0.06 μ M). The structure-activity relationship (SAR) of chromone derivatives as antimalarial agents could not be clearly deduced because the substituents types were not diverse enough. However, almost all of the 3-substituted chromones (R_3 = substituted benzoyl), except chromones **31** and **34**, were active as antimalarial agents.

Based on docking results, a series of newly designed chromones (**49a-49i**) were synthesized as Plm II inhibitors. The synthesis route was mainly divided into two parts. Firstly, the chromone core structure was prepared by Baker-Venkataraman rearrangement and subsequent intramolecular cyclization with a catalytic amount of strong acid. This synthesis pathway was practical and economical method for chromone structure preparation. Secondly, the esterification at positions 6 and 7 of the chromone structure was performed to provide the designed chromones. All of these newly synthesized compounds were evaluated for their antimalarial activity.

Chromone **49** was found to be the most active compound with $IC_{50} = 13.94 \mu M$ while the modified chromones **49a-49h** were inactive. The failure of chromones **49a-49h** might be due to the poor solubility of these compounds in solvent used in the assay.

REFERENCES

1. Greenwood BM, Bojang K, Whitty CJ, Targett GA, Malaria. Lancet 2005; 365: 1487- 98.
2. Banerjee R, Liu J, Beatty W, Pelosof L, Klemba M, Goldberg DE. Four plasmepsins are active in the *Plasmodium falciparum* food vacuole, including a protease with an active-site histidine. Proc Natl Acad Sci USA 2002; 99: 990-5.
3. Ersmark K, Samuelsson B, Hallberg A. Plasmepsin as potential target for new antimalarial therapy. Med Res Rev 2006; 26 (5): 626-66.
4. Bhaumik P, Gustchina A, Wlodawer A. Structural studies of vacuolar plasmepsins. Biochim Biophys Acta. 2012; 1824: 207-23.
5. Gupta D, Yedidi RS, Varghese S, Kovari LC, Woster PM. Mechanism-based inhibitors of the aspartyl protease plasmepsin II as potential antimalarial agents. J Med Chem 2010; 53 4234-47.
6. Martins TM, Demingos A, Berry C, Wyatt DM. The activity and inhibition of the food vacuole plasmepsin from the rodent malaria parasite *Plasmodium chabaudi*. Acta Trop 2006; 97: 212-8.
7. Parikh S, Liu J, Sijwali P, Gut J, Goldberg DE, Rosenthal P. Antimalarial effect of human immunodeficiency virus type 1 protease inhibitors differs from those of the aspartic protease inhibitor pepstatin. Antimicrob Agents Chemother 2006; 50: 2207-9.
8. Parikh S, Gut J, Istvan E, Goldberg DE, Havlir DV, Rosenthal P. Antimalarial activity of human immunodeficiency virus type 1 protease inhibitors. Antimicrob Agents Chemother 2005; 49 (7): 2983-85.
9. Ungwitayatorn J, Wiwat C, Samee W, Nunthanavanit P, Phosrithong N. Synthesis, *in vitro* evaluation, and docking studies of novel chromone derivatives as HIV-1 protease inhibitor. J Mol Struct 2011; 1001: 152-61.

10. Lehan AM, Saliba KJ. Common dietary flavonoids inhibit the growth of the intraerythrocytic malaria parasite. *BMC Res Notes* 2008; 1:26.
11. Yenjai C, Prasanphen K, Daodee S, Wongpanich V, Kittakoo P. Bioactive flavonoid from *Kaempferia parviflora*. *Fitoterepia* 2004; 75: 89-92.
12. Monbrison FD, Maitrejean M, Latour C, Bugnazet F, Peyron F, Baron D, *et al.* *In vitro* antimalarial activity of flavonoid derivatives dehydrosilibin and 8-(1;1)-DMA-kaempferide. *Acta Trop* 2006; 97: 102-7.
13. Auffer G, Labaied M, Frappier F, Rasoanaivo P, Grellier P, Lewin G. Synthesis and antimalarial evaluation of a series of piperazinyl flavones. *Bioorg Med Chem Lett* 2007; 17: 959-63.
14. Adkins JC, Faulds D. Amprenavir. *Drugs* 1998; 55(6): 837-42.
15. Morris GM, Huey R, Lindstrom W, Sanner MF, Belew RK, Goodsell DS, *et al.* Autodock 4 and autodocktools 4: Automated docking with selective receptor flexibility. *J Comput Chem* 2009; 30(16): 2785-91.
16. Desjardins RE, Canfield CJ, Haynes JD, Chulay JD. Quantitative assessment of antimalarial activity *in vitro* by a semiautomated microdilution technique. *Antimicrob Agents Chemother* 1979; 16 (6): 710-8.
17. Gao H, Kawabata J. Importance of the B ring and its substitution on the α -glucosidase inhibitory activity of baicalein, 5,6,7-trihydroxyflavone. *Biosci Biotechnol Biochem* 2004; 68 (9): 1854-64.
18. Riva C, Toma CD, Donadel L, Boi C, Pennini R, Motta G, *et al.* New DBU (1,8-Diazabicyclo[5.4.0]undec-7-ene) assisted one-pot synthesis of 2,8-disubstituted 4H-1-benzopyran-4-ones. *Synthesis* 1997: 195-201.
19. The World Health Organization. World Malaria Report 2008. Geneva: World Health Organization Press; 2008.
20. Mackintosh CL, Beeson JG, Marsh K. Clinical features and pathogenesis of severe malaria. *Trends Parasitol* 2004; 20: 597-603.
21. Francis SE, Sullivan DJ Jr, Goldberg DE. Hemoglobin metabolism I the malarial parasite *Plasmodium falciparum*. *Annu Rev Microbiol* 1997; 51: 97-123.
22. Skinner-Adams TS, Stack CM, Trenholme KR, Brown CL, Grembecka J, Lowther J, *et al.* *Plasmodium falciparum* neutral aminopeptidases: new targets for anti-malarials. *Trends Biochem Sci* 2010; 35 (1): 53-61.

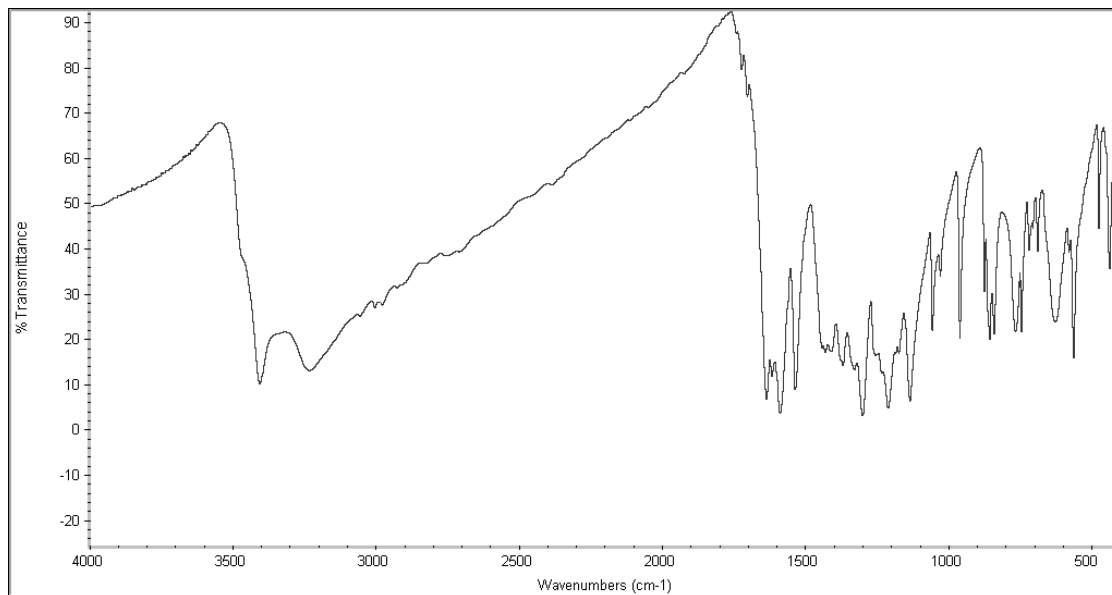
23. Greenwood D. The quinine connection. *J Antimicrob Chemother* 1992; 30:417-27.
24. Rosenthal PJ, editor. Antimalarial chemotherapy: Mechanisms of action, resistances, and new directions in drug discovery. New Jersey: Human Press; 2001.
25. Wongsrichanalai C, Pickard AL, Wernsdorfer WH, Meshnick SR. Epidemiology of drug-resistant malaria. *Lancet Infect Dis* 2002; 2: 209-18.
26. White NJ. Antimalarial combinations. *Lancet* 2004; 364: 285-94.
27. Fitvh CD. Ferriprotoporphyrin IX, phospholipids, and the antimalarial actions of quinine drugs. *Life Sci* 2004; 74: 1957-72.
28. Fernando D, Rodrigo C, Rajapakse S. Primaquine in vivax malaria: an update and review on management issues. *Malaria J* 2011; 10: 1-12.
29. Burger A, Wolff ME, editors. Burger's medicinal chemistry and drug discovery. Volume 5: Therapeutic Agents. New York: John Wiley & Sons; 1997.
30. Tang U, Dong Y, Wang X, Sriraghavan K, Wood JK, Vennerstrom JL. Dispiro-1,2,4-trioxane analogues of a prototype dispiro-1,2,4-trioxolane: Mechanistic comparators for artemisinin in the context of reaction pathway with iron (II). *J Org Chem* 2005; 70: 5103-10.
31. Gregson A, Plowe CV. Mechanisms of resistance of malarial parasites to antifolates. *Pharmacol Rev* 2005; 57: 117-45.
32. Woster PM. New therapies for Malaria. *Ann Rep Med Chem* 2003; 38: 203-11.
33. Olliaro PL, Yuthavong Y. An overview of chemotherapeutic targets for antimalarial drug discovery. *Pharmacol Ther* 1999; 81 (2): 91-110.
34. Craciun D, Isvoran A, Avram NM. Dose fractal characteristics of hemoglobin change from one organism to another. *Rom J Phys* 2009; (54): 569-75.
35. Yayon A, Vande Waa JA, Yayon M, Geary TG, Jensen JB. Stage-dependent effects of chloroquine on *Plasmodium falciparum* in vitro. *J Protozool* 1983; 30: 642-47.
36. Coombs GH, Goldberg DE, Klemba M, Berry C, Kay J Mottram JC. Aspartic protease of *Plasmodium falciparum* and other parasitic protozoa as drug targets. *Trends Parasitol* 2001; 17(11): 532-7.

37. Kamchomwongpaisan S, Samoff E, Meshnick SR. Identification of hemoglobin degradation products in *Plasmodium falciparum*. Mol Biochem Parasitol 1997; 86: 176-86.
38. Silva AM, Lee AY, Gulnik SV, Majer P, Collins J, Bhat TN, et al. Structure and inhibition of plasmepsin II, a hemoglobin-degrading enzyme from *Plasmodium falciparum*. Proc Natl Acad Sci USA 1996; 96: 10034-39.
39. Asojo OA, Gulnik SV, Afonina E, Yu B, Ellman JA, Haque TS, et al. Novel uncomplexed and complexed structures of plasmepsin II, an aspartic protease from *Plasmodium falciparum*. J Mol Biol 2003; 327: 173-81.
40. Matuz K, Motyan J, Li M, Wlodawer A, Tozser J. Inhibition of XMRV and HIV-1 protease by pepstatin A and acetyl-pepstatin. FEBS J 2012; 279: 3276-86.
41. Gutierrez-de-Teran H, Martin N, Eramark K, Liu P, Janka LK, Dunn B, et al. Inhibitor binding to the plasmepsin IV aspartic protease from *Plasmodium falciparum*. Biochemistry-US 2006; 45(35): 10529-41.
42. Peterson J, Dwyer J. Flavonoids: dietary occurrence and biochemical activity. Nutr Res 1998; 18: 1995-2018.
43. Scalebert A, Williamson G. Dietary intake and bioavailability of phenols. J Nutr 2000; 130: 2073S-85S.
44. Tasdemir D, Lack G, Brun R, Rüedi P, Scopozza L, Perozzo R. Inhibition of *Plasmodium falciparum* fatty acid biosynthesis: evaluation of FabG, FabZ, and FabI as drug target for flavonoids. J Med Chem 2006; 49: 3345-53.
45. Noedl H, Wongsrichanalai C, Wernsdorfer WH. Malaria drug-sensitivity testing: new assays, new perspectives. Trends Parasitol 2003; 19 (4): 175-81.
46. Kalra BS, Chawla S, Gupta P, Valecha N. Screening of antimalarial drugs: An overview. Indian J Pharmacol 2006; 1 (38): 5-12.
47. Gottlieb HE, Kotlyar V, Nudelman A. NMR chemical shift of common laboratory solvents as trace impurities. J Org Chem 1997; 62: 7512-5.
48. Trager W, Jensen JB. Human malarial parasites in continuous culture. Science 1976; 193: 673-5.

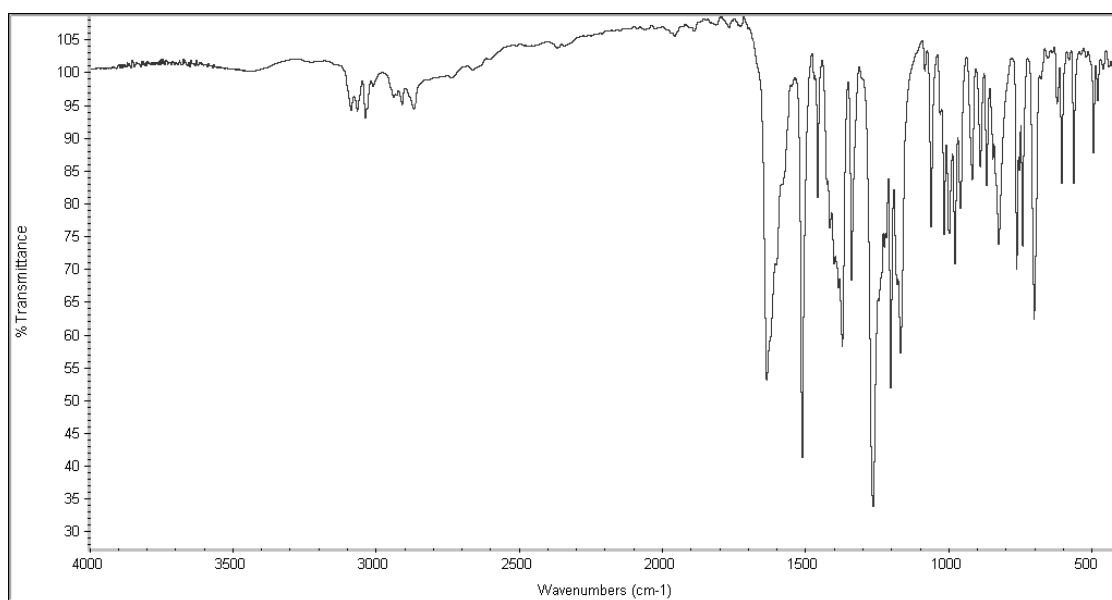
49. Bringmann G, Noll TF, Gulder T, Dreyer M, Grune M, Moskaru D. Polyketide folding in higher plant: biosynthesis of the phenylanthraquinone knipholone. *J Org Chem* 2007; 72 (9): 3247-52.
50. Aponte JC, Verástegui M, Málaga E, Zimic M, Quiliano M, Vaisberg AJ, *et al.* Synthesis, cytotoxicity, and anti-*Trypanosoma cruzi* activity of new chalcones. *J Med Chem* 2008; 51: 6230-4.
51. Saito S, Kawabata J. Effects of electron-withdrawing substituents on DPPH radical scavenging reactions of protocatechuic acid and its analogues in alcoholic solvents. *Tetrahedron* 2005; 61: 8101-8.
52. Fletcher S, Gunning PT. Mild, efficient and rapid O-debenzylation of ortho-substituted phenol with trifluoroacetic acid. *Tetrahedron Lett* 2008; 49: 4817-19.
53. Babu KS, Babu TH, Srinivas PV, Sastry BS, Kishore KH, Murty USN, *et al.* Synthesis and *in vitro* study of novel 7-O-acyl derivatives of oroxylin A as antibacterial agents. *Bioorg Med Chem Lett* 2005; 1: 3953-6.
54. Bray PG, Deed S, Fox E, Kalkanidis M, Mungthin M, Deady LW, *et al.* Primaquine synergises the activity of chloroquine against chloroquine-resistant *P. falciparum*. *Biochem Pharmacol* 2005; 70: 1158-66.

APPENDIX

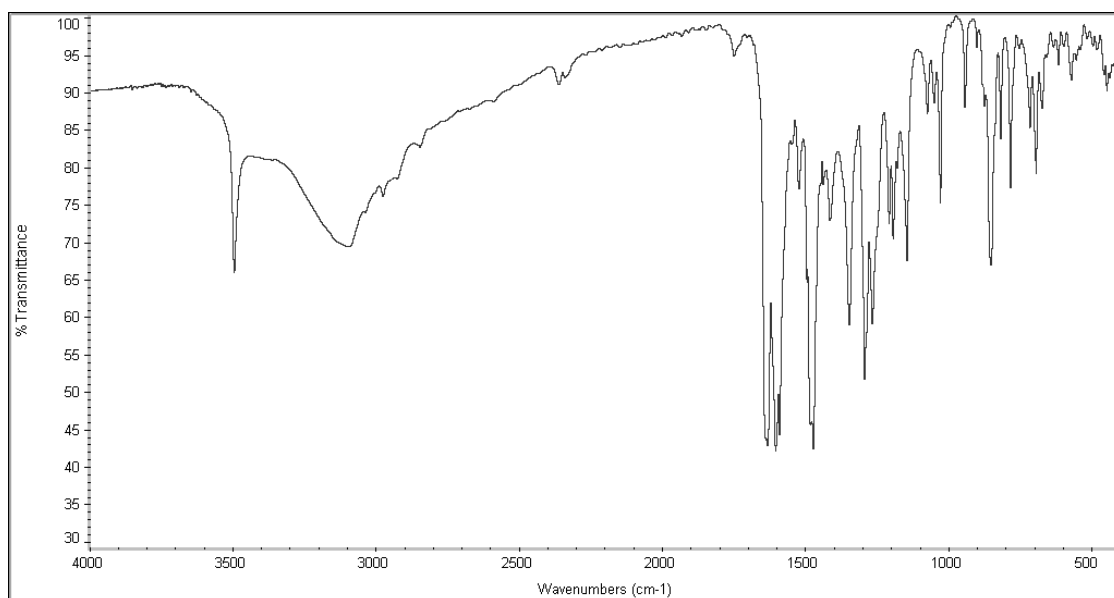
IR spectra



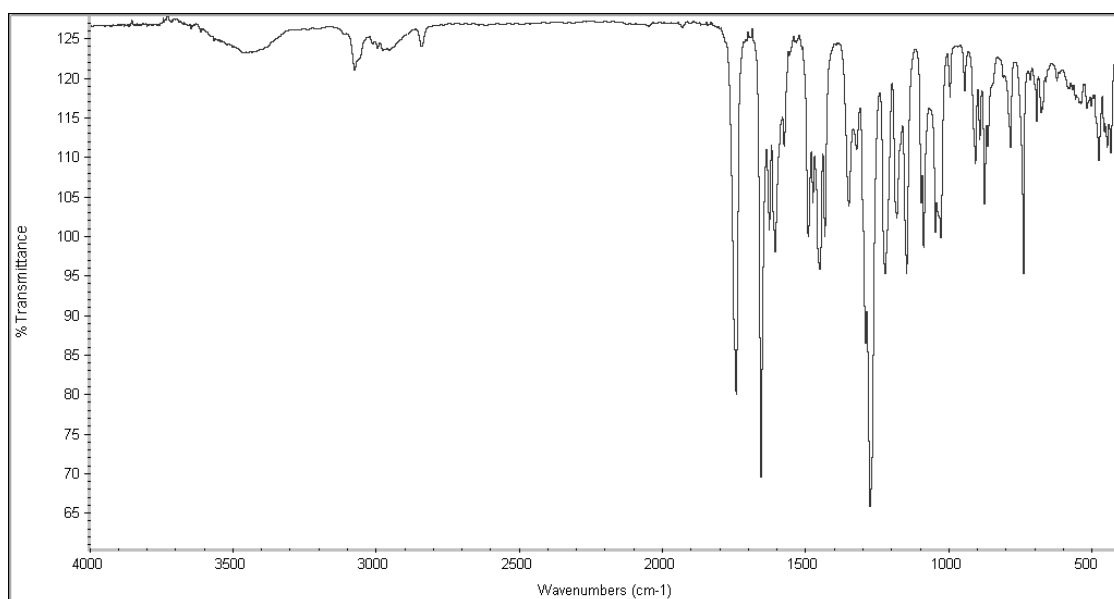
IR spectrum of 2,4,5-trihydroxyacetophenone



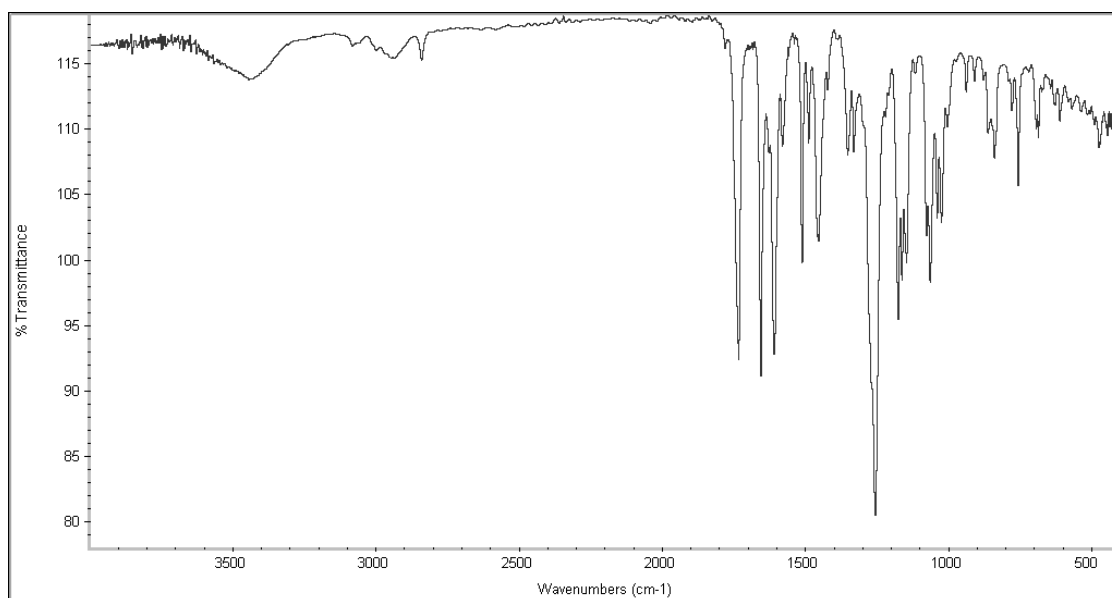
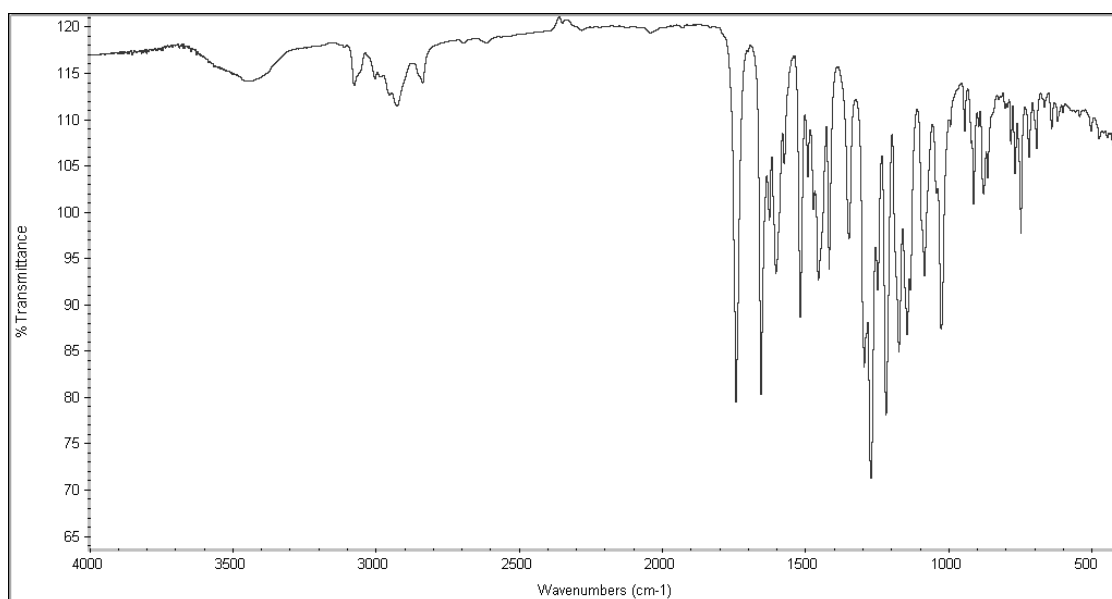
IR spectrum of 4,5-bisbenzyloxy-2-hydroxyacetophenone

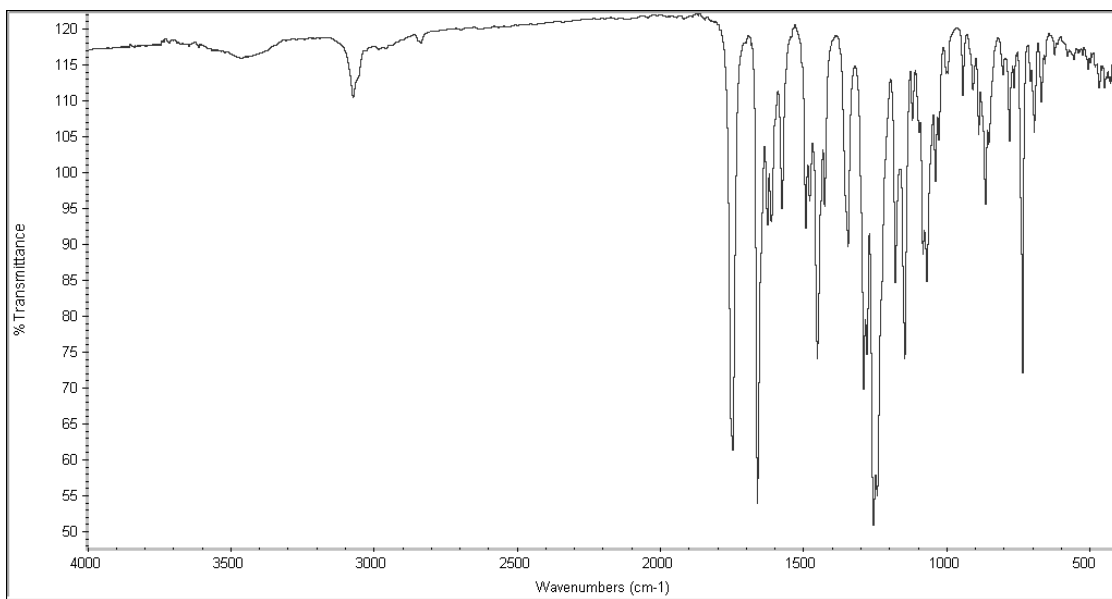


IR spectrum of chromone **49**

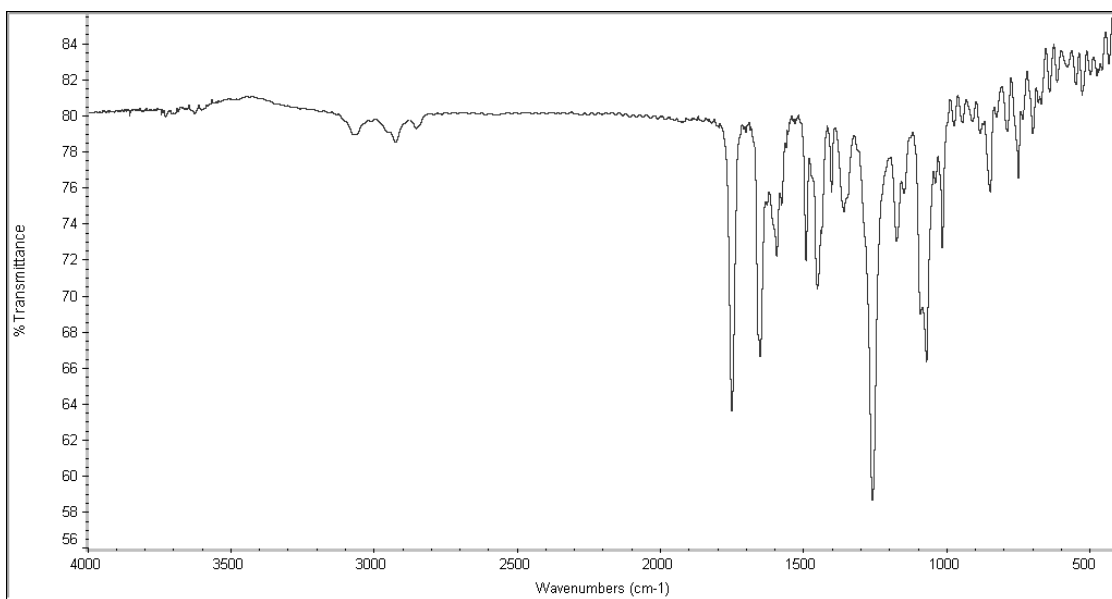


IR spectrum of chromone **49a**

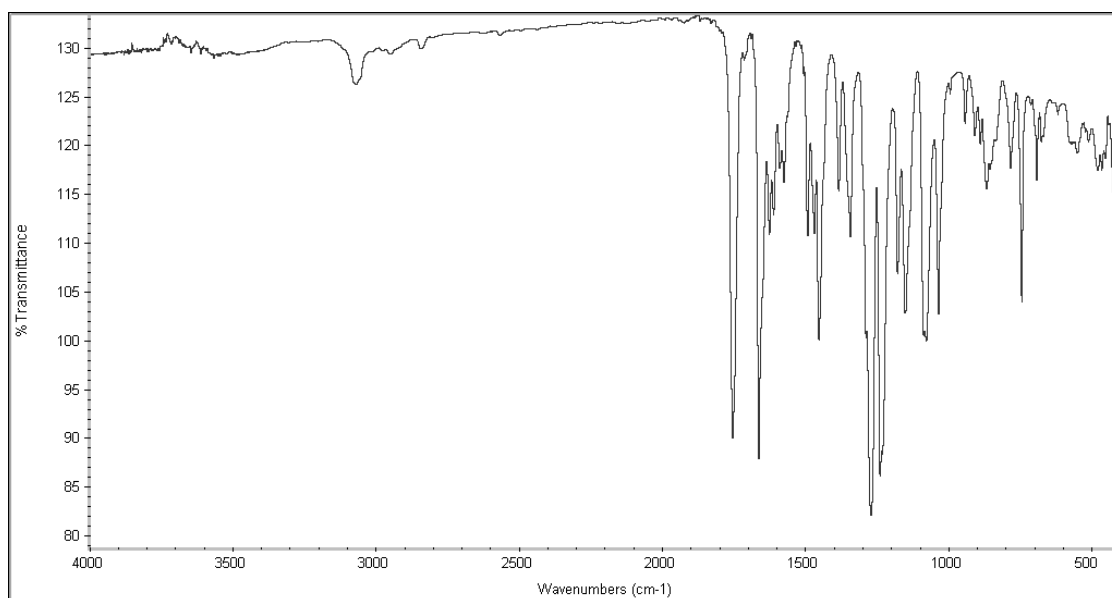
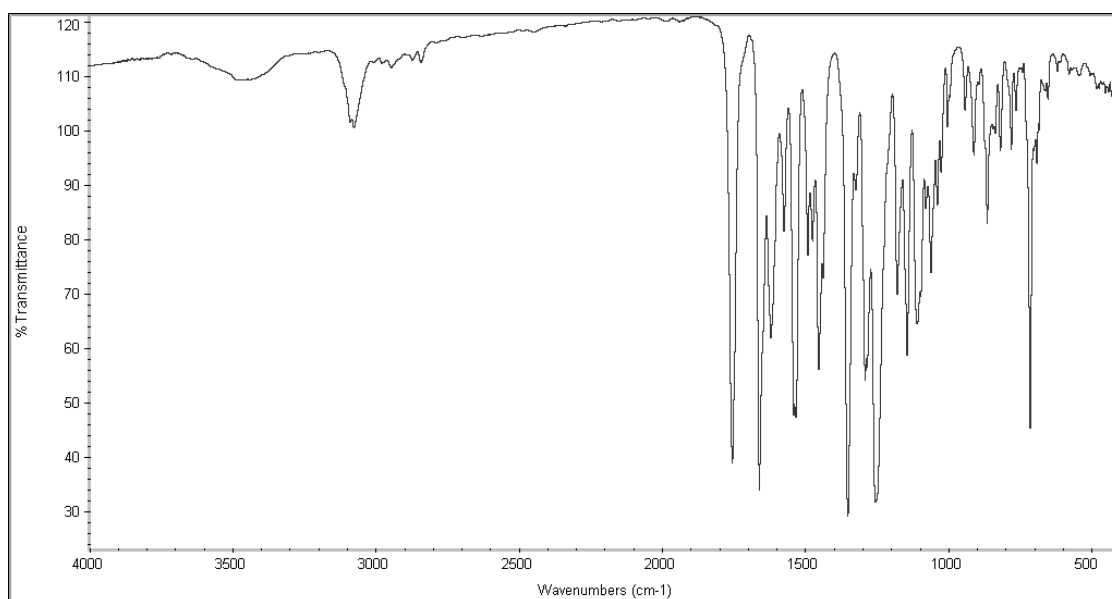
IR spectrum of chromone **49b**IR spectrum of chromone **49c**

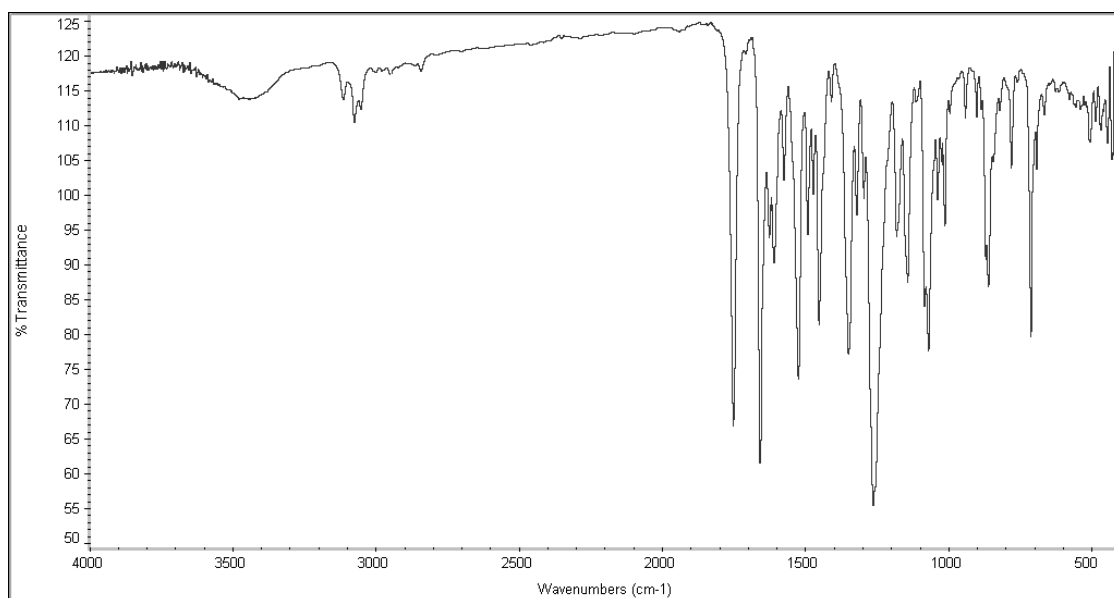


IR spectrum of chromone **49d**



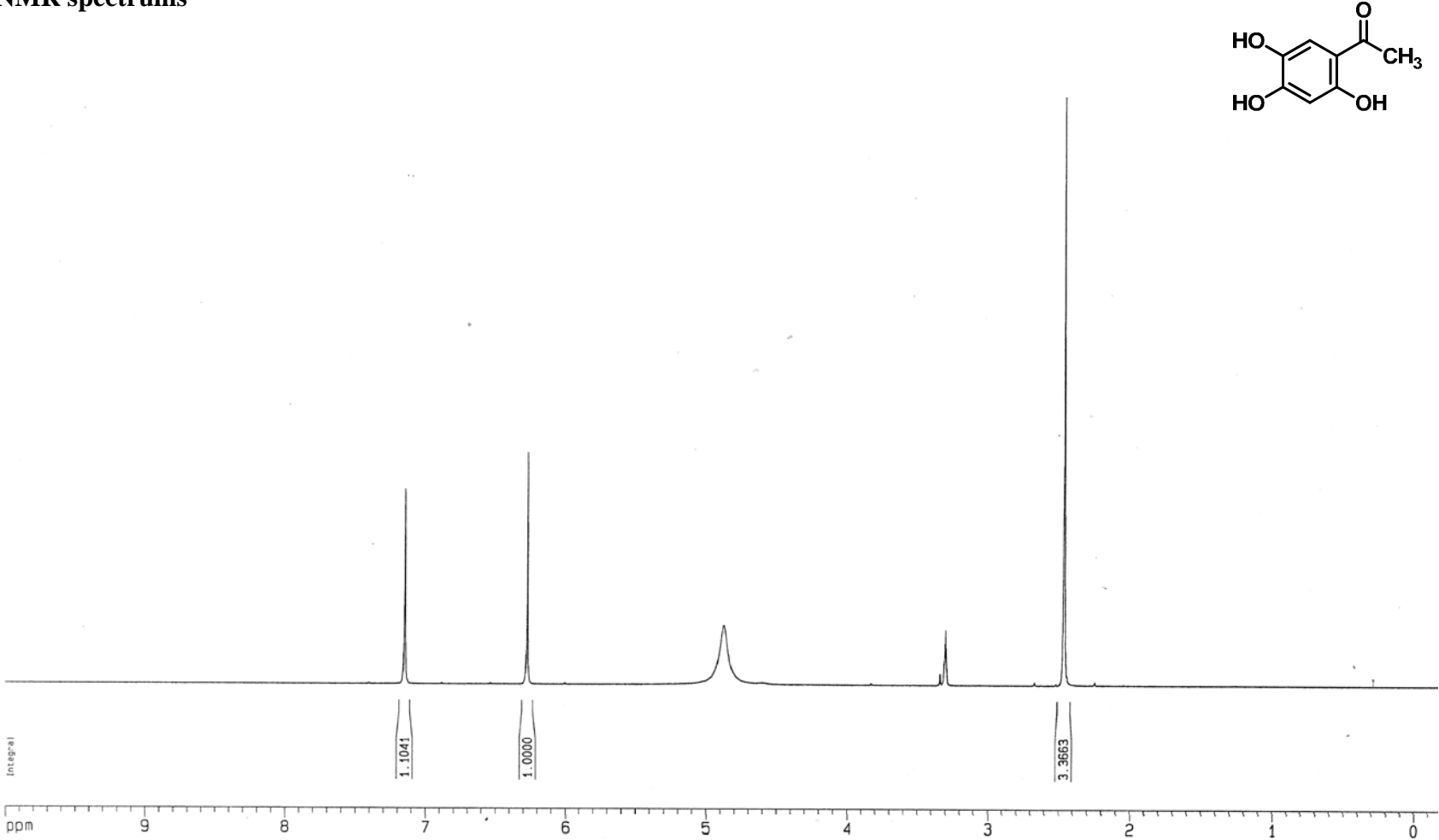
IR spectrum of chromone **49e**

IR spectrum of chromone **49f**IR spectrum of chromone **49g**

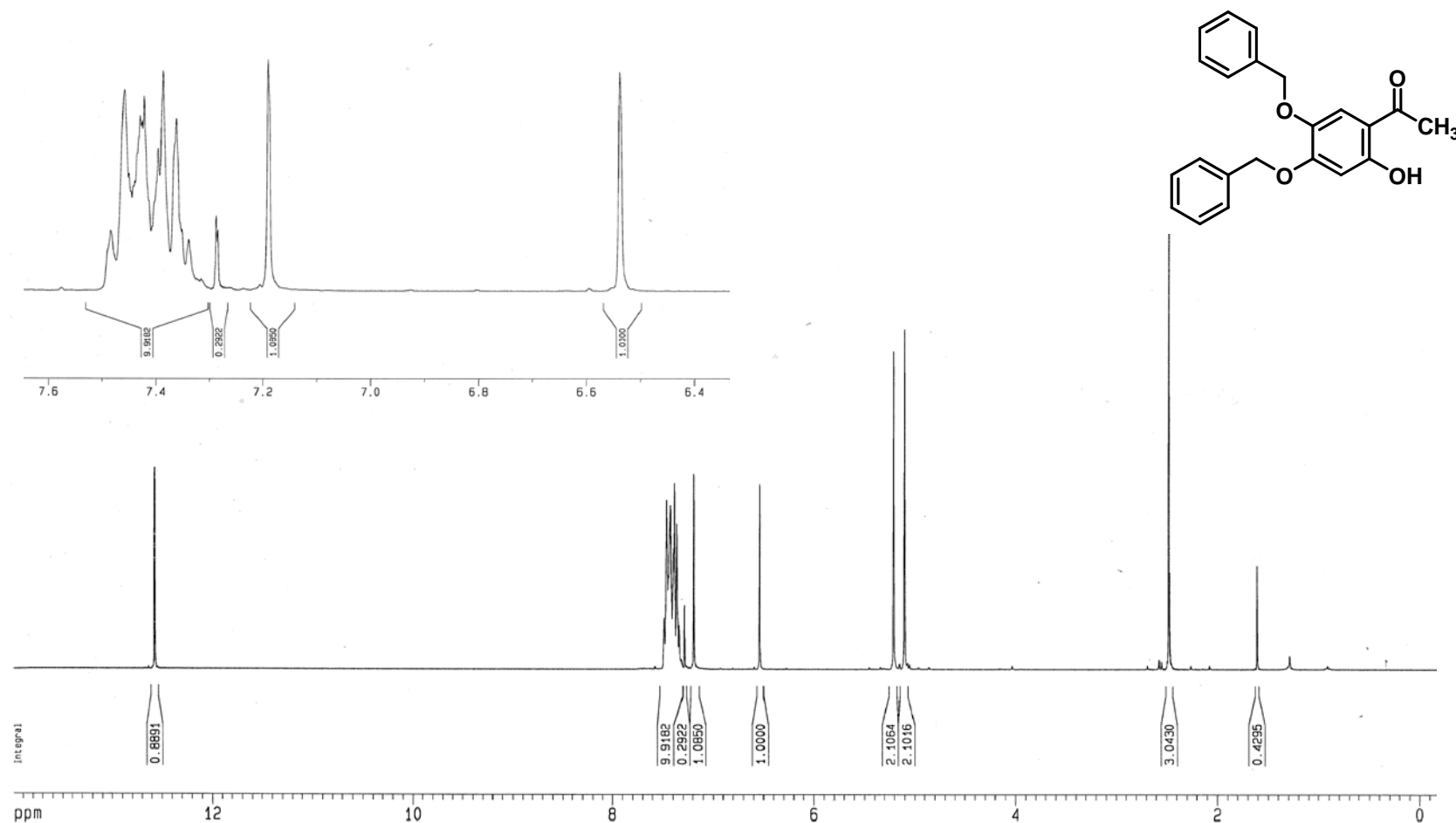


IR spectrum of chromone **49h**

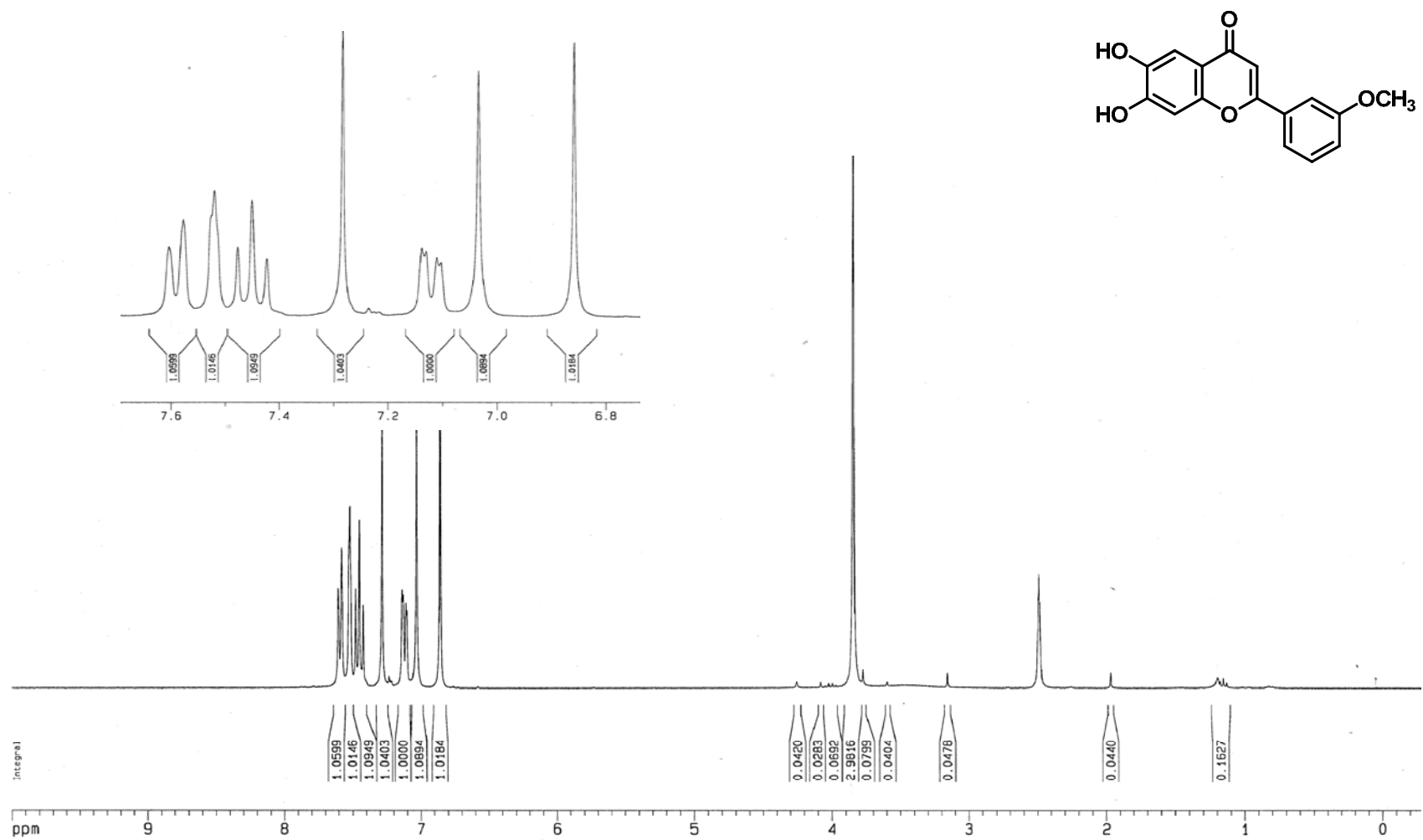
¹H-NMR spectra



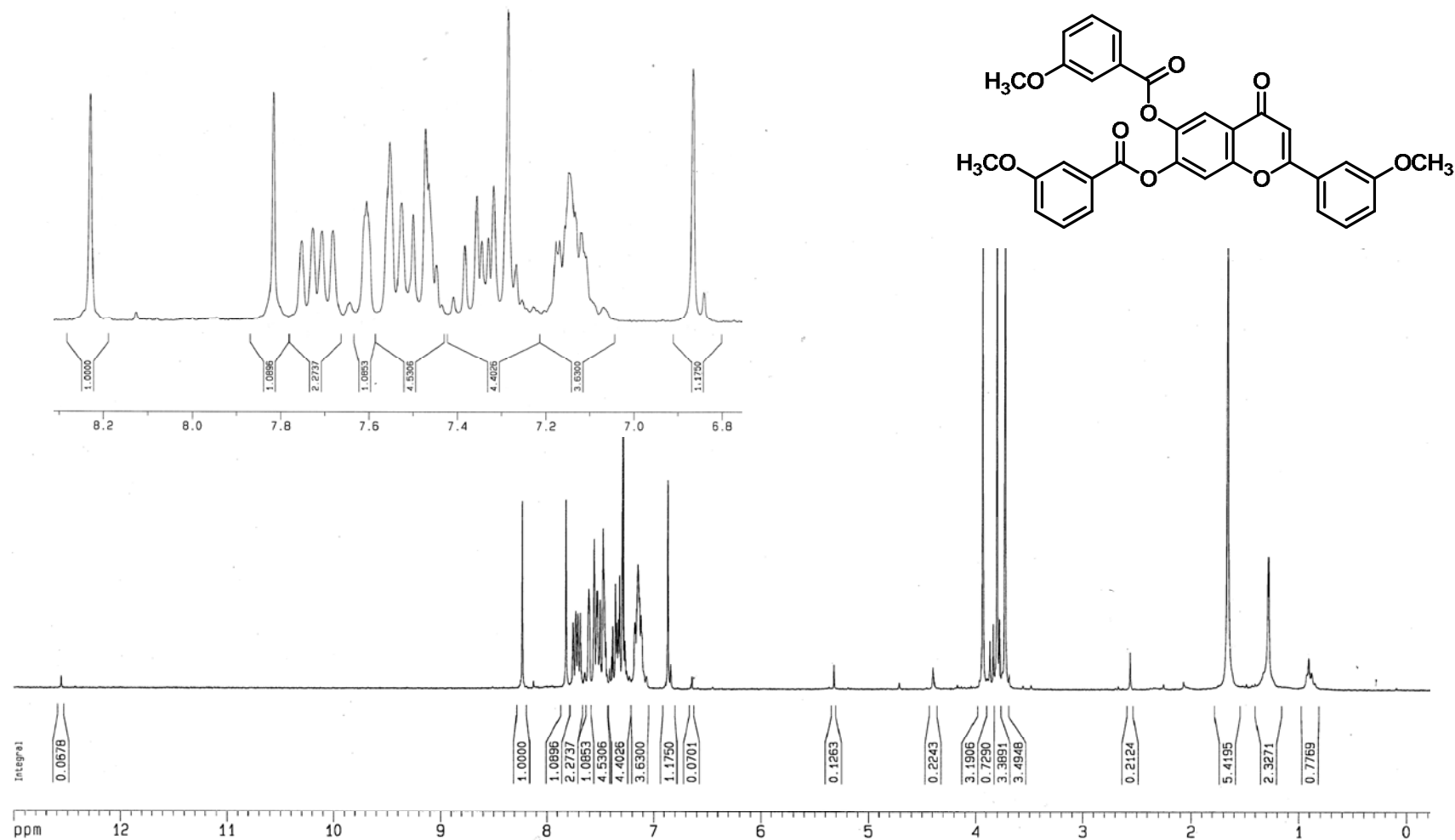
¹H-NMR spectrum (300 MHz) of 2,4,5-trihydroxyacetophenone in CD₃OD



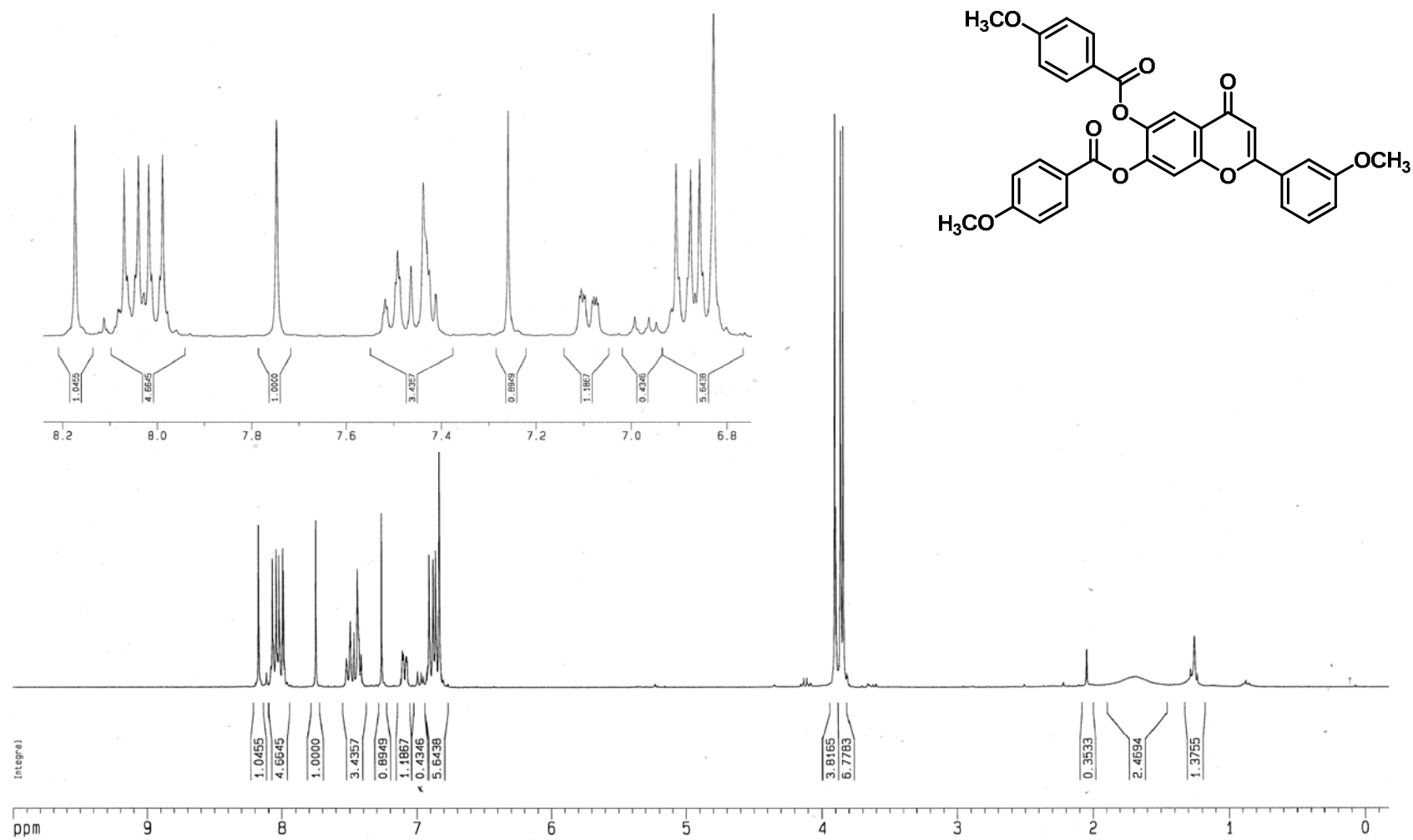
¹H-NMR spectrum (300 MHz) of 4,5-bisbenzyloxy-2-hydroxyacetophenone in CDCl₃



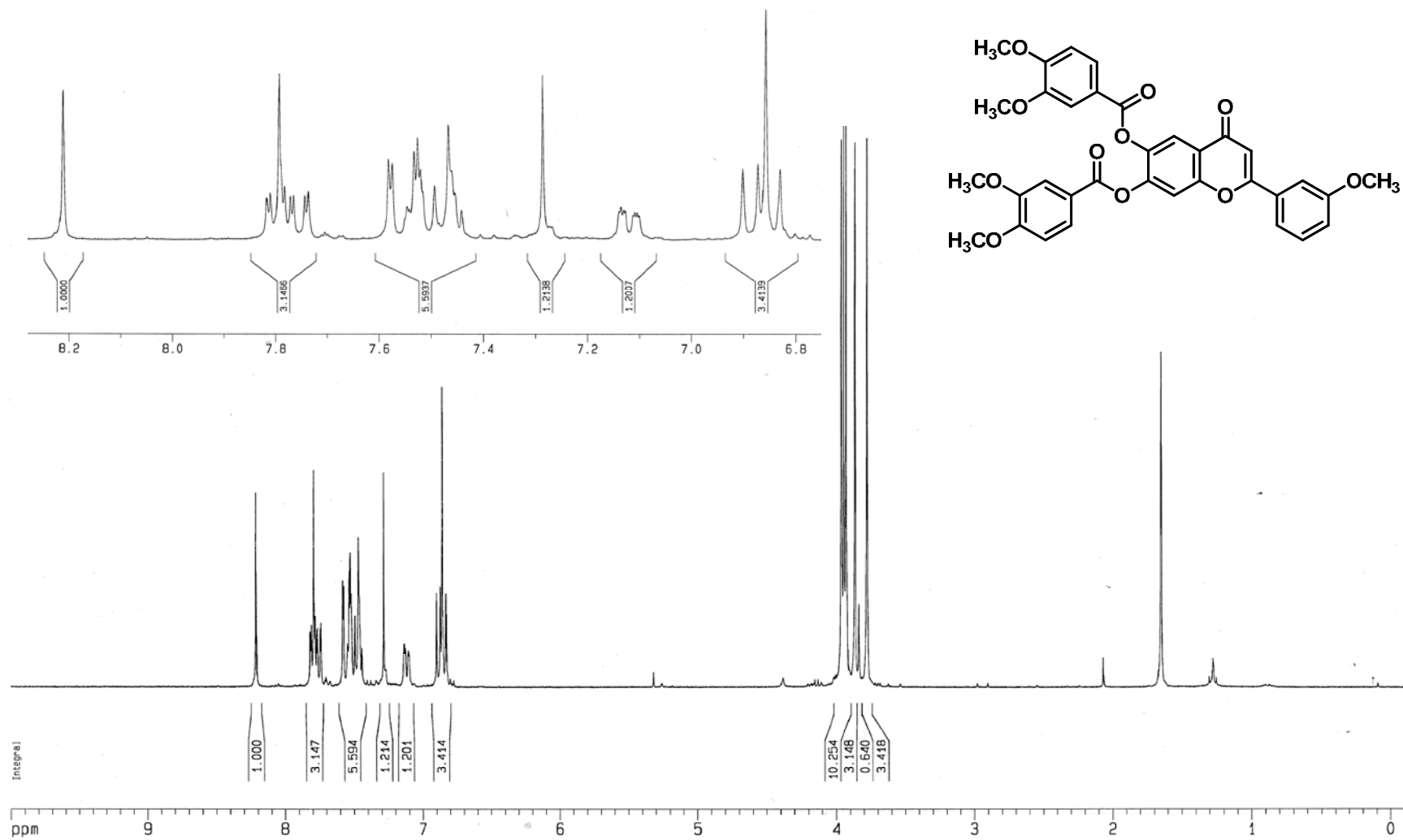
¹H-NMR spectrum (300 MHz) of chromone **49** in DMSO-d₆



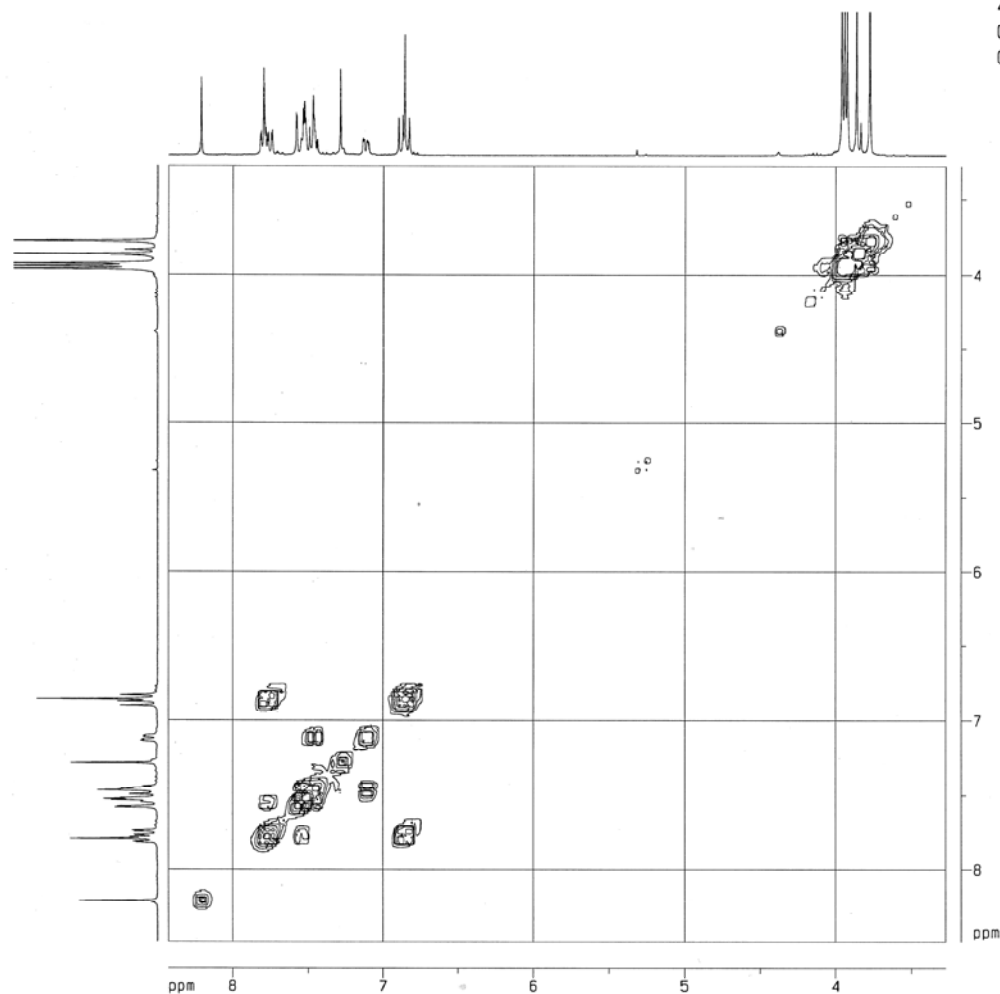
¹H-NMR spectrum (300 MHz) of chromone **49a** in CDCl₃



^1H -NMR spectrum (300 MHz) of chromone **49b** in CDCl_3



^1H -NMR spectrum (300 MHz) of chromone **49c** in CDCl_3



49c in CDCl₃
 055505009 (AVANCE300) SP
 COSY-45

```

Current Data Parameters
NAME      055505009
EXPNO     24
PROCNO     1

F2 - Acquisition Parameters
Date_     20120930
Time      14.23
INSTRUM   av800
PROBHD    5 mm BBO, 13C-1
PULPROG   zgpg30
TD         1664
SOLVENT   CDCl3
NS         16
DS         16
SWH        2620.540 Hz
FIDRES     0.000109 Hz
AQ          0.1564500 sec
RG          256
DE          190.800 usec
TE          300.2 K
D0          0.0000000 sec
D1          2.0000000 sec
d11         0.0000000 sec
C16         0.0000000 sec
IN0         0.00036161 sec

***** CHANNEL f1 *****
NUC1       1H
RG          7.00 usec
P1          7.00 usec
PL1         -3.00 dB
SF01       299.9314421 MHz

***** GRADIENT CHANNEL *****
GRNAME1    SINE,100
GRNAME2    SINE,100
GPR1       0.00 %
GPR2       0.00 %
GPR1       0.00 %
GPR2       0.00 %
GPR1       10.00 %
GPR2       10.00 %
P16        1000.00 usec

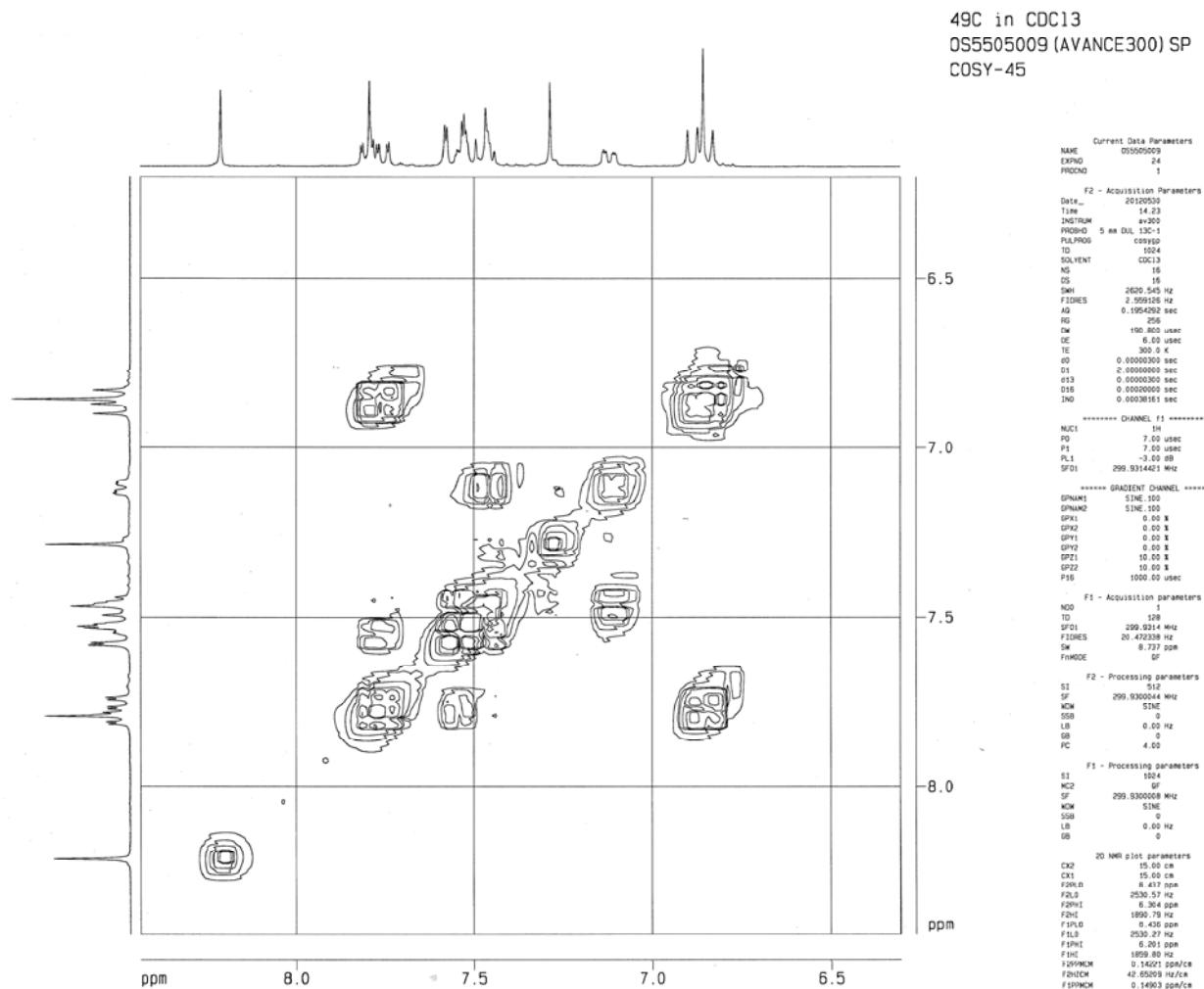
F1 - Acquisition parameters
NS          1
TD          128
SF01        299.9314 MHz
FIDRES      0.000109 Hz
SW           8.737 ppm
F0MODE      0F

F2 - Processing parameters
SI          512
SF          299.930044 MHz
WDW         SINE
SSB          0
LB           0.00 Hz
GB           0
PC           4.00

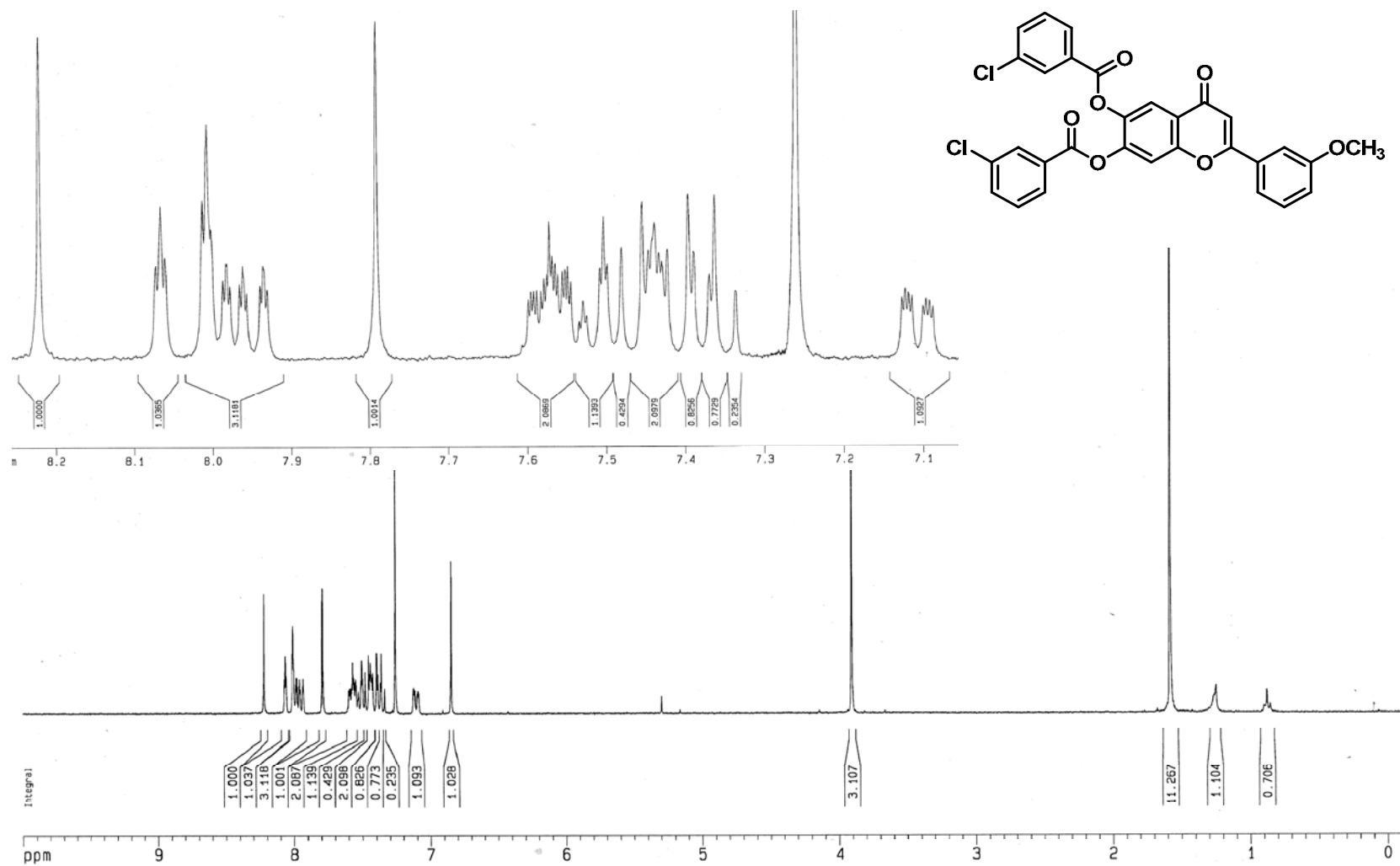
F1 - Processing parameters
SI          1024
MC2         0F
SF          299.930008 MHz
WDW         SINE
SSB          0
LB           0.00 Hz
GB           0

2D NMR plot parameters
CK2          15.00 cm
CK1          15.00 cm
F2P0         8.428 ppm
F2L0         2567.81 Hz
F2PH1        3.274 ppm
F2H1         862.15 Hz
F2P0         8.491 ppm
F2L0         2546.72 Hz
F2PH1        3.278 ppm
F2H1         863.15 Hz
F2P0MCH      0.34257 ppm/cm
F2H2MCH      103.04748 Hz/cm
F2P0MCH      0.34754 ppm/cm
F2H2MCH      104.23832 Hz/cm
  
```

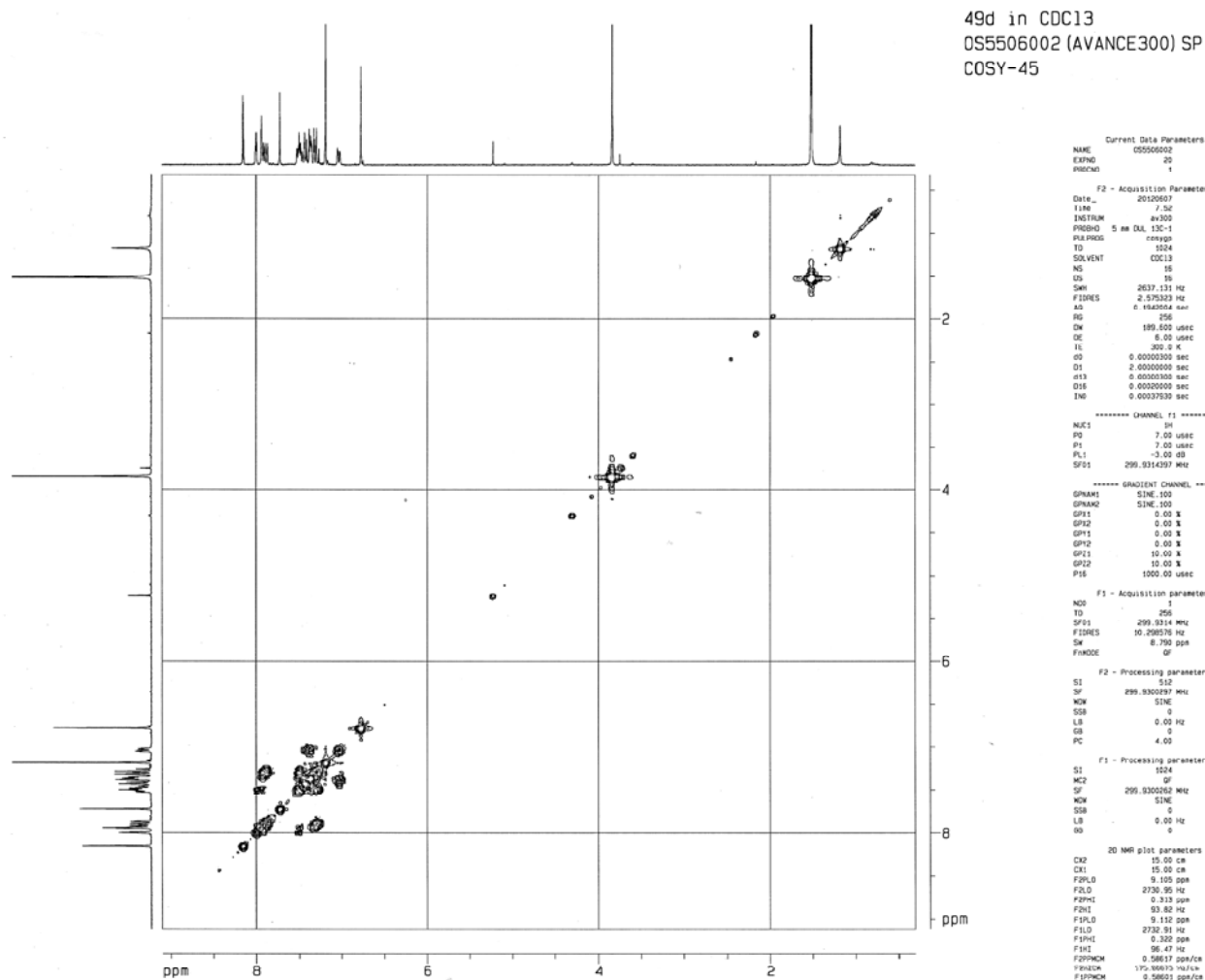
¹H-¹H COSY spectra (300 MHz) of chromone **49c** in CDCl₃



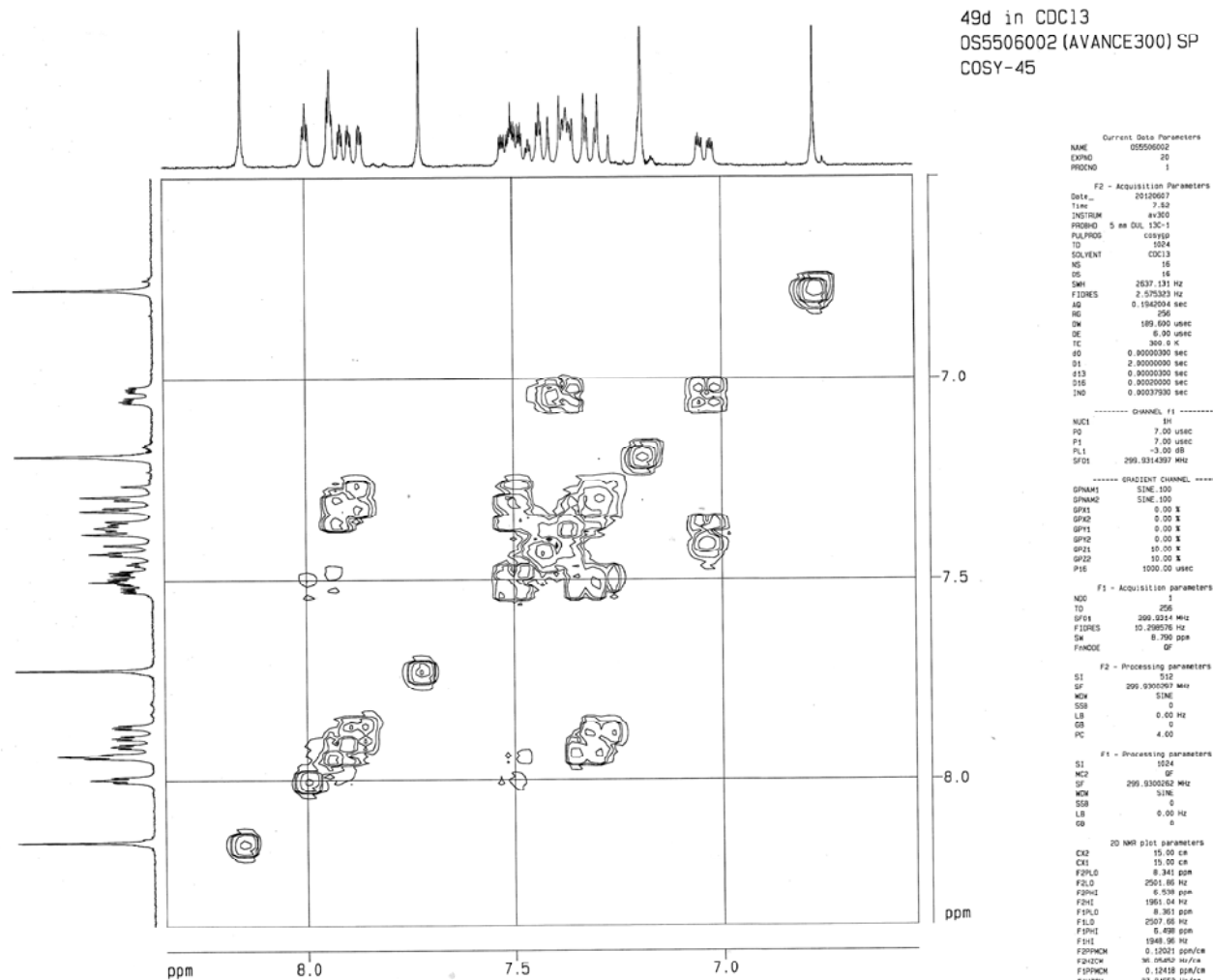
Expand ¹H-¹H COSY spectra (300 MHz) of chromone **49c** in CDCl₃

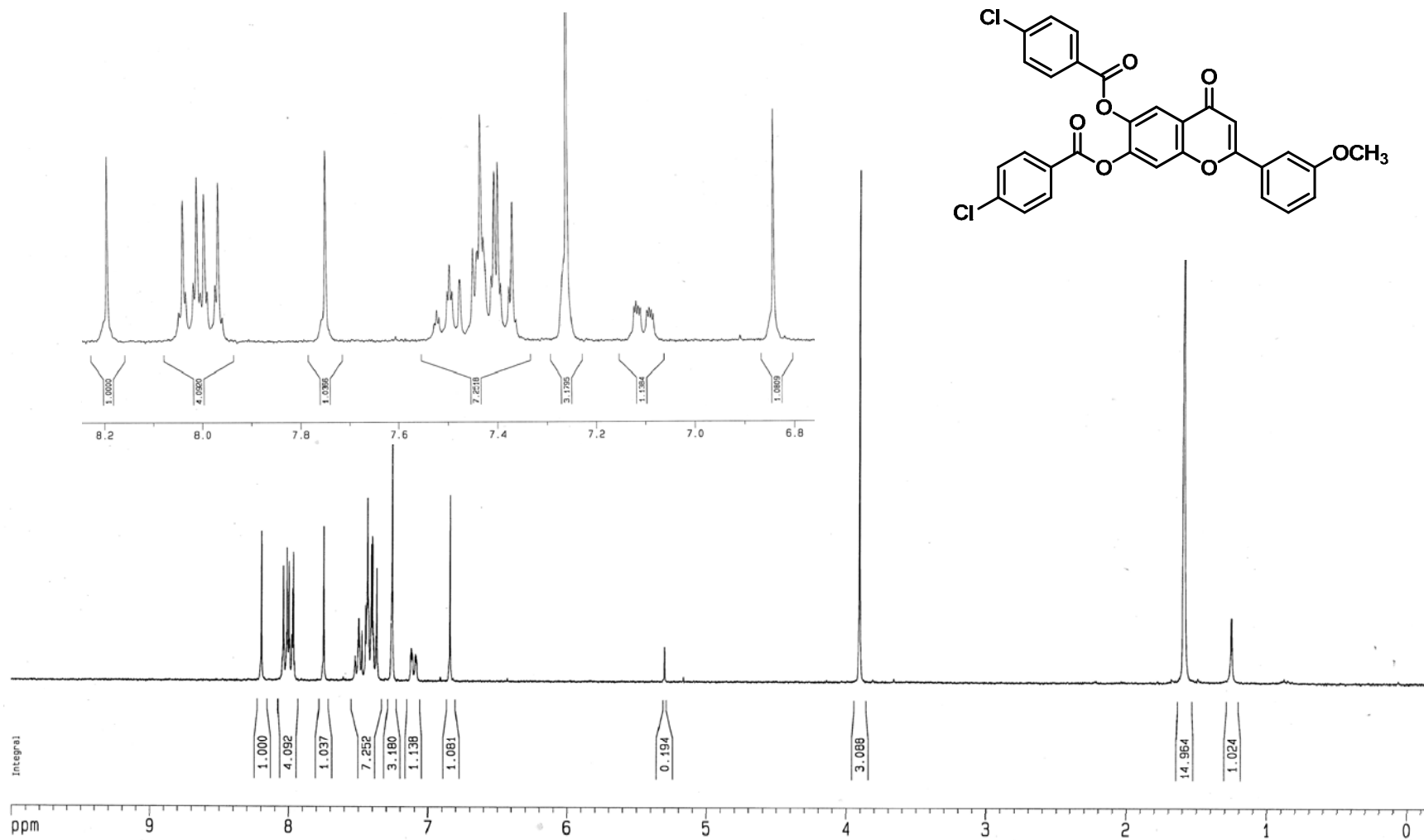


¹H-NMR spectrum (300 MHz) of chromone **49d** in CDCl₃

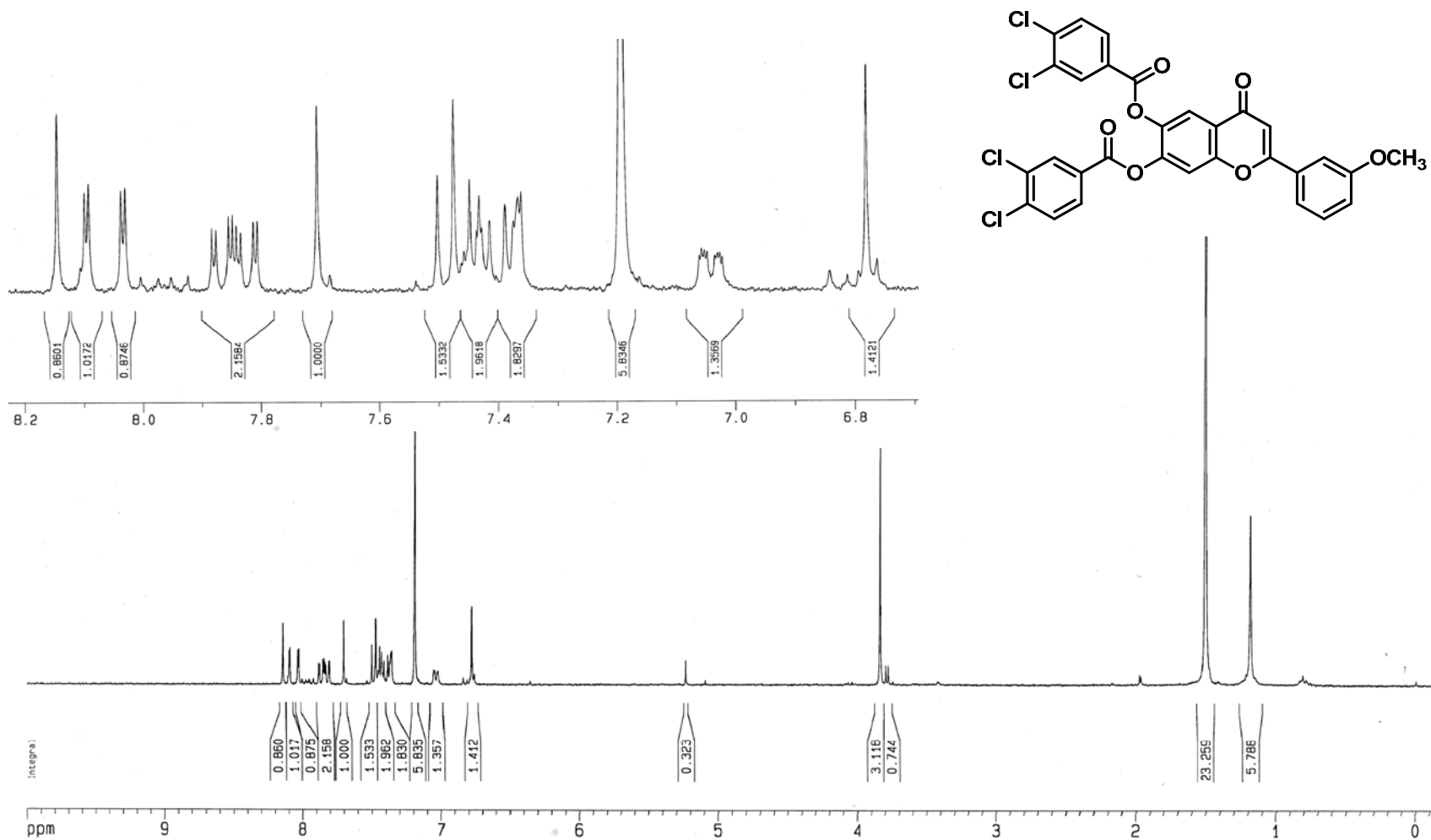


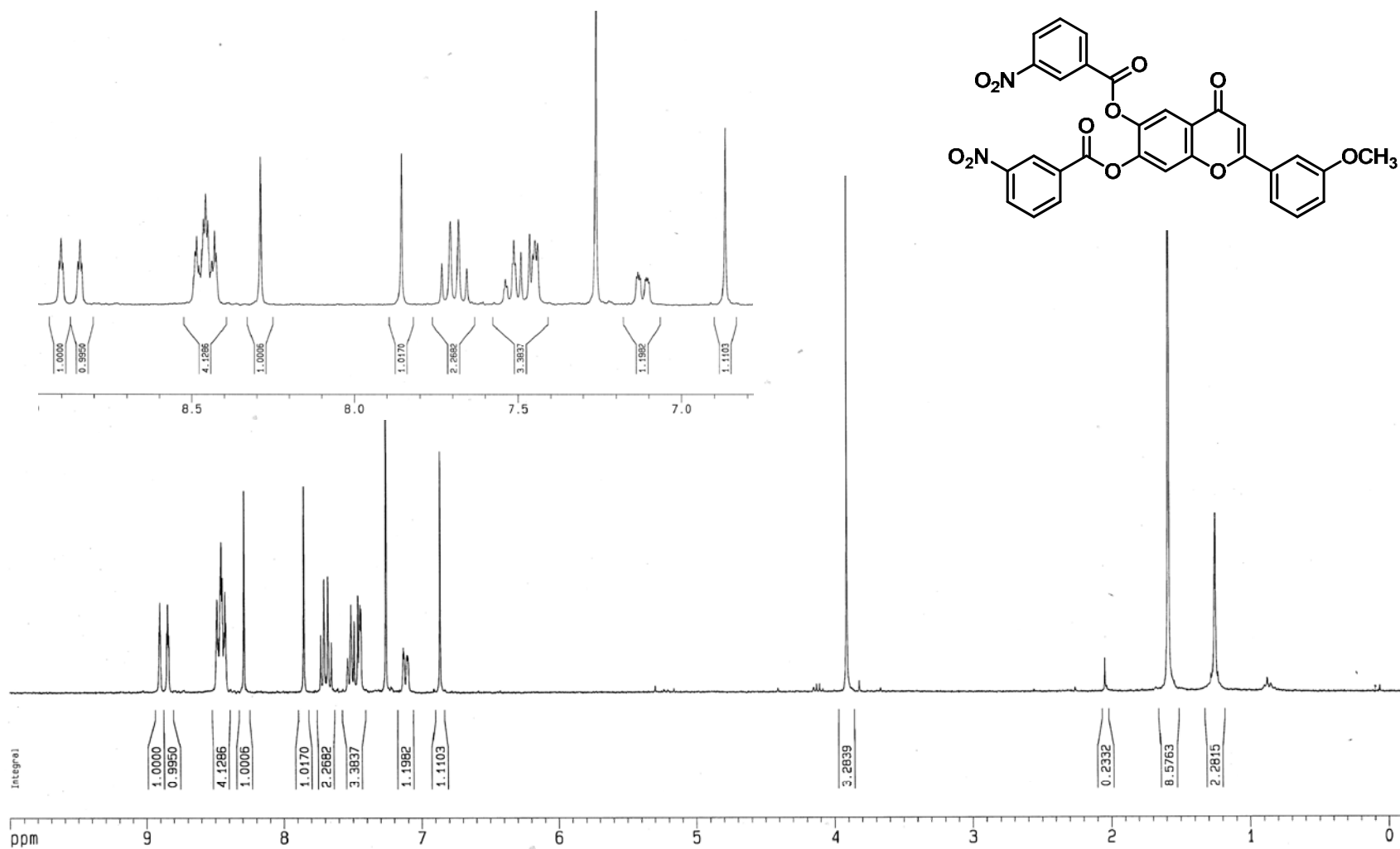
¹H-¹H COSY spectra (300 MHz) of chromone **49d** in CDCl₃

Expand ¹H-¹H COSY spectra (300 MHz) of chromone **49d** in CDCl₃

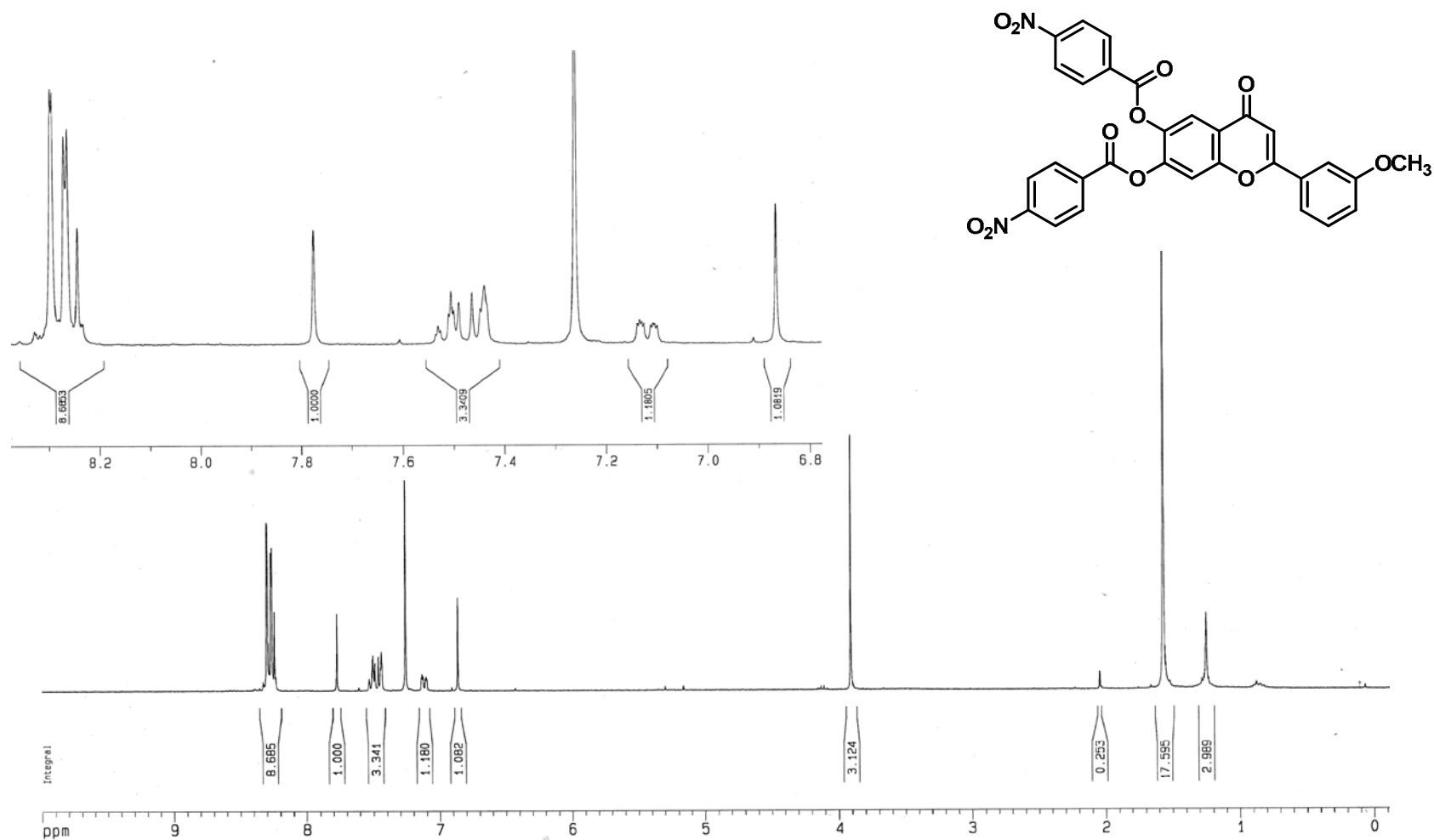


¹H-NMR spectrum (300 MHz) of chromone **49e** in CDCl₃

 ^1H -NMR spectrum (300 MHz) of chromone **49f** in CDCl_3

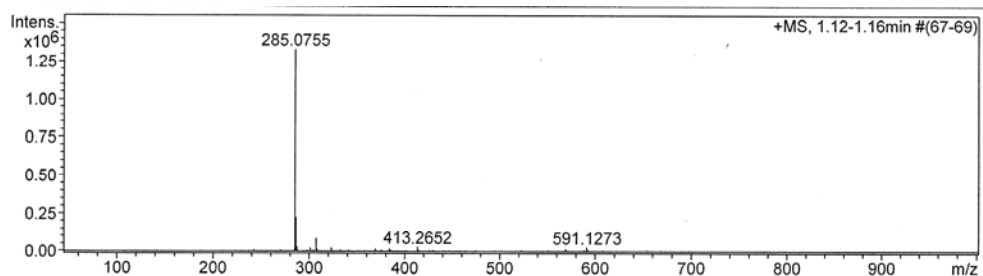


^1H -NMR spectrum (300 MHz) of chromone **49g** in CDCl_3

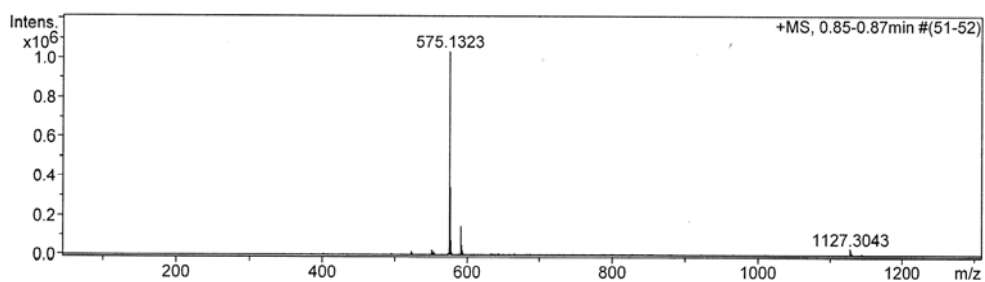


^1H -NMR spectrum (300 MHz) of chromone **49h** in CDCl_3

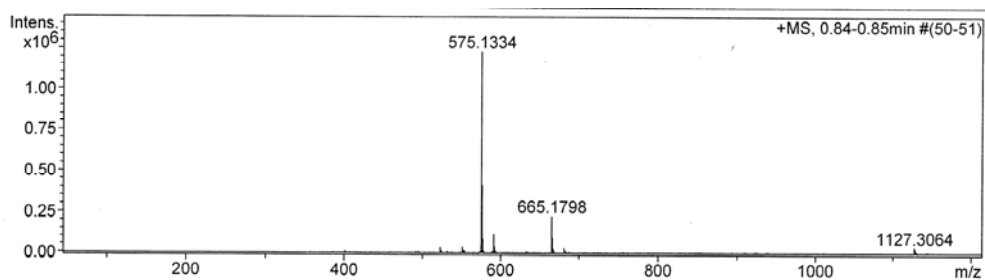
High resolution mass spectrums



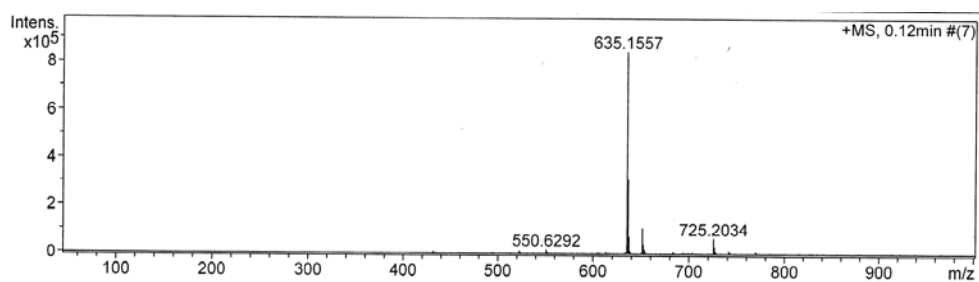
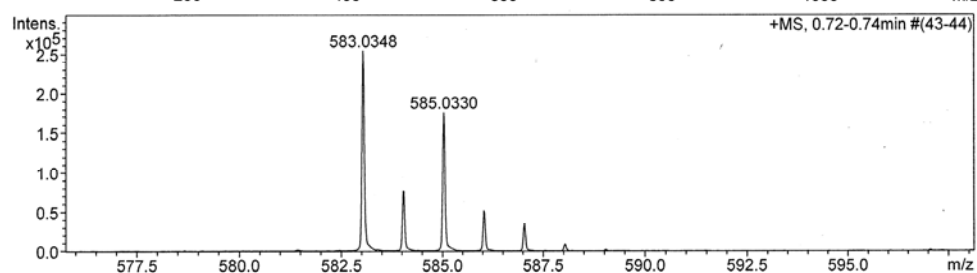
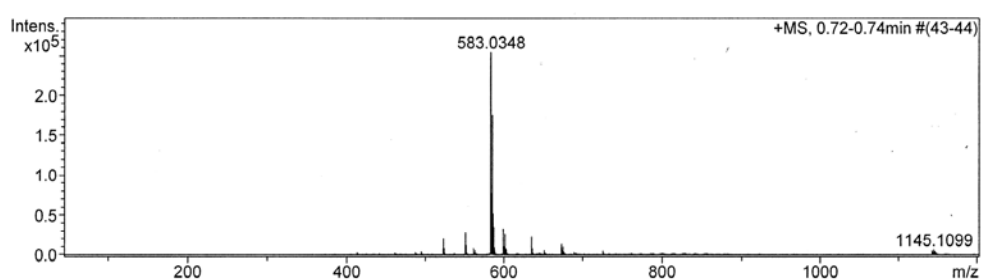
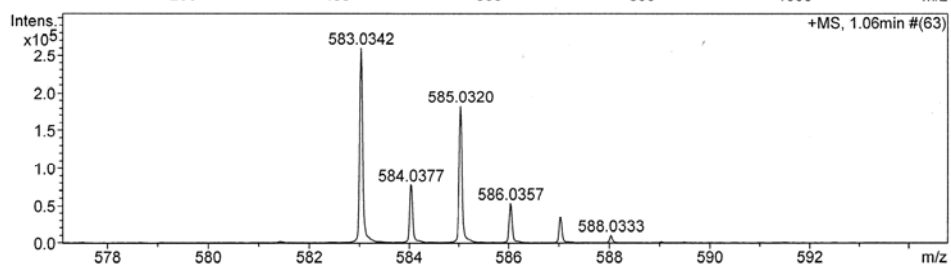
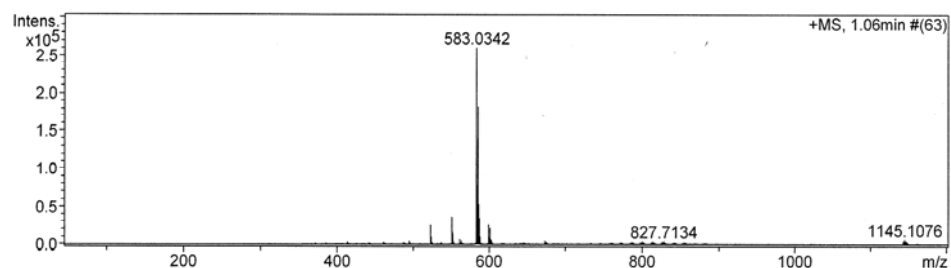
High resolution mass spectrum of chromone **49**

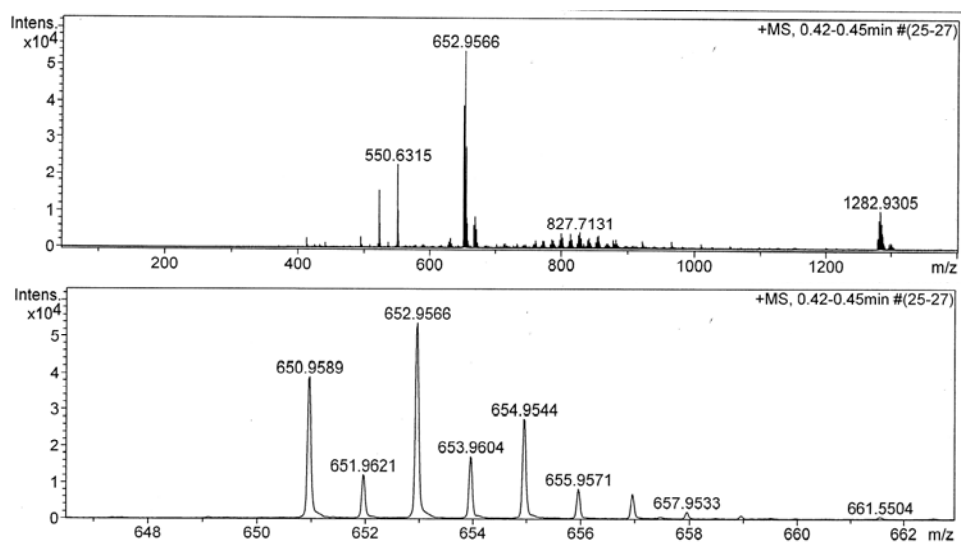
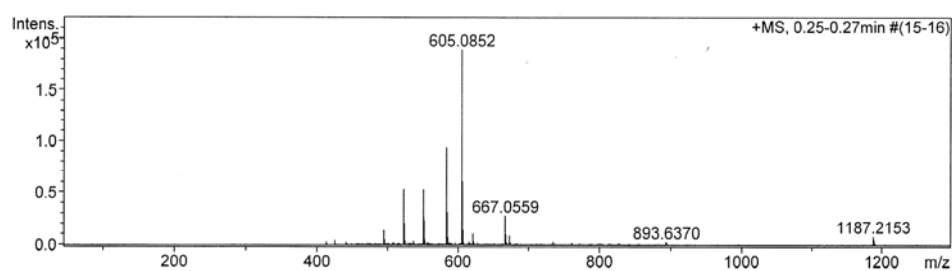
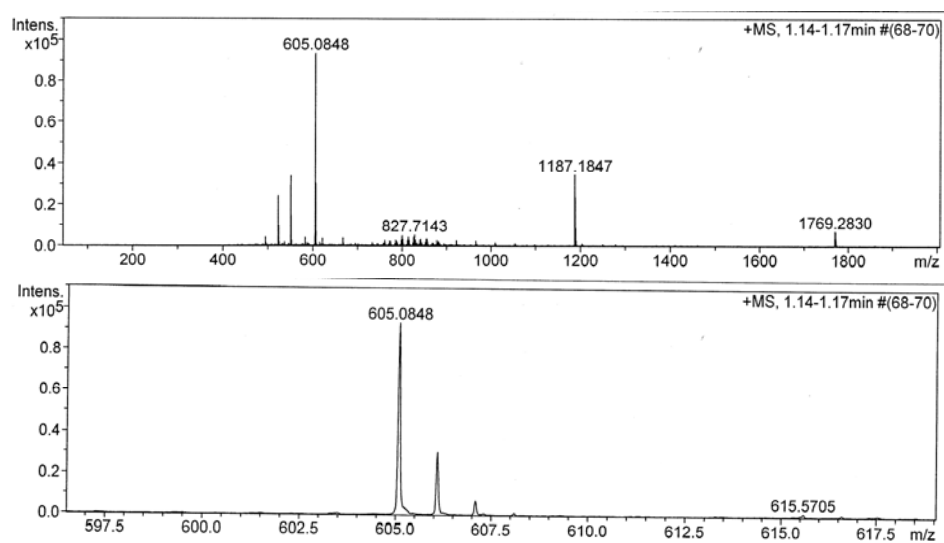


High resolution mass spectrum of chromone **49a**



High resolution mass spectrum of chromone **49b**

High resolution mass spectrum of chromone **49c**High resolution mass spectrum of chromone **49d**High resolution mass spectrum of chromone **49e**

High resolution mass spectrum of chromone **49f**High resolution mass spectrum of chromone **49g**High resolution mass spectrum of chromone **49h**

BIOGRAPHY

NAME	Mr. Pradith Lersirisuk
DATE OF BIRTH	April 8, 1987
PLACE OF BIRTH	Bangkok, Thailand
INSTITUTIONS ATTENDED	Kasetsart University, 2005-2008: Bachelor of Science (Chemistry) (Hon. 2nd class) Mahidol University, 2009-2012: Master of Science (Pharmaceutical Chemistry and Phytochemistry)
HOME ADDRESS	55/109 Ngamwongwan Rd., Toung-song-hong, Laksi, Bangkok 10210 E-mail : uz_ping@hotmail.com l.pradith@yahoo.com